



**Acta Technica Napocensis: Civil Engineering & Architecture  
Vol. 54 (2011)**

Journal homepage: <http://constructii.utcluj.ro/ActaCivilEng>

**ISSN 1221-5848**



**ISSN: 1221-5848**

**WWW:** <http://constructii.utcluj.ro/ActaCivilEng>

**Editor-In-Chief: Prof. Cosmin G. Chiorean**

(Tech. Univ. of Cluj-Napoca, Romania)

Phone/Fax: 40-264-594967

E-mail: [cosmin.chiorean@mecon.utcluj.ro](mailto:cosmin.chiorean@mecon.utcluj.ro)

**Affiliation to Organization:**

Technical University of Cluj-Napoca, Faculty of Civil Engineering, Romania

**Editorial Office Address:**

Technical University of Cluj-Napoca

15 C Daicoviciu Str., 400020 Cluj-Napoca, Romania

**Published by:**

UTPRESS

34 Observatorului Str., 400775 Cluj-Napoca, Romania

Phone: 40-264-401999

E-mail: [utpress@biblio.utcluj.ro](mailto:utpress@biblio.utcluj.ro)

Fax: 40-264-430408

**Abstracting and Indexing**



**CNCS Rating**

Romanian National Council of Scientific Research in Higher Education (CNCS) is rating the journal in B+ category.



**Aims and Scope:** *Acta Technica Napocensis: Civil Engineering & Architecture* provides a forum for scientific and technical papers to reflect the evolving needs of the civil and structural engineering communities. The scope of *Acta Technica Napocensis: Civil Engineering & Architecture* encompasses, but is not restricted to, the following areas: infrastructure engineering; earthquake engineering; structure-fluid-soil interaction; wind engineering; fire engineering; blast engineering; construction materials; structural mechanics; water resources; hydraulics and coastal engineering; structural reliability/stability; life assessment/integrity; structural health monitoring; multi-hazard engineering; structural dynamics; optimization; expert systems and neural networks; experimental modeling; performance-based design; engineering economics, constructional management; architecture; planning and built environment studies. *Acta Technica Napocensis: Civil Engineering & Architecture* also publishes review articles, short communications and discussions, book reviews, and a diary on national and international events related to any aspect of civil engineering and architecture. All articles will be indexed by the major indexing media, therefore providing maximum exposure to the published articles.

## **Editorial Board**

### **Editor-in-Chief**

**Prof. Cosmin G. Chiorean**

*Technical University of Cluj-Napoca, Faculty of Civil Engineering,  
15 C. Daicoviciu Str., 400020, Cluj-Napoca, Romania*

### **Vice Editor-in-Chief**

**Dr. Stefan GUTIU**

*Technical University of Cluj-Napoca, Romania*

### **Editorial Board**

**Prof. Horia-Aurel ANDREICA**

*Technical University of Cluj-Napoca, Romania*

**Prof. Pavel ALEXA**

*Technical University of Cluj-Napoca, Romania*

**Prof. Iacob BORS**

*Technical University of Cluj-Napoca, Romania*

**Prof. Gheorge BADEA**

*Technical University of Cluj-Napoca, Romania*

**Prof. Alexandru CATARIG**

*Technical University of Cluj-Napoca, Romania*

**Prof. Corneliu CISMASIU**

*New University of Lisbon, Portugal*

**Dr. Ildi CISMASIU**

*New University of Lisbon, Portugal*

**Dr. Vasile FARCAS**

*Technical University of Cluj-Napoca, Romania*

**Prof. Mihai ILIESCU**

*Technical University of Cluj-Napoca, Romania*

**Prof. Adrian IOANI**

*Technical University of Cluj-Napoca, Romania*

**Prof. Zoltan KISS**

*Technical University of Cluj-Napoca, Romania*

**Prof. Ludovic KOPENETZ**

*Technical University of Cluj-Napoca, Romania*

**Prof. Cornelia MAGUREANU**

*Technical University of Cluj-Napoca, Romania*

**Prof. Petru MOGA**

*Technical University of Cluj-Napoca, Romania*

**Prof. Adriana MATEI**

*Technical University of Cluj-Napoca, Romania*

**Prof. Ioan MOGA**

*Technical University of Cluj-Napoca, Romania*

**Prof. Traian ONET**

*Technical University of Cluj-Napoca, Romania  
(Romanian Technical Science Academy)*

**Prof. Vasile PACURAR**

*Technical University of Cluj-Napoca, Romania*

**Prof. Augustin POPA**

*Technical University of Cluj-Napoca, Romania*

**Prof. Laszlo POKORADI**

*University of Debrecen, Hungary*

**Prof. Iordache VLAD**

*Technical University of Civil Engineering, Bucharest, Romania*

***Contents of Acta Technica Napocensis: Civil Engineering & Architecture  
Vol. 54 No. 1 2011***

V. Stoian, D. Dan, A. Fabian	<i>Composite Shear Walls with Encased Profiles, New Solution for Buildings Placed in Seismic Area</i>	Pages 6-12
O. Prodan, Ioana Ladar, P. Alexa	<i>Seismic risk mitigation via supplemental viscous damping</i>	Pages 13-27
M. Cristutiu, L. Nunes.	<i>Local and global stability of single storey frames made of welded plate elements with tapered web</i>	Pages 28-37
Mihai Nedelcu	<i>GBT-based Analysis of Tapered Thin-Walled Members: Recent Developments</i>	Pages 38-49
Mircea Păstrav	<i>Full Scale Test of a Prestressed Concrete T-Beam</i>	Pages 50-59
Corina Moldovan	<i>Semirigidity. Past and Present</i>	Pages 60-73
V. Sav, Cristina Campian, M. Senila , H. Constantinescu	<i>Composite Steel-Concrete Columns with High Strength Concrete versus Normal Strength Concrete</i>	Pages 74-81
Dana Opincariu	<i>Structural Systems and the Quality of Daylight in Buildings</i>	Pages 82-92
Mihai Grecu	<i>Proposal for a network of urban motorways in the Cluj-Napoca urban area</i>	Pages 93-111
M. Dragomir, C. Petit	<i>Thermal shrinkage bending test in characterizing reinforcement advantages over bituminous mixtures</i>	Pages 112-121

## Composite Shear Walls with Encased Profiles, New Solution for Buildings Placed in Seismic Area

V. Stoian <sup>\*1</sup>, D. Dan<sup>1</sup>, A. Fabian<sup>1</sup>

<sup>1</sup> Politehnica University of Timisoara, Faculty of Civil Engineering, Department of Civil Engineering, Timisoara, Romania

Received 29 May 2011; Accepted 15 August 2011

### Abstract

*The concrete advantages in terms of higher stiffness, good fire protection, buckling prevention, recommends composite elements made by steel and concrete to be used in high-rise buildings placed in seismic areas. The steel concrete composite shear walls are used as lateral loads resisting systems for high-rise buildings as an alternative to reinforced concrete shear walls. Composite steel concrete shear walls are structural walls where at the boundary elements of the wall are encased steel profiles. The information's about this type of elements are poor also in the literature and in the design provisions for composite structures and for structures subjected to lateral loads from earthquake. A research program is in ongoing process at the Department of Civil Engineering from Politehnica University of Timisoara, which studies the behavior of composite steel concrete shear walls under cyclic lateral loads. Six scaled experimental elements were tested in laboratory under combined vertical and cyclic lateral loads. The paper presents the behavior of the experimental elements under lateral loads including the strain analysis in structural steel and reinforcements and the failure modes experienced by all tested elements. The results obtained during the experimental tests shown that the behavior of composite steel concrete shear walls is a ductile one, no brittle failure being experienced by the tested elements.*

### Rezumat

*Avantajele betonului în termeni de rigiditate sporită, asigurare a protecției la foc și împiedecare a flambajului, recomandă utilizarea elementelor compozite oțel beton la realizarea clădirilor înalte amplasate în zone seismice. Pereții structurali compoziți oțel beton sunt utilizați ca alternativă a pereților structurali din beton armat în cadrul sistemelor structurale acționate preponderent de încărcări laterale. Pereții structurali compoziți structurali sunt pereți din beton armat cu profile metalice înglobate la capete. Informațiile legate de acest tip de element structural sunt reduse în normele de proiectare pentru elemente compozite oțel beton cât și în normele referitoare la proiectarea structurilor la cutremur. Un program de cercetare este în derulare la Departamentul de Construcții Civile din cadrul Universității Politehnica din Timișoara și are ca scop studiul comportării pereților compoziți oțel beton supuși acțiunilor laterale ciclice. Șase elemente experimentale supuse unor acțiuni verticale constante și unor orizontale ciclice au fost testate în laborator. Lucrarea de față prezintă comportarea elementelor experimentale supuse la acțiunea combinată a încărcărilor verticale și orizontale cu accent pe analiza deformațiilor specifice din oțelul structural și armături precum și a modurilor de cedare ale elementelor testate. Rezultatele obținute arată că pereții structurali compoziți oțel beton au o comportare ductilă.*

---

\* Corresponding author: Tel./ Fax.: 40 256 403 952 / +40 256 403 958  
E-mail address: [valeriu.stoian@ct.upt.ro](mailto:valeriu.stoian@ct.upt.ro)

**Keywords:** composite elements, lateral loads, strain analysis, behavior

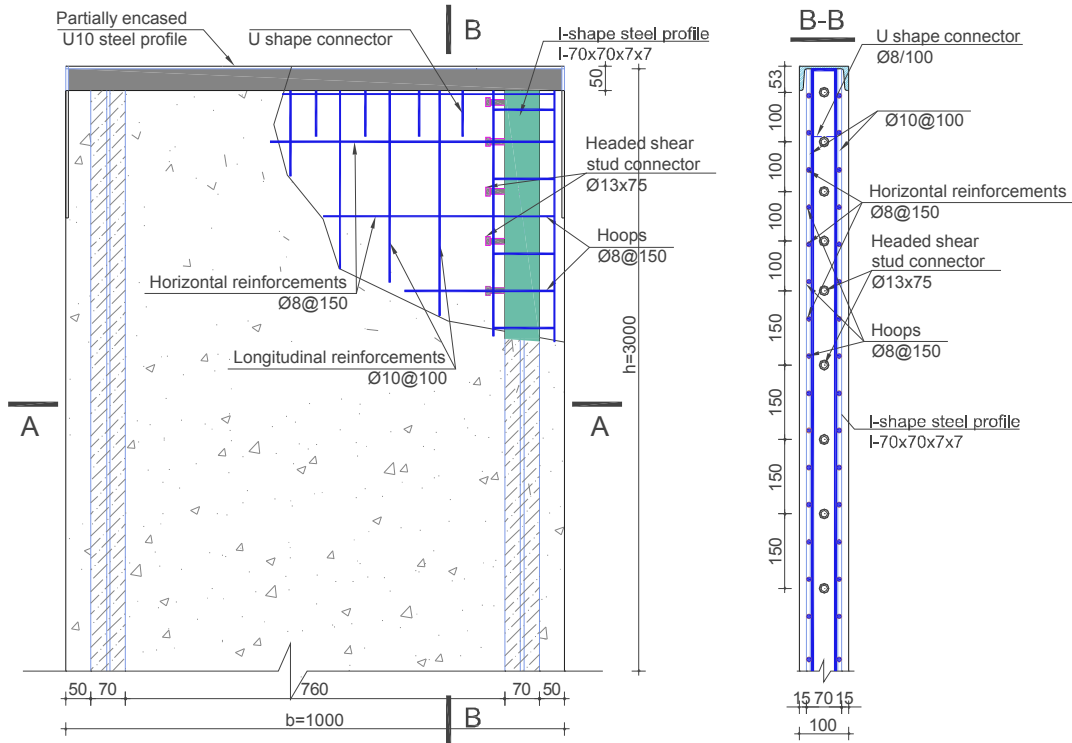
## 1. Introduction

Composite steel concrete elements made by steel and concrete are used in world wide almost as soon as the two materials became available for structural engineers, taking into account the two main advantages of these materials, good compression strength of concrete and higher tension strength of steel. A composite element which can be used together with perimeter frames in obtaining dual systems is the composite wall obtained from encasing steel shapes in the reinforced concrete wall. Composite walls are reinforced concrete walls with additional steel shapes or plates, being subjected to combined vertical and horizontal loads. Walls with additional shapes referred as composite steel-concrete shear walls, contain one or more encased steel shapes, usually located at the ends of the wall. The design principles of composite shear walls are included in specific codes- design of composite steel and concrete structures [1, 2] and in provisions regarding the design of buildings for earthquake resistance [3]. Also the design principles for reinforced concrete and for steel structures may be used in some cases. In Eurocode 8 part 7.10 are defined three types of composite structural systems: Type 1 – Steel or composite frame with concrete infill, Type 2 – Concrete walls reinforced by vertical steel sections, Type 3 – Concrete shear wall coupled by steel or composite beams, the studied walls belonging to Type 2. Although the research and specifications for composite construction, especially columns and beams, started very early, the design principles regarding composite steel concrete shear walls show a poor level of knowledge's and in order to complete the design prescriptions, are in process, experimental studies in major laboratories and research centers.

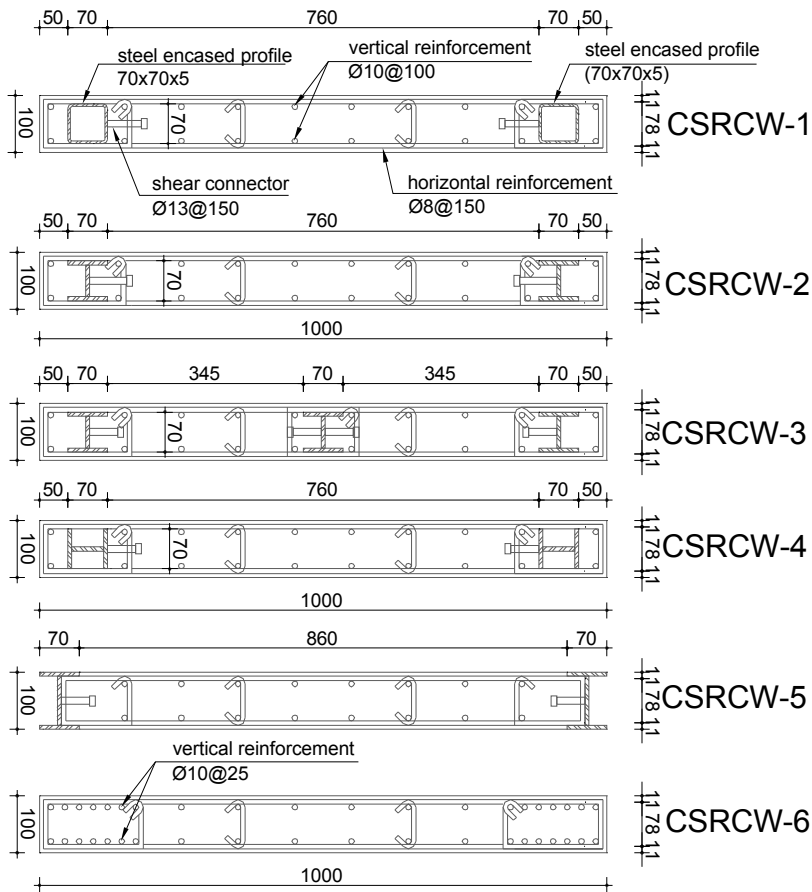
## 2. Experimental program

### 2.1 *Experimental elements design*

The experimental program was developed in the Civil Engineering Department at the Politehnica University of Timișoara, Romania and consists in quasi-static reversed cyclic loads performed on 1:3 scaled composite steel concrete wall specimens. Six different types of experimental elements were designed and tested in laboratory in order to investigate the nonlinear behavior, stress distribution, crack distribution, structural stiffness at various loads, and load bearing capacity. The specimens were designed and conceived to investigate the effects of some parameters into the behavior of the composite walls. The studied parameters are: the type of vertical reinforcement bars, the position of structural steel in the cross section, the structural steel shape. The experimental specimens had 3000 mm height, 1000mm width and 100 mm in thickness. The wall panels were fixed in reinforced concrete foundations with 1500 mm length, 400 mm height and 350 mm width. The structural steel profiles were connected with the concrete web by headed shear stud connectors with  $d=13$  mm diameter and  $h=75$  mm length placed every 100 mm. For all specimens the reinforcements of the RC web panel consists of  $\text{Ø}10/100$  mm vertical bars and  $\text{Ø}8/150$  mm horizontal bars. Vertical and horizontal reinforcements were placed on the both faces of the wall and were connected together with  $\text{Ø}8/400/450$  mm steel ties [4]. The materials used for elements construction were tested in laboratory in order to determine their specific properties. The compression strength of concrete at the testing moment varies between 46 and 65  $\text{N/mm}^2$ . The average yield strength ( $f_y$ ) for the horizontal reinforcements was 479  $\text{N/mm}^2$  and for the vertical reinforcements 548  $\text{N/mm}^2$ , whilst the ultimate strength ( $f_u$ ) was 616  $\text{N/mm}^2$  and 622  $\text{N/mm}^2$  respectively. The average yield strength for the structural steel was 328  $\text{N/mm}^2$ , whilst the ultimate strength was 516  $\text{N/mm}^2$ . For all materials three samples were provided and tested. The design details of all six types of composite steel-concrete shear walls are shown in Fig. 1.



a) Elevation



b) A-A Sections

Figure 1. Details of the composite steel-concrete walls

## 2.2 Test set-up and instrumentation

All specimens were tested under constant vertical load and cyclically increasing horizontal (lateral) loads. The lateral loads were applied alternatively from left and right. The test specimens were placed in the same plane as the loading frame and were anchored into the reaction floor, as shown in Fig. 2. The horizontal force was applied using two 400 kN hydraulic jacks, whereas the vertical force was realized by a 250 kN hydraulic cylinder. The vertical force was provided in order to obtain an axial stress level (the ratio between the induced axial stress and the characteristic cube strength of the concrete) between 1.5 and 2.2%.

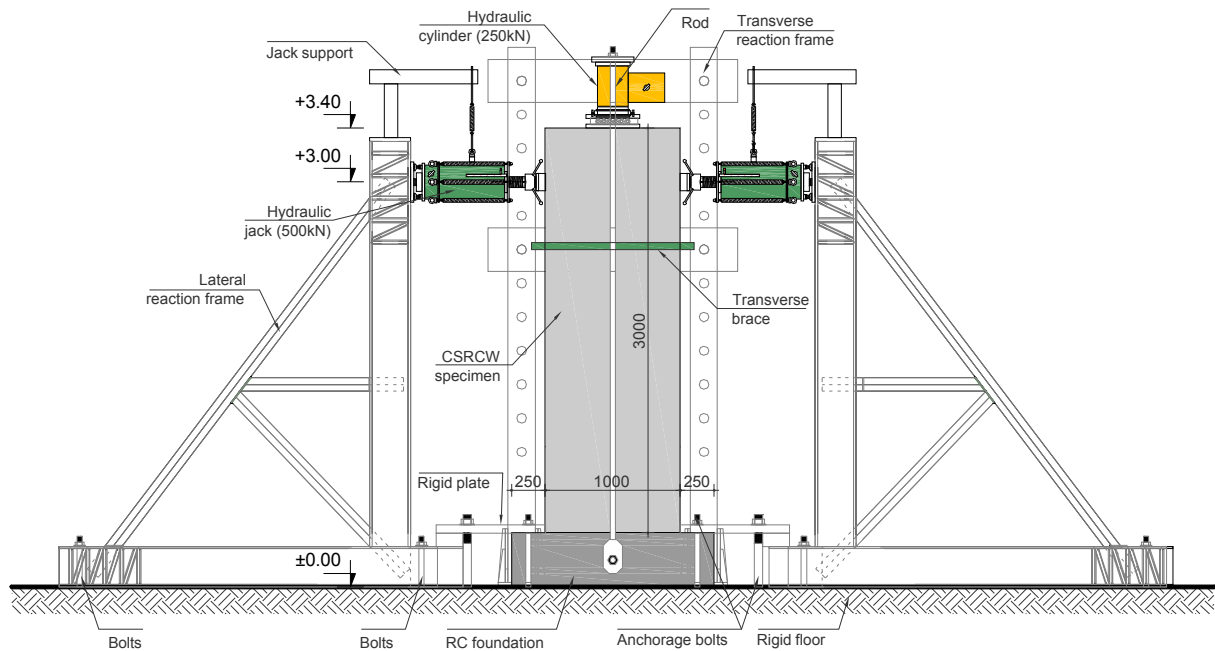


Figure 2. Test set-up

The recommended ECCS short testing procedure was used for the cyclic tests [5]. The tests were performed in displacement control. After the elastic limit, for each displacement level, three cycles were performed. The horizontal forces were applied under controlled cyclic displacements, until the strength of the specimens decreased to 85 % of the peak horizontal load [6]. Similar procedure was adopted by other experiments [7, 8]. The behavior of the experimental specimens was monitored by pressure transducers, displacement transducers (D), strain gauges glued on the reinforcement bars and on the structural steel (G) and by optical laser measurements.

## 2.3 Experimental observations

The experimental tests show quite similar behaviour for the different tested elements. In the followings, a general comment about the behaviour of the specimens is presented.

At the beginning horizontal cracks appeared in the tensioned zone near the base of the wall, after that, as the horizontal load level increased, the cracks began to develop on the height of the element. Diagonal cracks appear in the elements after the top displacement exceeded 20 mm, and develop until practically the entire surface is separated into a series of rhombic concrete blocks. At this load level, the measured strains indicated yielding of the vertical reinforcing bars located at the extremities and yielding of the steel profiles. In this moment the element was considered in yield, a nonlinear behaviour occurring after that.

The specimens attained their ultimate strength at a displacement level between 100 and 125 mm.



After this moment the lateral load began to decrease with an increasing of the horizontal displacement. The failure of the element was considered when the horizontal load decreased to a value of 85 % of the maximum load.

The connection provided by shear studs between the steel profiles and the concrete was monitored and no visible separation at the interface occurred during the transfer of stresses between the steel encased profiles and the concrete. For element CSRCW2, the connection between the steel and the concrete failed in tension at 2% drift cycle due to a missing shear stud, probably fractured in the manufacturing process.

The tested composite shear walls with steel encased profiles showed a bending failure mode, with the crushing of the compressed concrete and the tearing of the tensioned steel. The vertical reinforcement placed at the extremity of the elements yielded in tension, but never failed. In the compression zone, the local buckling of the steel profile and vertical reinforcements occurred after the concrete crushing. The behaviour of the specimens was in accordance with the design process for all tested specimens.

### 3. Test results

The horizontal loads versus lateral displacement envelope curves are shown in Fig. 3. The maximum horizontal load ( $P_{max}$ ) was attained by element CSRCW3 and represents 127% of the ultimate lateral load of the reinforced concrete wall CSRCW6. Note that the steel encased sectional area from the extremities of the wall has the same value as the vertical reinforcement area of the reinforced concrete element. It can be mentioned that composite wall had a higher initial stiffness than the reinforced concrete wall. The value of the element stiffness prior to failure is higher for the composite wall than for the reinforced concrete wall. The diagrams show symmetrical behaviour of the tested elements until the final stage. The differences between the values obtained for positive and negative directions of loading, are due to the last loading stage, when the element was tested until failure.

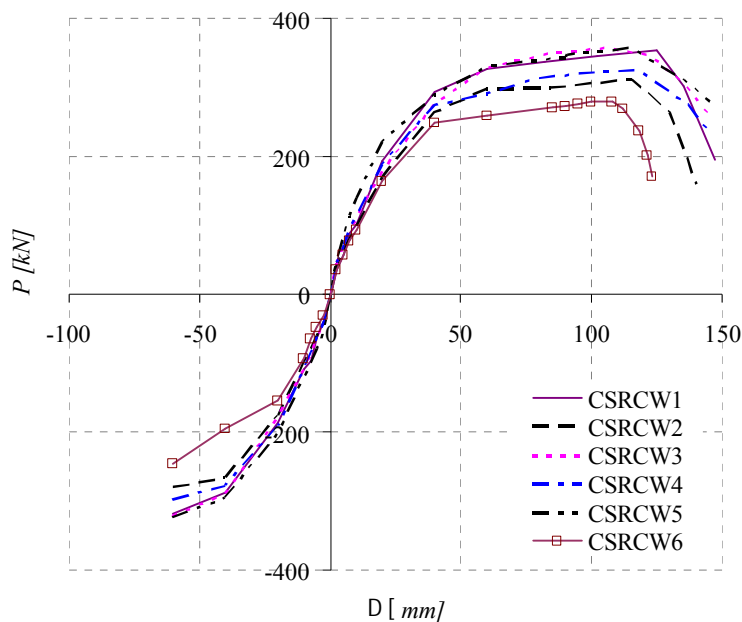


Figure 3. Comparative load displacement experimental curves

The recorded values for horizontal loads and the corresponding horizontal displacements in some characteristic stages are presented in Table 1.

Table 1: Forces and displacements in characteristic stages

Specimen	Initial cracking		Element yielding		Limit stage		Failure stage	
	$P_{cr}$ (kN)	$D_{cr}$ (mm)	$P_y$ (kN)	$D_y$ (mm)	$P_{max}$ (kN)	$D_{max}$ (mm)	$P_{85\%}$ (kN)	$D_u$ (mm)
CSRCW1	80.5	7.54	228.2	26.5	354.4	125.1	301.5	135.4
CSRCW2	80.6	7.53	204.7	25.7	311.2	115.0	262.1	130.0
CSRCW3	91.6	7.52	209.2	25.2	357.8	106.03	304.2	135.7
CSRCW4	94.6	7.56	238.6	26.4	324.8	117.75	275.4	137.2
CSRCW5	84.0	5.00	258.3	26.3	357.3	115.1	303.7	135.2
CSRCW6	77.0	7.41	185.8	24.6	279.6	108.1	237.6	118.2

In Fig. 4(a) is represented the relation between lateral loads ( $P$ ) and the longitudinal steel strain ( $\epsilon_{steel}$ ) in the steel encased profiles for two specimens. The  $P - \epsilon_{steel}$  relation is linear until the major diagonal crack develops in concrete. After that phase,  $\epsilon_{steel}$  increases more rapidly, and the yielding strain is attained when the maximum displacement reaches values between 15 and 21 mm. As an observation, with the exception of element CSRCW4, when yielding occurred in the same time for vertical reinforcements and vertical steel encased profile, it occurred first in steel encased profiles and after that in the vertical reinforcements. In Fig. 4(b) are represented the  $\epsilon_{sw}$  strain, measured on the first layer of the vertical bars located near the steel encased profile, at the extremity of element.

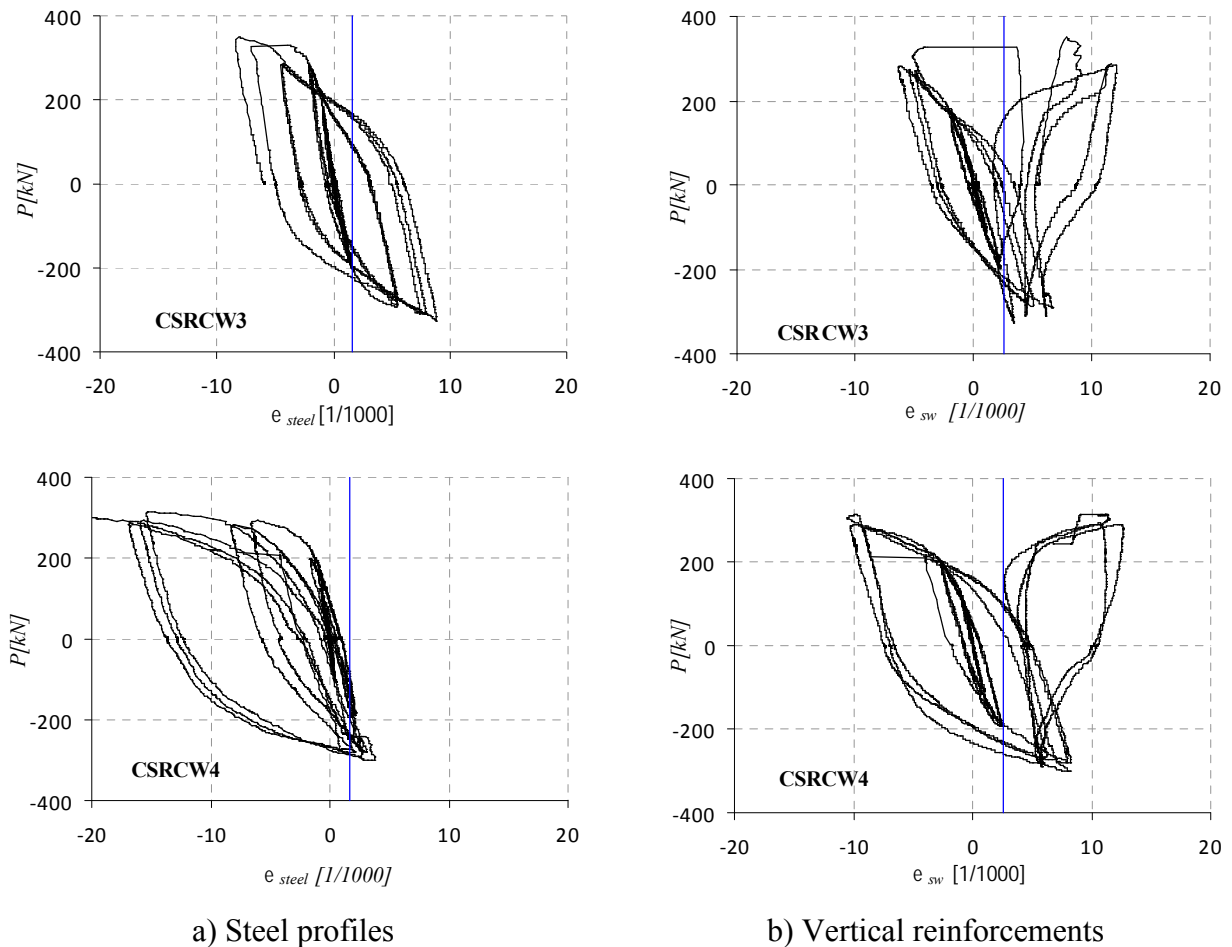


Figure 4. Load – steel strain relations

In Fig. 5 are presented some aspects regarding the failure conditions of the tested specimens.

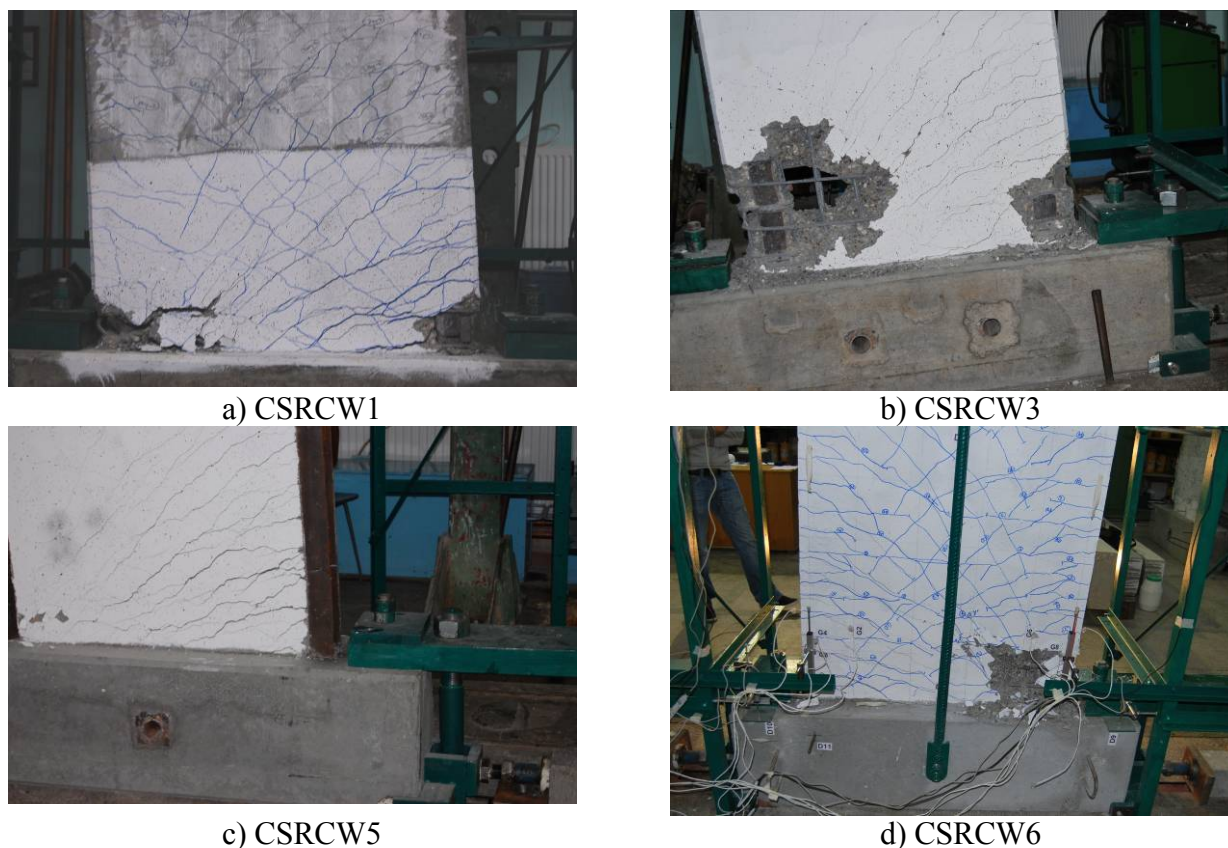


Figure 5. Failure conditions of tested specimens

## 5. Conclusions

The performed studies show that the failure mode of the tested elements is in bending, with the crushing of the compressed concrete and the tearing of the tensioned steel. The behaviour of CSRCW is nonlinear. The nonlinearities are caused by the steel yielding which occurred in steel profiles and vertical reinforcement, plastic deformations occurred in concrete, steel concrete connection and due to shear stud connector's behavior. The vertical reinforcement placed at the extremity of the elements yielded in tension, but never failed. In the compression zone, the local buckling of the steel profile and vertical reinforcements occurred after the concrete crushing. The local buckling of the steel profiles flanges of element CSRCW5 was more evident. The shear stud connectors that were used to assure the connection between steel and concrete provided a full connection, no slip between the two materials occurred during the experimental tests. The behavior of the specimens was in accordance with the design process for all tested specimens.

Further studies are needed to extend the range of the test data and to investigate other variables like the influence of higher axial load ratios, different height/width ratios and other possible connection between steel and concrete.

## Acknowledgements

The presented work was supported by research grant ID\_1004 founded by the National University Research Council, Romania, entitled „Innovative Structural Systems Using Steel-Concrete Composite Materials and Fiber Reinforced Polymer Composites”.

## 6. References

- [1] EN 1992-1-1. Eurocode 2: Design of concrete structures, part 1-1, general rules and rules for buildings.
- [2] EN 1994-1-1. Eurocode 4: Design of composite steel and concrete structures, part 1-1, general rules and rules for buildings.
- [3] EN 1998-1. Eurocode 8: Design of structures for earthquake resistance.
- [4] Dan D., Fabian A., Stoian V., “Theoretical and experimental study on composite steel–concrete shear walls with vertical steel encased profiles” *Journal of Constructional Steel Research*, Vol. 67, pp. 800 – 813, 2011.
- [5] ECCS - Recommended testing procedure for assessing the behaviour of structural steel elements under cyclic loads, European Convention for Constructional Steelwork, 1999.
- [6] Liao F.Y., Han L.H., Tao Z, “Seismic behavior of circular CFST columns and RC shear wall mixed structures: Experiments”, *Journal of Constructional Steel Research*, Vol. 65, pp. 1582 – 1596, 2009.
- [7] Liao, F.Y., Han, L.H., Tao Z. Experimental behaviour of RC shear walls framed with steel reinforced concrete (SRC) columns under cyclic loading. *Steel & Composite Structures 2010, Proc. of the 4-th International Conference*.
- [8] Guo, L., Ma., X., Zhang, S., Guan, N.: Experimental research on seismic behaviour of two-sided steel-concrete composite shear walls. *Proc. of Eurosteel 2008*, Graz, Austria, 3-5 September 2007.

# Seismic risk mitigation via supplemental viscous damping

Ovidiu PRODAN<sup>\*1</sup>, Ioana LADAR<sup>2</sup>, Pavel ALEXA<sup>2</sup>

<sup>1,2</sup> Technical University of Cluj-Napoca, Faculty of Civil Engineering, 15 C Daicoviciu Str., 400020, Cluj-Napoca, Romania

Received 21 April 2011; Accepted 27 June 2011

## Abstract

*Present contribution focuses on a special aspect of seismic mitigation of steel skeletal structures via viscous supplemental damping. The response reduction due to added viscous damping is expressed in terms of associated static and kinematical parameters as well as synthetic parameters and refers to several degrees of added viscous damping. Seismic response is computed by classical technique of nonlinear time history type analysis allowing for elastic – plastic behavior of structure. The time history analysis is carried out by two accelerograms: recorded accelerogram of Vrancea 1977 earthquake and an artificial sinusoidal calibrated accelerogram of constant amplitude (that is used in order to avoid the reduction of the seismic response due to the reduction in the seismic action). The analyses are conducted on a performance based approach and encompass a set of steel planar frames of different heights, ranging from a six level five bay frame to a 15 level five bay frame of office serviceability located in a highly seismically zone. The set of analyzed structures is part of a larger study focused on assessing (technically and economically) the seismic protection of steel skeletal structures by supplemental damping.*

## Rezumat

*Lucrarea prezintă câteva aspecte referitoare la eficiența protecției seismice a structurilor de tip cadre metalice multi-etajate prin amortizare vâscoasă suplimentară. Reducerea răspunsului seismic prin amortizare suplimentară este exprimată în valori ale unor parametri statici, cinematici și sintetici asociați câtorva niveluri de amortizare vâscoasă. Răspunsul seismic este calculat prin metoda clasică a analizei dinamice neliniare în domeniul de comportare elasto – plastică a structurii. Analiza dinamică folosește două accelerograme: accelerograma înregistrată Vrancea 1977 și o accelerograma sinusoidală calibrată. Aceasta din urmă este utilizată pentru a decela reducerea răspunsului seismic datorită amortizării suplimentare de reducerea acestui răspuns datorită reducerii intensității cutremurului. Analizele efectuate se referă la o structură metalică multi-etajată etajată având 12 niveluri amplasată într-o zonă cu seismicitate ridicată. Structurile analizate sunt proiectate pentru un amplasament având  $a_g = 0,24 g$  și fac parte dintr-un set mai larg vizând modalități de evaluare a eficienței amortizării suplimentare în protecția antiseismică.*

**Keywords:** skeletal steel structures, added viscous damping, performance based analysis, mitigation assessment

## 1. Introduction

The main problem of earthquake acted upon structures is the kinetic energy induced by the natural

---

\* Corresponding author: Tel./ Fax.: +40-745934864/+40-260660466  
E-mail address: Ovidiu.prodan@mecon.utcluj.ro

phenomenon (earthquake) into the artificially created structure. Induced kinetic energy is transformed into deformation potential energy, a transformation that induces a vibratory motion into the structure. While the continuous process of reciprocal transformation of mechanical energy goes on, another physical phenomenon is present by altering the conservation of mechanical energy. It is the damping, the natural or inherent class of damping associated to mechanical vibrations. In the case of earthquake acting upon the structure, the damping effect is exhibited by the reduction of response (seismically induced) parameters amplitudes. Nevertheless, one has to note that the reduction in (mainly the amplitudes of) seismically induced parameters is, intrinsically, associated to the reduction of the intensity of seismic action itself. The beneficial effect of natural / inherent damping in protecting the structural and nonstructural elements during the seismic action is as old as the construction activity itself. Even the additional damping purposely introduced into the structure has been in use *avant la lettre*, while ancient Greeks built up the Temple of Artemis on a soft layer of wool stuffed sacks capable of absorbing a good part of seismic base shear in the same way as the modern base isolators do. What about so many other buildings erected before Temple of Artemis but not mention in ancient history?

The problem of absorbing kinetic energy – irrespective of its source (wind, earthquakes) - in order to prevent its transformation into potential energy, is an important aspect of modern seismic design though, it is, by no means, only a subsequent step in seismic protection of structures. The first step is the correct conceiving of the structure by observing the seismic design principles. Only a correctly conceived structure located in a seismic area “deserves” to be further protected by more or less modern means. A high-rise structure that does not observe the fundamental rules of seismic design will not be able to further benefit of modern seismic mitigation equipment introducing added damping.

One of this means is increasing the level of natural damping by supplemental damping provided via modern equipments or hardware. The added damping will increase the natural (inherent) level of internal damping of the structure. However small this internal damping level may be, it has to be modeled in terms of static and kinematical parameters involved in the induced vibratory motion. In the case of internal damping, the damping force may be the result of several physical phenomena: Coulomb friction, yielding of metal elements, deforming viscous fluids, forcing viscous fluids through small orifices. By the nature of these phenomena, one may note the dependence of (damping) force upon either the (induced) displacement or upon (induced) velocity. The dependence of damping force upon the displacement (as in the metallic yielding case) confers to the force – displacement relationship a hysteretic feature Fig. 1, while the dependence of damping force upon the velocity (as in the case of viscous damping), confer to the force – displacement relationship a closed cycle aspect Fig. 2.

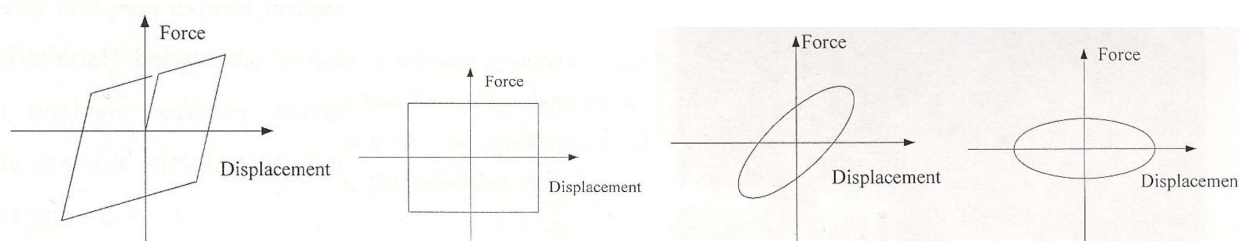


Figure 1. Hysteretic force – displacement relationship of displacement dependent damping      Figure 2. displacement relationship in the case of velocity dependent damping

Whatever is the source and the nature of the damping, the graphical and associated analytical models are idealizations of the real damping phenomena. As the earthquake induced structural motion exhibits a vibratory feature, the associated state of deformation is, also of cyclic form. During such a cyclic deformation, the material response, in terms of stress – strain relationship,

takes a hysteretic form as well. The area enclosed in a loop of the hysteretic stress – strain relationship is a good estimate of the amount of dissipated kinetic energy.

Referring to viscous type damping, the stress – strain relationship is specific to the structural material (via Young modulus  $E$ ) and it is frequency dependent, i.e., it depends on the rate of deformation. Most of the literature considers the Kelvin – Voigt model of viscous - elastic damping as very appropriate for practical use. At the unit stress ( $\sigma$ ) – specific deformation ( $\varepsilon$ ), Kelvin – Voigt model of viscous - elastic damping reads:

$$\sigma = E \cdot \varepsilon + E^* \cdot d\varepsilon/dt \quad \text{Eq. (1)}$$

where  $E^*$  is the complex modulus of elasticity and  $d\varepsilon/dt$  is the rate of the specific deformation. The elastic component  $E \cdot \varepsilon$  of the stress takes no part in damping process. The inelastic stress component  $E^* \cdot d\varepsilon/dt$  is generating (internal) damping. The main characteristic of this term – responsible for damping – is its independency of frequency  $\omega$  of vibrations since neither  $E^*$ , nor the rate of deformation change  $d\varepsilon/dt$  depend on frequency.

The more important is the weighted contribution of non-elastic component  $E^* \cdot d\varepsilon/dt$  in the stress  $\sigma$ , the larger is the damping level of the structure. But the design of real structures has to take into account the irreversible feature of this component. It is responsible not only for the (internal) damping of the structure, but, also, for plastic behaviour of structural (and non-structural) elements. Indeed, this term generates both, damping and plastic zones. The generation of plastic zones may be desirable in terms of seismic mitigation but it is not at all desirable in terms of plastic zones in (mainly) structural elements. What the supplemental damping actually does, is to shift the unavoidable plastic zones from structural elements to some elements / equipments capable of both, developing plastic deformations and introducing supplemental damping. The idea of mitigating seismic effects by supplemental damping is not new, as it has been pointed out, but equipments developed during recent years are innovative and efficient. The innovations not only enriched the general level of damping but are capable of automatically adapting this level to the instantaneous structural necessity during the earthquake action. Among these innovative equipments, an important place is taken by the viscous-fluid dampers. These devices, by the very principle they function, (deforming viscous fluids) constitute zones of plastic deformations outside structural (or non-structural) elements, therefore, saving structural and non-structural damages that are associated to seismic action.

Viscous dampers not only increase the general level of damping (up to 30% of the critical ratio), but, also, allow the structural designer to predict and control the structural response. Additional damping may lead to a reduction in structural stiffness (mainly lateral) which, in its turn is associated to larger vibration periods, therefore, to lower seismic base shear force. Viscous fluid dampers develop (damping) forces dependent on velocity of induced motion. Fluid viscous dampers may be considered as 100% velocity dependent, therefore, they do not add stiffness to the structure but damping only. The role and place of fluid viscous dampers in seismic mitigation can be emphasized by the energy balance during seismic action. During a seismic action on a structure, the ground motion induces into the structure an amount  $E_i$  of (mechanical) energy. A part  $E_s$  of this induced energy is stored in the structure (in the form of elastic and kinetic energy), while the rest is dissipated within the structure through internal (inherent) damping and possible plastic deformations. A first form of energy balance (law of conservation of mechanical energy) of a seismically unprotected structure reads:

$$E_i = E_s + E_d \quad \text{Eq. (2)}$$

The amount of stored energy  $E_s$  takes, in its turn, the form of elastic strain energy  $E_e$  (responsible for elastic deformations) and kinetic energy  $E_k$  that generates the vibratory motion. That is:

$$E_s = E_e + E_k \quad \text{Eq. (3)}$$

Dissipated energy  $E_d$  is made up of energy dissipated by plastic deformations  $E_p$  and energy dissipated by internal inherent damping (supposed of viscous nature)  $E_h$ .

That is:

$$E_d = E_p + E_h \quad \text{Eq. (4)}$$

In the case of a seismically protected structure, the term  $E_d$  is artificially increased via seismic protection devices with an amount  $E_s$  due to the supplemental damping. Energy approach to seismic mitigation may be expressed, again, as a condition of conservation of mechanical energy produced by seismic action upon a structure equipped with mitigation devices - fluid viscous dampers in this case:

$$E(t) = E_k(t) + E_e(t) + E_p(t) + E_h(t) + E_s(t) \quad \text{Eq. (5)}$$

where:

All energy terms are expressed as functions of time  $t$ . While in the case of a structure without supplemental damping equipment, the term  $E_s = 0$ , the only contribution to dissipation of input energy is brought about by the (usually) small amount (from 2% to 5%) of internal damping ( $E_d$ ) and by the undesirable plastic deformations ( $E_p$ ). The energy balance expressed by Eq. (5) emphasize the possibility of transferring the task of energy dissipation by plastic deformations of structural elements ( $E_p$ ) to the equipment providing supplemental damping ( $E_s$ ), saving the structure of plastic deformations, therefore of damages. The possibility of inserting damping generating equipment into the structure is both, a way of avoiding plastic (irreversible) deformation and a way of controlling the seismic structural response. Possibility of controlling structural response (to seismic action, for instance) is not just a way of mitigating seismic behaviour, but a new approach to structural design affecting all its components: structural engineering, economical consequences, the use of new materials.

There is a very large option spectrum of incorporating the equipment providing supplemental damping into the structure. In the case of skeletal steel structures equipped with viscous dampers, the dampers may be connected to structural elements (columns and beams) as a new “bracing” system Fig. 3.

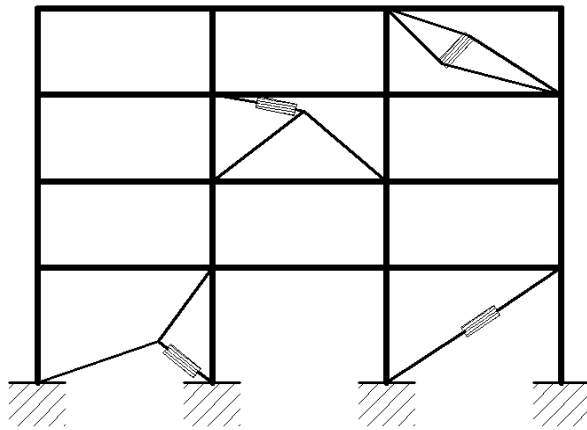


Figure 3. Several possibilities of damper location

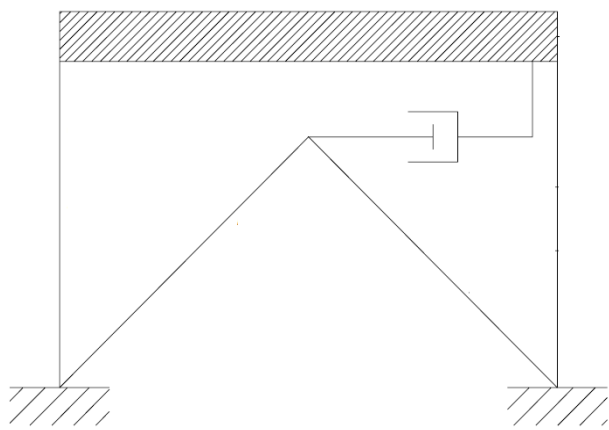


Figure 4. Chevron arrangement of a damper

It has to be emphasized that a damper placed into a non – horizontal position is less effective than a damper placed in a horizontal position coinciding with the seismically horizontal induced motion. A Chevron type arrangement (Fig. 4) of viscous dampers is supposed to use up its entire damping capacity.

As in the case of internal damping, the most important characteristic of the supplemental damping provided by modern equipment is the relation between the damping force and induced displacement (force - displacement relationship). In the case of fluid viscous dampers, the force generated by the damper is velocity dependent.

The present contribution introduces several numerical results associated to seismic behaviour of steel multi-storey frames provided with supplemental damping via viscous nonlinear fluid dampers. Also, a versatile and simple approach to assess the effectiveness of seismic protection is proposed. It consists of envelope curves collecting the peak values of seismically induced kinematical parameters (lateral displacements, lateral accelerations, etc.).



## 2. Analyzed structure

The two frames (a seismically unprotected frame and a seismically protected frame) have the same general and sectional geometry. The 12 stories reference frame Fig. 5 has been designed according to current Romanian design provisions for steel structures. [4] and observe, also, European recommendations [5] for steel skeletal structures. Loading combination includes both, gravitational loads and seismic action. A general level of stressing of approximately 75% of full (bending) capacity of the frame members is reached. The sections of elements, also, observe design provisions with reference to local stability and deformation state.

Regarding the aspect of the global level of damping induced into the structure via viscous dampers, it has been dealt with by using seismic response displacement code spectra for several levels of damping [6]. Induced level of damping has been equated to the damping level of code displacement spectra that yields (produces) the same displacements. Substituting displacements by accelerations into above equating process, the obtained results are close.

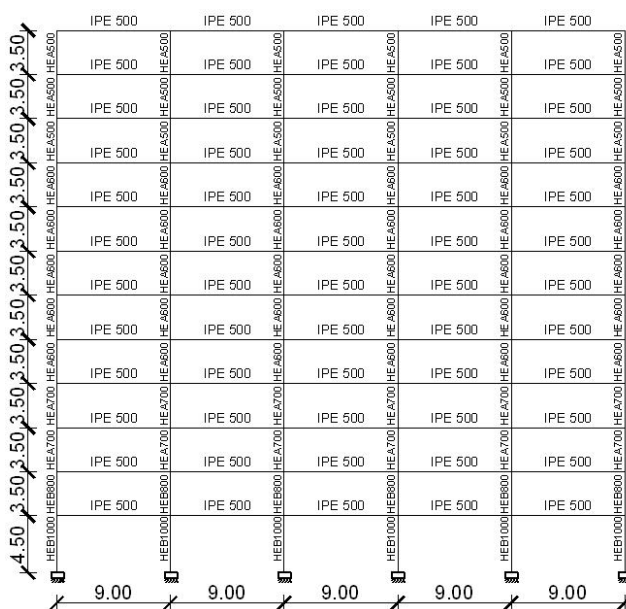


Figure 5. Frame with viscous dampers

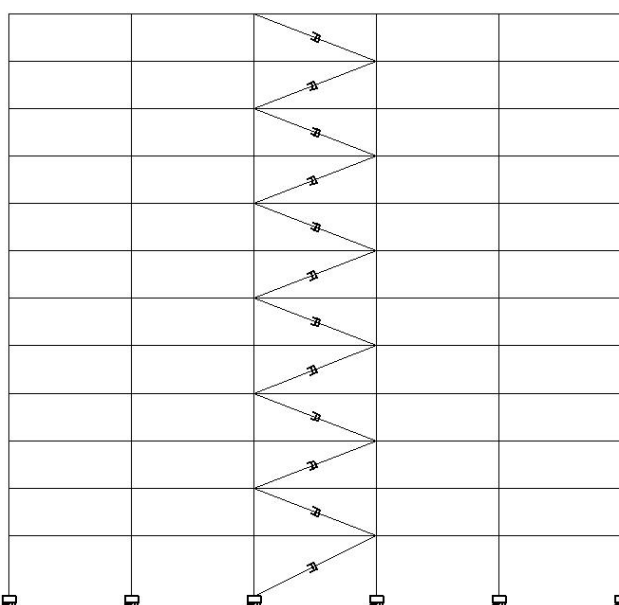


Figure 6. Twelve stories reference frame

A previous study, regarding the influence of dampers location in the frame on protection efficiency, lead to the present placement: in the central bay along the entire height of the structure (Fig. 2) for all frames.

The intensity of sinusoidal accelerogram Fig. 8 has been fixed at 0.2g, corresponding to the maximum value of recorded Vrancea N-S (March 1977, Romania) accelerogram Fig. 7. Vrancea 1977 earthquake. By its destructions and casualties, Vrancea 1977 earthquake is considered a reference earthquake in this country.

The sinusoidal accelerogram Fig. 8 acts, rather as a dynamic action of indefinite duration in time. By this artificial action, no reduction in seismically induced effects is recorded due the diminishing of the (seismic) action itself as it happens in the case of a recorded accelerogram. The sinusoidal accelerogram may be compared to a dynamic force of constant amplitude, therefore the mitigation effects of added damping will exhibit only the amount of mitigation (reduction) not the duration and location of the mitigation interval allowing for a better assessment of added damping. In spite of leading to larger values of seismic response (in displacements, for instance), the sinusoidal “accelerogram” allows a more accurate evaluation of seismic protection effectiveness as it eliminates the mitigation due to the fading away of seismic action itself.

The dampers are of FIP INDUSTRIALE type and are of nonlinear viscous type. The damping force

of each damper is given by  $F_a = c * v^{0.15}$  [7], where  $c$  is an adaptable damping coefficient (its values have been computed for each global damping level) and  $v$  is velocity of motion and it is implicitly computed. The nonlinearity is generated by the exponential factor  $v^{0.15}$ .

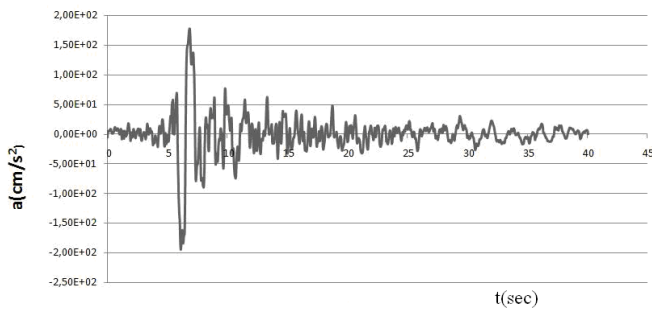


Figure 7. Vrancea 1977 accelerogram

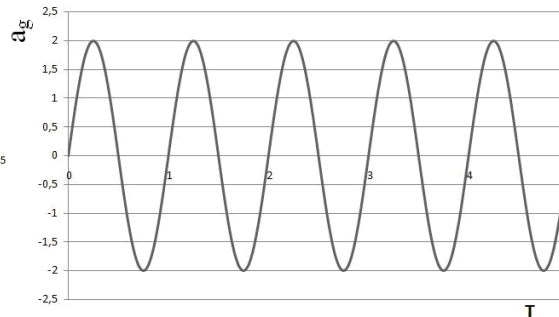


Figure 8. Sinusoidal accelerogram

### 3. Numerical Results

Several sets of numerical results have been obtained. The focus of this contribution is especially on the mitigation interval of lateral top displacements and lateral top accelerations. Seismic protection efficiency is expressed, both graphically and numerically by computed (envelop) seismic protection efficiency curves (SPEC's) that collect the peak values of induced top lateral displacements. In the case of recorded Vrancea 1977 accelerogram, and in the case of sinusoidal type accelerogram, the displacements versus time presented diagrams have been extracted from the entire diagram (associated to the real duration of earthquake, approximately 50 seconds), such that "extracted segments" comprise the mitigation intervals in order to allow for a better assessment of the length and slope of SPEC's. The computed numerical results are presented in a comparative manner: the cases of supplemental damping are presented versus the homologous results related to the reference structure.

The seismic protection efficiency curves (SPEC's) have been computed as envelope curves of peak (positive and negative) values of displacement versus time diagrams. In this way, the steepness of these envelope curves expresses both, the length (in time) of the mitigation interval and the amount of reduction in the peak values of the kinematical parameters (displacements and accelerations, in this case). When the reduction in the displacements values reaches approximately 70% of their maximum values, the steady state motion is considered initiated.

#### 3.1 Variation of displacements

The results referring to the variation of top lateral displacement in the case of 12 stories frame acted upon by Vrancea earthquake Fig. 7 for the reference frame and three levels of supplemental damping are presented together as follows: reference frame and 10% supplemental general level of damping Fig. 9, reference frame and 15% supplemental damping Fig. 10 and reference frame and 20% supplemental damping Fig. 11. The frames acted upon by sinusoidal acceleration exhibit their seismic responses in top lateral displacements: reference frame and 10% supplemental general level of damping Fig. 12, reference frame and 15% supplemental damping Fig. 13 and reference frame and 20% supplemental damping Fig. 14. Expressing the efficiency of seismic protection in number of cycles of seismically induced vibrations proves to be more perceptible.

The proposed SPEC's are presented in the same comparative manner as the displacements: reference frame and 10% supplemental general level of damping Fig. 15, reference frame and 15% supplemental damping Fig. 16 and reference frame and 20% supplemental damping Fig. 17. The frames acted upon by sinusoidal acceleration exhibit their seismic responses in top lateral displacements via SPEC's as follows: reference frame and 10% supplemental general level of

damping Fig. 18, reference frame and 15% supplemental damping Fig. 19 and reference frame and 20% supplemental damping Fig. 20.

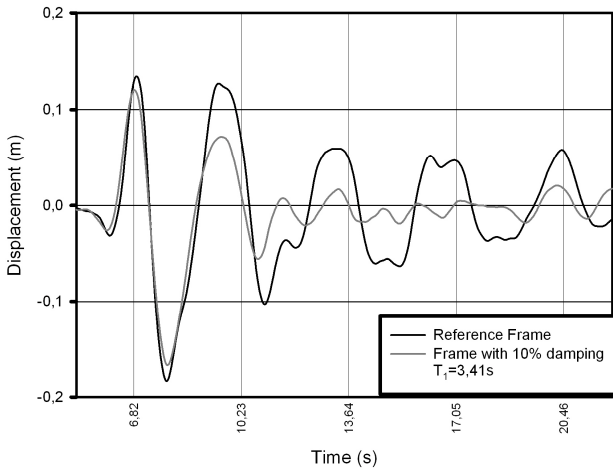


Figure 9. Displacements - reference frame versus frame with 10% damping (Vrancea)

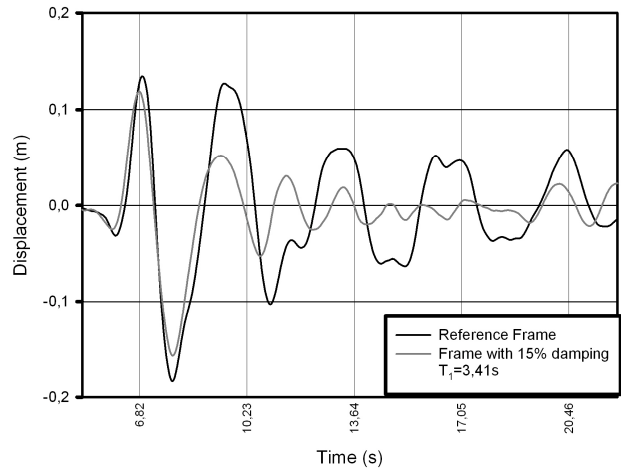


Figure 10. Displacements - reference frame versus frame with 15% damping (Vrancea)

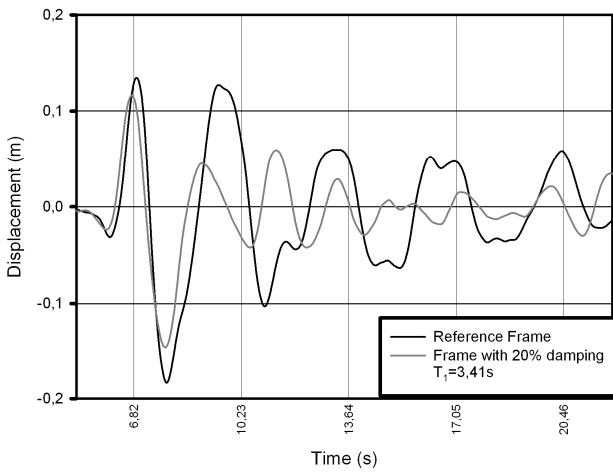


Figure 11. Displacements - reference frame versus frame with 20% damping (Vrancea)

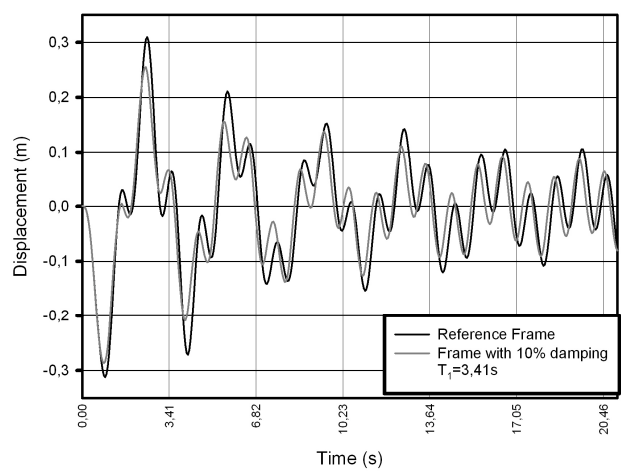


Figure 12. Displacements - reference frame versus frame with 10% damping (Sinusoidal)

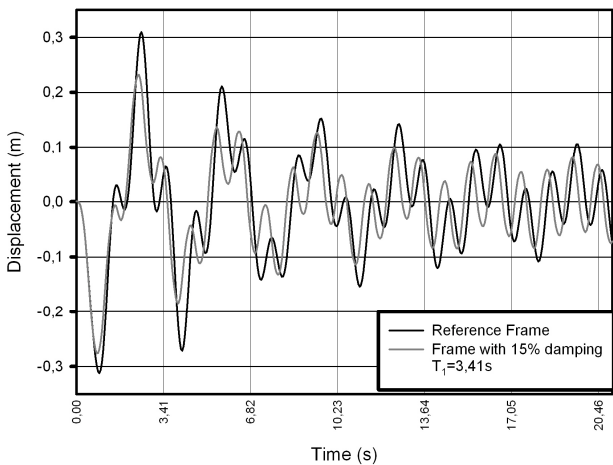


Figure 13. Displacements - reference frame versus frame with 15% damping (Sinusoidal)

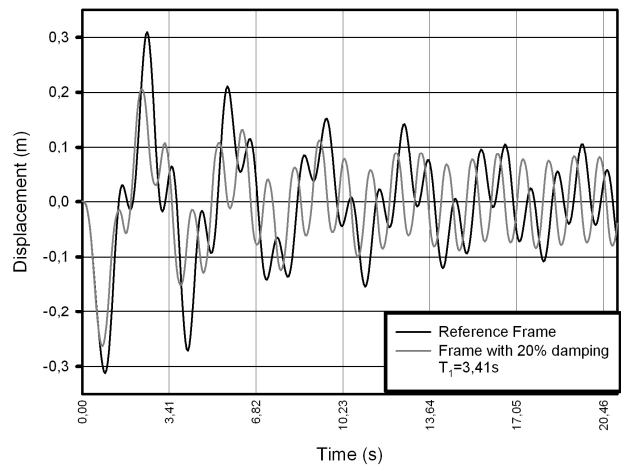


Figure 14. Displacements - reference frame versus frame with 20% damping (Sinusoidal)

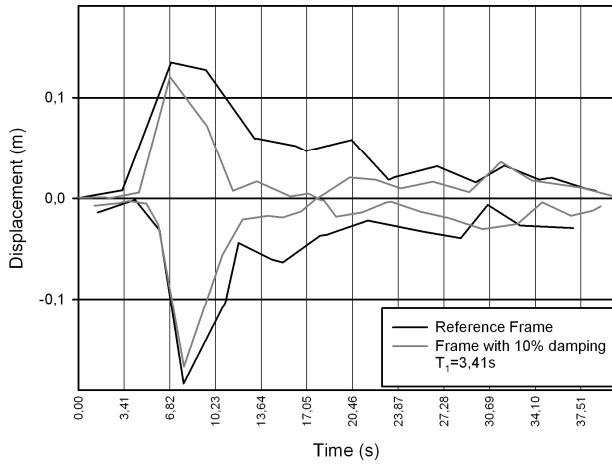


Figure 15. Displacement mitigation curves - reference versus 10% damping frame (Vrancea)

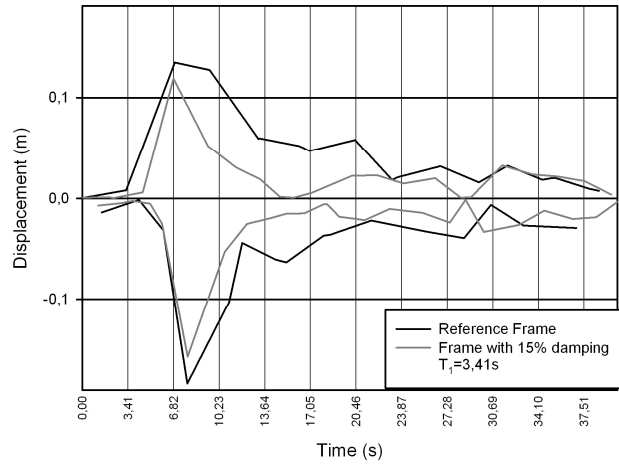


Figure 16. Displacement mitigation curves - reference versus 15% damping frame (Vrancea)

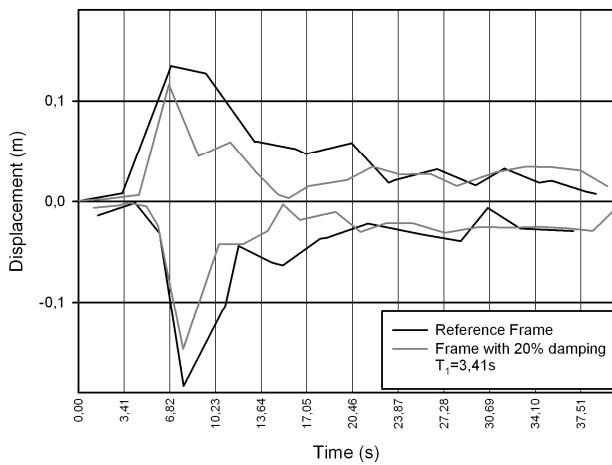


Figure 17. Displacement mitigation curves - reference versus 20% damping frame (Vrancea)

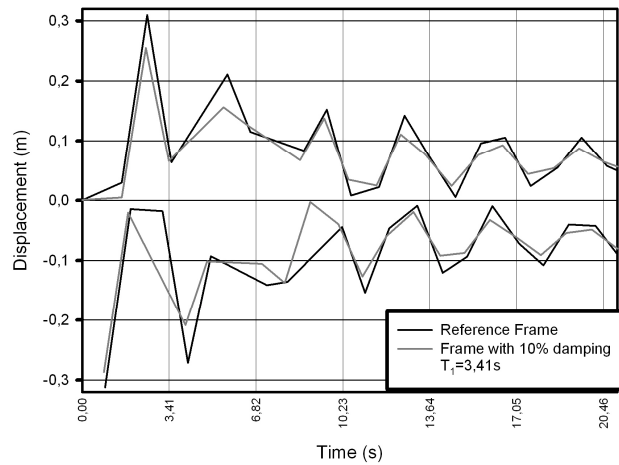


Figure 18. Displacement mitigation curves - reference versus 10% damping frame (sinusoidal)

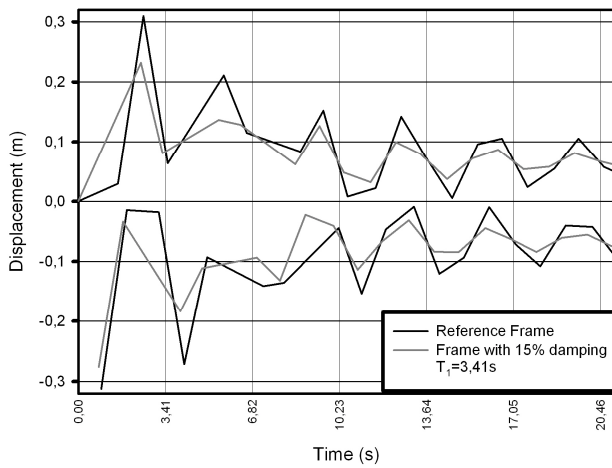


Figure 19. Displacement mitigation curves - reference versus 15% damping frame (sinusoidal)

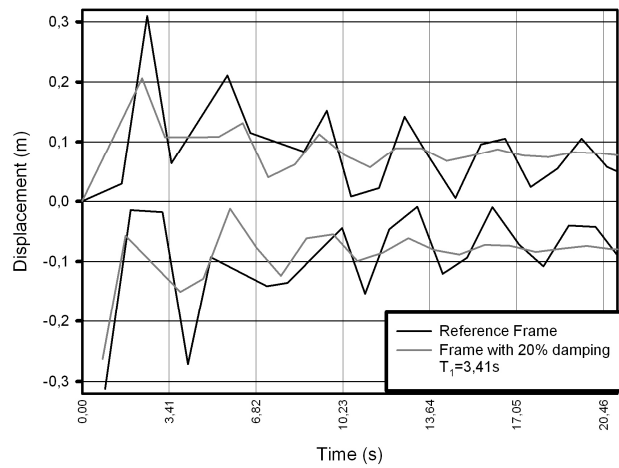


Figure 20. Displacement mitigation curves - reference versus 20% damping frame (sinusoidal)

### 3.2 Variation of accelerations

At this stage, a short statement of “why (induced) accelerations” and “not only (induced) displacements” have been considered for assessing the seismic protection efficiency is necessary. Indeed, what else than lateral displacements of top level may better express induced seismic effects? The displacements (mainly lateral top displacements, in the case of skeletal multi-storey structures) are both, very discernible and very popular as they, actually, perform the seismically induced lateral sway motion of these structures. Present contribution is part of a larger study that includes several seismically induced, both kinematical (displacements, velocities, accelerations, story drifts, ductility coefficients) and static (base shear, statically equivalent seismic forces) parameters. Computed induced accelerations have been selected in the present work, as the reductions in their (peak) values are not spectacular. The (small) reductions in induced accelerations are rather disappointing when compared to the reductions in displacements and, also, when compared to the amount of added damping (up to 4 times the inherent damping amount). Nevertheless, the accelerations are very eloquent when they are regarded in relation with statically equivalent seismic forces. A straightforward and direct proportionality relate accelerations to statically equivalent seismic forces. Therefore, even if displacements are dramatically reduced, only the accelerations “tell the truth” about reduction in seismic effects. As long as the structural seismic design process follows the “statically equivalent seismic forces” pattern, the seismic mitigation has to be assessed in terms of accelerations rather than in terms of displacements. Reduction in (peak values of) induced accelerations is the real reward to the supplemental damping introduced into the structure via viscous dampers.

The small reduction in induced accelerations (as compared to the larger reduction in induced displacements) is, also, a direct consequence of the apparently insignificant change in natural period / circular frequency of vibrating mechanical systems in the presence of viscous damping versus the values of homologous parameters computed in the case of undamped vibrations [8], [9], [10]. Nevertheless, a small amount of reduction in induced accelerations has to be always related to the large values of vibrating masses of multi - storey structures. The results referring to the variation of top lateral acceleration in the case of 12 stories frame acted upon by Vrancea earthquake Fig. 7 for the reference frame and three levels of supplemental damping are presented together as follows: reference frame and 10% supplemental general level of damping Fig. 21, reference frame and 15% supplemental damping Fig. 22 and reference frame and 20% supplemental damping Fig. 23. The frames acted upon by sinusoidal acceleration exhibit their seismic responses in top lateral accelerations: reference frame and 10% supplemental general level of damping Fig. 24, reference and 15% supplemental damping Fig. 25 and reference and 20% supplemental damping Fig. 26.

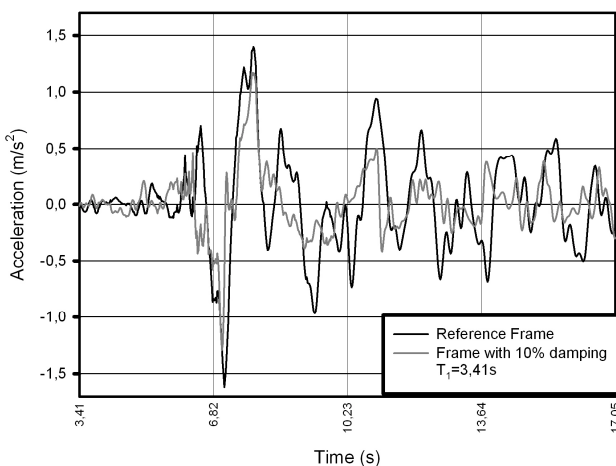


Figure 21. Accelerations - reference frame versus frame with 10% damping (Vrancea)

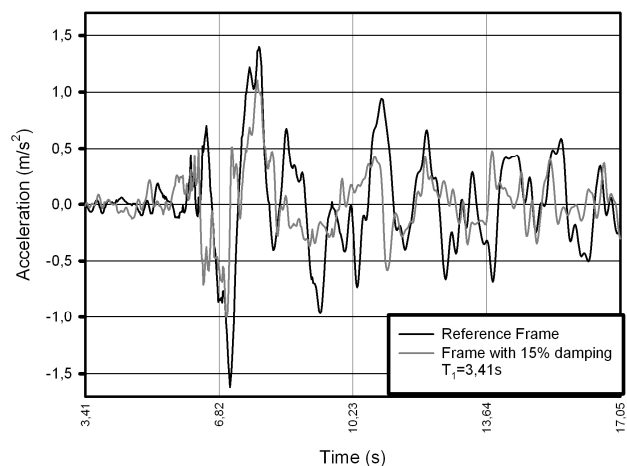


Figure 22. Accelerations - reference frame versus frame with 15% damping (Vrancea)

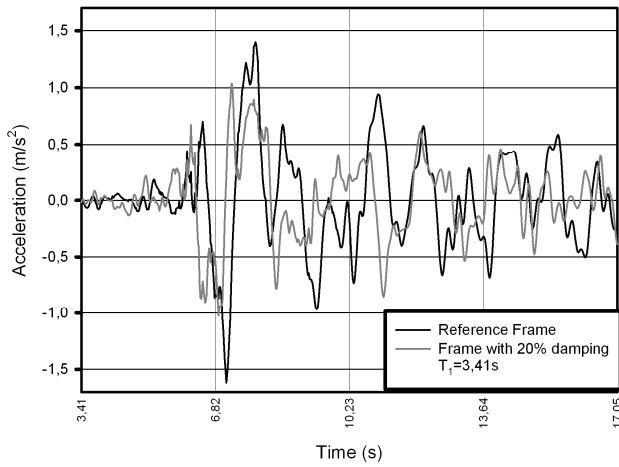


Figure 23. Accelerations - reference frame versus frame with 20% damping (Vrancea)

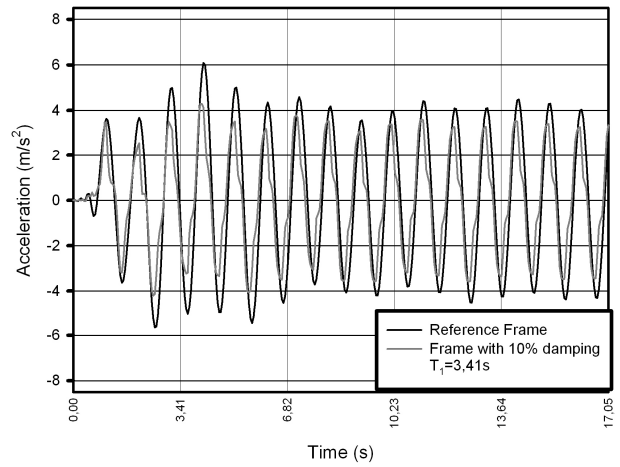


Figure 24. Accelerations - reference frame versus frame with 10% damping (sinusoidal)

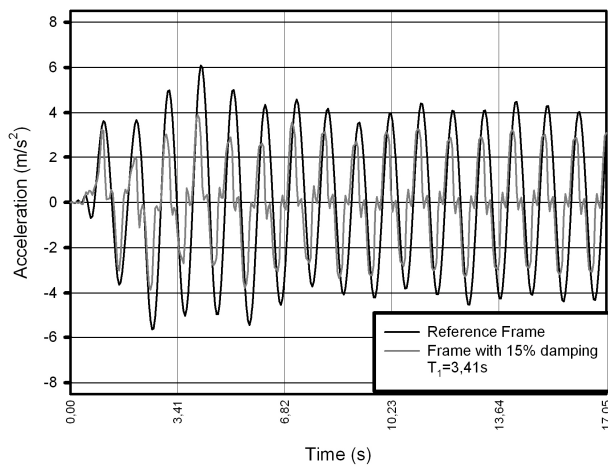


Figure 25. Accelerations - reference frame versus frame with 15% damping (sinusoidal)

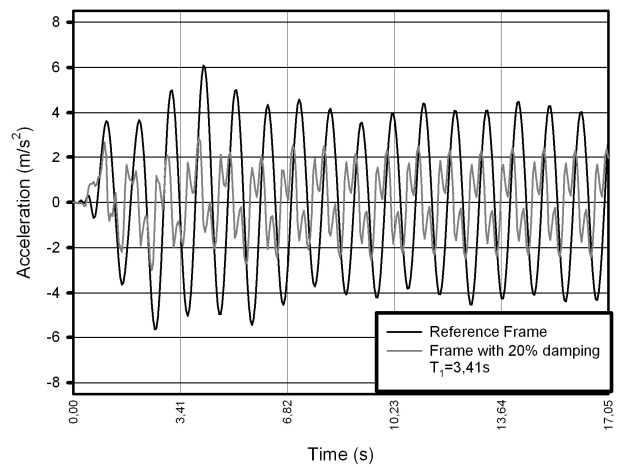


Figure 26. Accelerations - reference frame versus frame with 20% damping (sinusoidal)

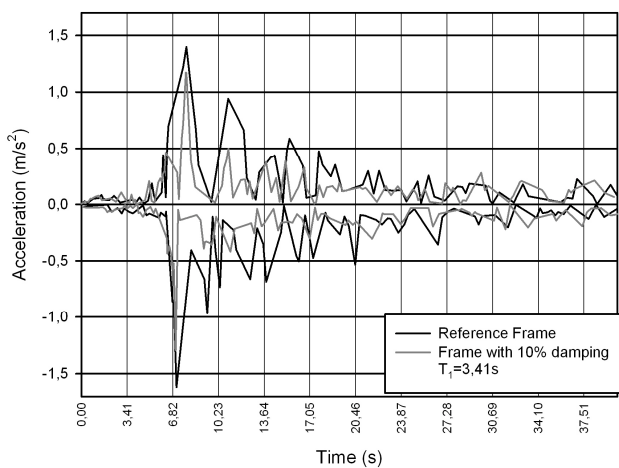


Figure 27. Acceleration mitigation curves - reference versus 10% damping frame (Vrancea)

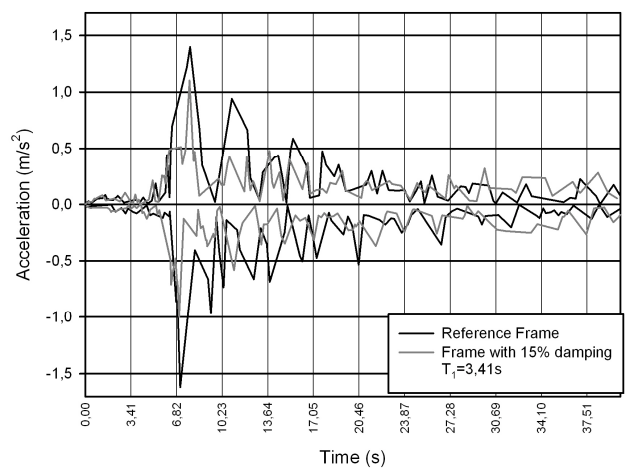


Figure 28. Acceleration mitigation curves - reference versus 15% damping frame (Vrancea)

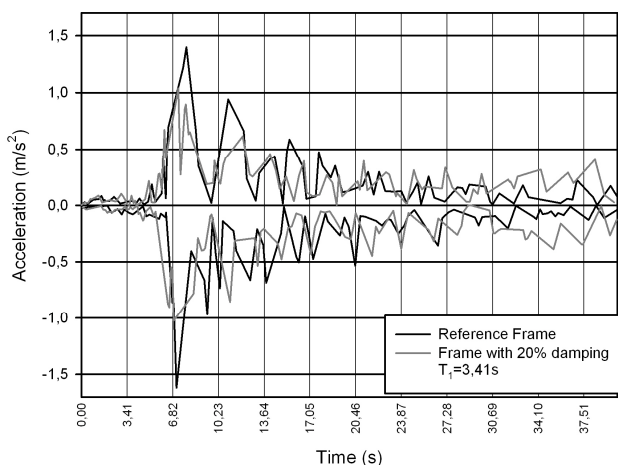


Figure 29. Acceleration mitigation curves - reference versus 20% damping frame (Vrancea)

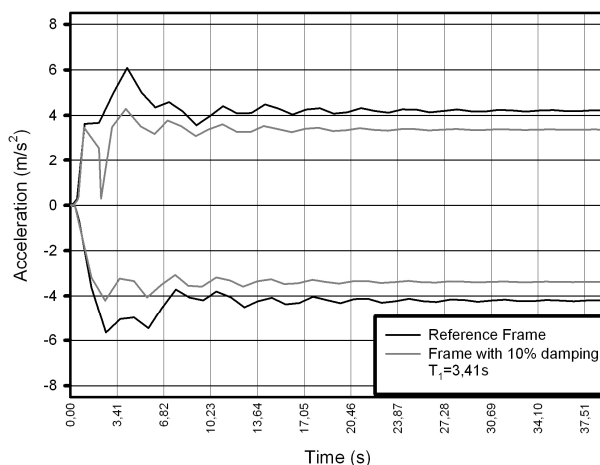


Figure 30. Acceleration mitigation curves - reference versus 10% damping frame (sinusoidal)

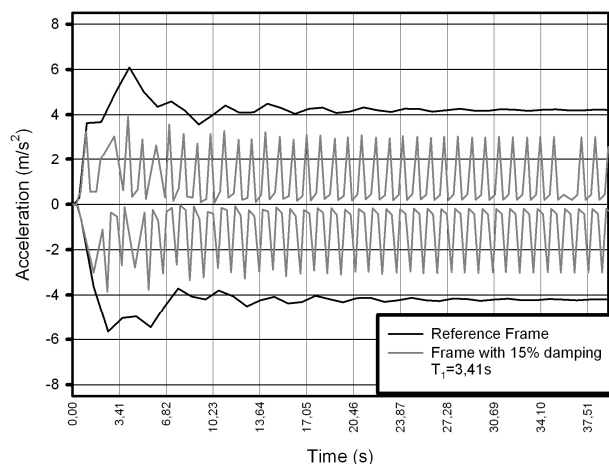


Figure 31. Acceleration mitigation curves - reference versus 15% damping frame (sinusoidal)

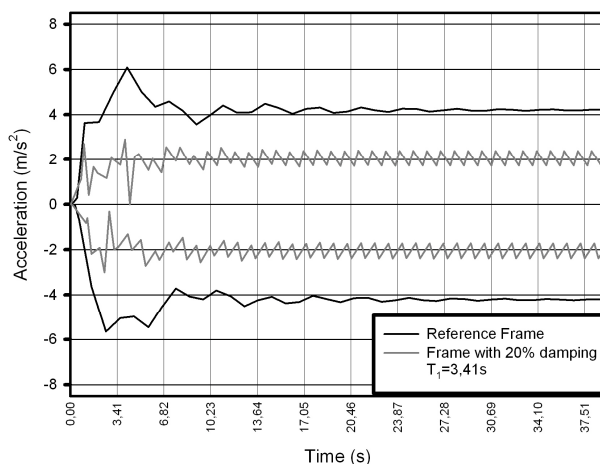


Figure 32. Acceleration mitigation curves - reference versus 20% damping frame (sinusoidal)

Scaling the seismic mitigation interval in terms of (fundamental) natural period of the structure, rather than in time units, allows for expressing the efficiency of seismic protection (level of supplemental damping) in number of cycles of seismically induced vibrations. In this way, the proposed seismic protection efficiency curves (SPEC's) underline – by their slope and length - the duration and rapidity of the seismic mitigation in terms of the natural fundamental periods of vibration of analysed structure.

The proposed SPEC's are presented in the same comparative manner as the accelerations: reference frame and 10% supplemental general level of damping Fig. 27, reference frame and 15% supplemental damping Fig. 28 and reference frame and 20% supplemental damping Fig. 29. The frames acted upon by sinusoidal acceleration exhibit their seismic responses in top lateral displacements via SPEC's as follows: reference frame and 10% supplemental general level of damping Fig. 30, reference frame and 15% supplemental damping Fig. 31 and reference frame and 20% supplemental damping Fig. 32.

Eloquent conclusions may be inferred from the efficiency of added damping versus number of stories. For this, a number of 4 sets of 6 stories, 9 stories, 12 stories and 15 stories, respectively have been analyzed. Indeed, it may be concluded that in the case of high-rise structures, reduction in lateral displacements decrease versus the case of structures with less that 12 to 15 stories. This tendency appears to preserve no matter the global level of damping.

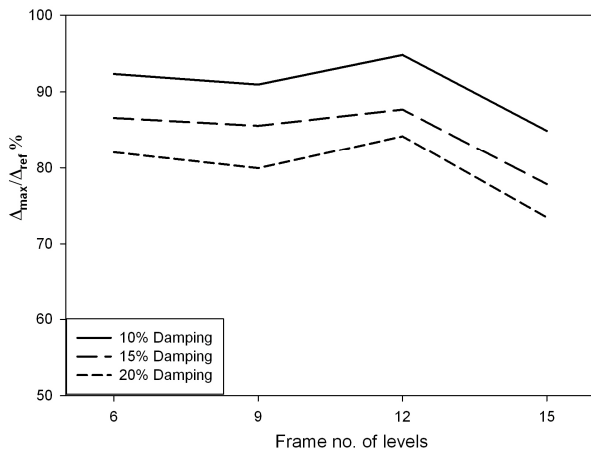


Figure 33. Damping reduction curves negative values (Vrancea)

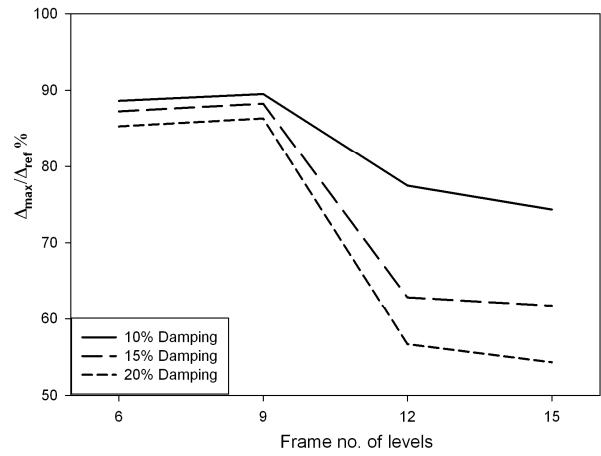


Figure 34. Damping reduction curves positive values (Vrancea)

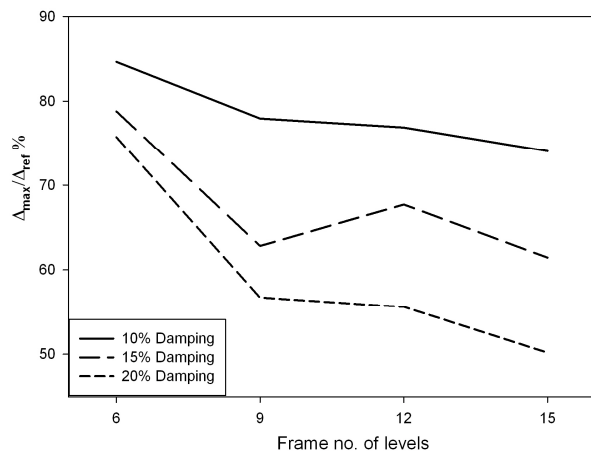


Figure 35. Damping reduction curves negative values (sinusoidal)

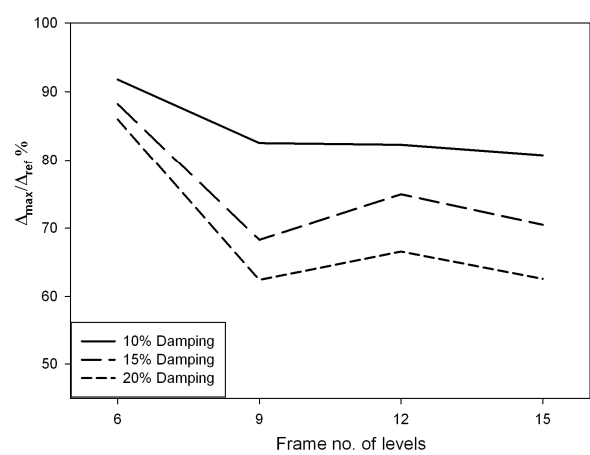


Figure 36. Damping reduction curves positive values (sinusoidal)

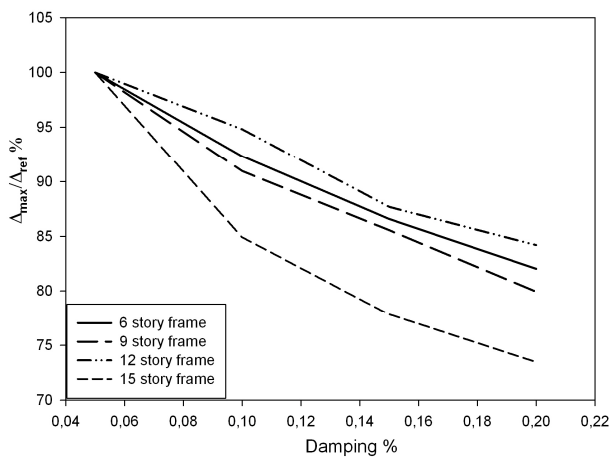


Figure 37. Damping reduction curves negative values (Vrancea)

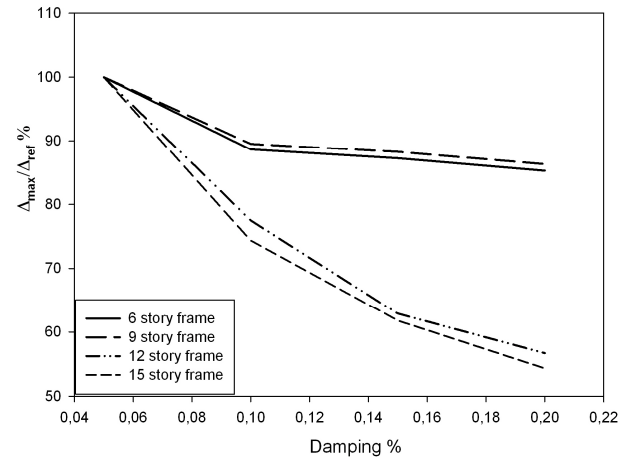


Figure 38. Damping reduction curves positive values (Vrancea)



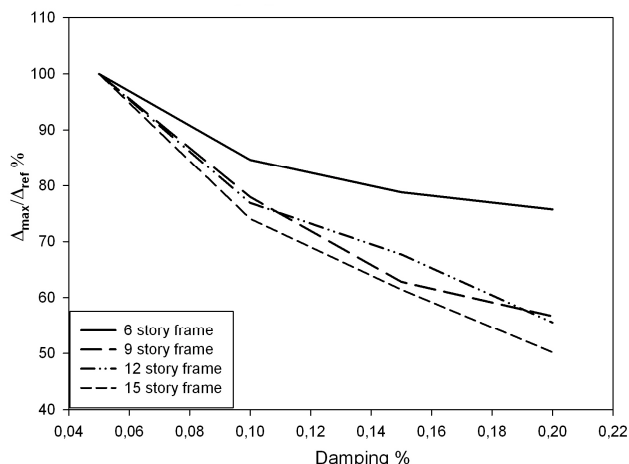


Figure 39. Damping reduction curves negative values (sinusoidal)

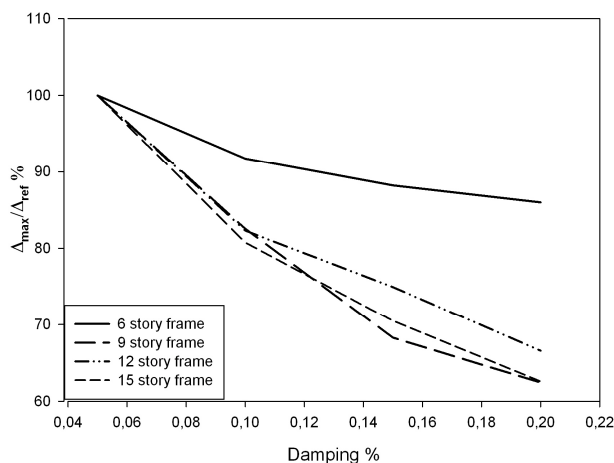


Figure 40. Damping reduction curves positive values (sinusoidal)

Due to the total asymmetry of seismic action, the reduction in lateral displacements has been analyzed in terms of their both, positive and negative values of top lateral displacements. Associated numerical results are presented in Fig. 33 to Fig. 40.

## 4. Conclusions

Literature associated to seismic devices aiming at mitigating seismic structural response [11], [12], [13], [14] focuses on the efficiency of proposed techniques with reference to both, induced displacements and accelerations.

The final inferred conclusions refer to the efficiency of the seismic protection via viscous dampers and, mainly, to the possibility of assessing this efficiency via proposed seismic mitigation envelope curve (SPEC). An inherent [8] damping level of 5% is considered as a standard unit of damping level. Therefore, a damping level of 10% is equivalent with a two unit level, a damping level of 15%, is referred to, as a 3 unit level, while a 20% (highest in this study) damping level will be a 4 unit damping level.

### 4.1 Remarks regarding SPEC's associated to displacements

Using such a scaled damping level, it may be concluded that a doubling in the damping level (from standard 5% to 2 unit level of 10%) results in a reduction in top lateral displacements of 10 %, while a threefold increase induces a decrease of 14 % in lateral top displacements. The (20%) level of damping is equivalent to a reduction of 16% (in the case of Vrancea accelerogram). Similar reductions in lateral top displacements (of 21%, 30% and 50%), respectively are associated to the case of sinusoidal excitation. The proposed mitigation envelope curves (SPEC's) are eloquent in terms of the length of the interval expressed in the natural fundamental period. In the case of reference 12 story frame, the length of the mitigation interval is reduced from  $7T_1$  to  $3T_1$  in the case of 10% added damping and Vrancea accelerogram, Fig. 15. Similarly, SPEC's associated to 15% and 20% levels of added damping are, also, computed Fig. 16, Fig. 17. Associated results for the sinusoidal type excitations are presented in the same manner: in the case of 10% supplemental damping Fig. 18, in the case of 15% added damping Fig. 19 and in the case of 20%, respectively Fig. 20.

#### 4.2 Remarks regarding SPEC's associated to accelerations

Regarding the efficiency of passive protection via viscous damper – expressed in induced accelerations of lateral motion of top level - it may be concluded that the damping level do not affect the values of induced accelerations. The accelerations are, in fact, related to the statically equivalent seismic forces and the seismic forces (seismic base shear) do not depend on, not do they change in any way with the amount of damping the structure is provided with.

What does, nevertheless, the damping level change in induced accelerations? It shortens the time interval of transitory (seismically induced) vibratory motion. This effect is of real importance in seismically induced structural vibrations. Multi-storey steel structures may undertake quite large lateral displacements without dramatic effect in its stress state, while an alternative (vibratory) motion associated with even smaller lateral displacements will significantly affect this state.

The mitigation envelope curves (acc. SPEC's) are, also, very suggestive in terms of the length of the interval expressed in fundamental period of structural vibrations. In the case of reference frame, the length of the mitigation interval is reduced from  $4.5T_1$  to  $2.5T_1$  in the case of 10% added damping and Vrancea accelerogram Fig. 21. Similarly, the mitigation curves associated to the other levels (15% and 20%) of added damping and for the case of sinusoidal excitation are presented: a reduction to  $2T_1$  in the case of 15% damping level Fig. 22, a reduction to  $1.5T_1$  Fig. 23 for 20% damping level versus reference 5%. In the case of sinusoidal input accelerogram, reduction in the length of mitigation interval (from  $5T_1$  – in the case of reference frame) is down to  $4T_1$ , for 10% damping level Fig. 24, down to  $3.5T_1$ , for 15% damping level Fig. 25 and down to  $2.5T_1$ , in the case of 20% damping level Fig. 26.

#### 4.3 General conclusions

In what regards proposed mitigation enveloped curves, they prove to be a direct tool of assessing the efficiency of supplemental damping. Their expressing in terms of fundamental period of the structure allows a rapid and synthetic evaluation of supplemental damping efficiency. As it has been pointed out, if the structure vibrates at peak values of its kinematical parameters, incipient or even full shakedown type behaviour is induced. A vibration “stage” along a time interval up to two fundamental periods ( $2T_1$ ) will save the structure of shakedown behaviour and, consequently, of remanent deformations. Also, the decrease in the values of associated parameter (top lateral displacements in this study) offers immediate asses of the measure of reductions in these values.

It has to be emphasized that the obtained numerical results referring to reduction in the values of seismic response components, are, only, partially due to seismic protection, since a part of induced kinetic energy is dissipated via remanent deformations.

Finally, it may be emphasized that the versatility of mitigation envelope curves and their synthetic feature opens the possibility of incorporating them in the set of performance criteria of seismically protected (via viscous dampers) steel structures.

### 5. References

- [1] Constantinou, M.C. and Symans, M.D., Experimental study of seismic response of buildings with supplemental fluid dampers. Structural design of tall buildings. Vol II,93-132, 1993
- [2] Chopra, A.K., Dynamics of Structures. Theory and Applications to Earthquake Engineering, Prentice Hall International, Inc., 1995
- [3] Soong, T.T. and Dargush G.F., Passive Energy Dissipation Systems in Structural Engineering, Wiley, Chichester – England, 1997
- [4] P100/1 – 2006
- [5] EUROCODE 8 – EN 1998
- [6] Constantinou, M.C., Fluid dampers for applications of energy dissipation and seismic isolation, 2007
- [7] Baldo, P., Tomaselli, F. and Pimenta, F., Loureiro viaduct seismic protection: Testing of non-linear

viscous dampers. SEISMICA 2004 Congresso Nacional de Sismologia e Engenharia Sismica, 2004, pp. 679-690.

- [8] de Silva, C.W., *Vibration Damping, Control, and Design*, CRC Press, 2007
- [9] Beards, C. F., *Engineering vibration analysis with application to control systems*, Edward Arnold, London – Great Britain, 1995
- [10] Cheng, F. Y., Jiang, H., Lou, K., *Smart structures: innovative systems for seismic response control*, CRC Press, 2008
- [11] Nastac, S., Leopa, A., *New Structural Configurations for Vibroisolation Devices with High Isolation Performances*, WSEAS TRANSACTIONS on APPLIED and THEORETICAL MECHANICS Issue 5, Volume 3, May 2008
- [12] Bratosin, D., *Nonlinear Effects in Seismic Base Isolations*, WSEAS TRANSACTIONS on APPLIED and THEORETICAL MECHANICS Issue 4, Volume 3, April 2008
- [13] Bajpai, V.K, Garg, T.K., Gupta, M.K., *Vibration-dampers for smoke stacks*, 3rd WSEAS International Conference on Applied and Theoretical Mechanics, Spain, December 14-16, 2007, pp.124-130.
- [14] Ashwani Jain and D. K. Soni, *Foundation Vibration Isolation Methods*, Proceedings of the 3rd WSEAS International Conference on APPLIED and THEORETICAL MECHANICS, Spain, December 14-16, 2007, p.163-167.

## Local and global stability of single storey frames made of welded plate elements with tapered web

Mircea I. Cristutiu<sup>\*1</sup>, Luis D. Nunes<sup>2</sup>

<sup>1</sup> Politehnica University of Timisoara, Faculty of Architecture. 2 T. Lalescu Str., 300223, Timisoara, Romania

<sup>2</sup> Politehnica University of Timisoara, Faculty of Civil Engineering. 1 I. Curea Str., 300224, Timisoara, Romania

Received 29 May 2011; Accepted 15 August 2011

### Abstract

*Modern industrial halls and not only, possess a steel main frame usually made of welded plate elements with tapered web classified as class 3 and 4. In case of class 3 sections, when they are restrained against lateral or/and torsional buckling, the interaction between sectional plastic buckling and overall elastic buckling of the members in compression and/or in bending is possible. When class 4 sections are used, which generally is the case of the rafter in the maximum height of the tapered web, the sectional buckling (e.g. local buckling of walls or distortion) may occur in elastic domain. If no lateral restrains, or when they are not enough effective, the lateral torsional mode characterizes the global behavior of frame members and, again, interaction with sectional buckling modes may occur. The paper summarises a systematic numerical study performed by authors on a relevant series of such type of frames. A series of frames of different spans and heights have been analyzed. The frames were designed to withstand the vertical loads and satisfy the ULS and SLS criteria. Also different types of lateral restraints had been considered within the analysis. For the purpose of the work, nonlinear elastic plastic analyses and eigen buckling analyses with FEM were performed.*

### Rezumat

*Halele industriale moderne si nu numai au structura de rezistență realizată din cadre metalice, având elemente zvelte cu secțiune variabilă de clasă 3 și 4. În cazul elementelor cu secțiuni de clasă 3, prevăzute cu blocaje laterale împotriva flambajului si/sau răsucirii , și supuse la compresiune și/sau încovoiere, este posibilă apariția interacțiunii între flambajul plastic local și flambajul elastic global. În cazul în care se utilizează elemente cu secțiuni de clasă 4, flambajul local se poate dezvolta in domeniul elastic, prin voalarea inimii. Dacă nu sunt prevăzute blocaje laterale suficiente sau acestea sunt ineficiente, modurile de flambaj pot fi caracterizate prin flambaj local, flambaj global, sau o interacțiune între cele două moduri. Lucrarea prezintă un studiu parametric realizat pe un număr de cadre, având tipo-dimensiuni utilizate in mod curent în practică. Cadrele au fost proiectate la incarcari gravitaționale pentru a satisface condițiile specifice pentru SLU si SLEN. Au fost considerate, diferite tipuri de blocaje laterale. S-au realizat analize ne-liniare elasto-plastice si analize elastice de flambaj cu MEF, pentru studia comportarea cadrelor sub efectul încărcărilor gravitaționale.*

**Keywords:** pitched roof portal frames, tapered elements, stability, FEM, lateral restraints, initial imperfections

---

\* Corresponding author: Mircea I. Cristutiu Tel./ Fax.:+40.723.281.859/+40.361.814.159  
E-mail address: mircea.cristutiu@arh.upt.ro

## 1. Introduction

Structural stability is the fundamental security criterion for buildings both during their functioning period and construction life. The present draft of SR-EN 1993-1[1] (EN 1993-1[2]) which was implemented in Romania at the beginning of 2010, contains numerical procedures for buckling verification of component elements from steel structures, which differs from the traditional simplified procedures. These last ones were only covering regular geometrical shapes, simple load cases and classical fixing (rigid or pinned). Advanced numerical computer aided analyses can be performed nowadays which allow the investigation of complex structures by using these new procedures. This allows one to use a greater number of factors that affect the structure in what concerns their stability: geometrical imperfections, material imperfections, production residual stresses, element lateral restraining, and real element boundary conditions.

The design, execution and erection of steel structures must take place under certain limit constraints. If in the design process, one must ensure strength, stability and rigidity to the structure, in the manufacturing and erection process certain admissible tolerance limits must be accounted for. EN 1090-2[3] is the European standard that establishes the values of admissible limit tolerances for the manufacturing and erection of steel structures. The last version allows for a maximum linearity deviation of manufactured/erected elements a value of  $L/750$  ( $L$ =length of the element). This is less strict than previous requirements ( $L/1000$ ), which were the basis for the present European buckling curves (EN 1993-1). Also the Romania norm [1] contains provisions for several initial imperfections (vertical deviation and initial arc imperfections), which take values function of the considered buckling curve ( $a_0, a, b, c, d$ ) and buckling mode (minimum or maximum axis). If the values for manufacturing/erection allowable tolerances are higher than those of the above mentioned imperfections, further investigations are required in order to establish if the partial safety factor ( $\gamma_{M0} = 1,00$ ), given in SR-EN 1993-1-1 is still enough.

Steel structural elements with variable cross section, made of welded plates, are largely used in construction industry for both beams and columns in accordance with the stress and stiffness demand in the structure. Due to nonrectangular shape of the element, thin web section may be obtained at the maximum cross section height. Usually class 3 to class 4 web results for the case of double T welded cross section. The buckling strength of these structures is directly influenced by the lateral restraining, end support and initial imperfections [1]. If no lateral restrains, or when they are not effective enough, global behaviour of frame members is characterized by the lateral torsional mode and interaction with sectional buckling modes may occur.

The main objective of the paper is to analyze the sensitivity of single storey steel structures made of variable cross section to different type of lateral restraints and supplementary to manufacturing and erection imperfections. The previous studies [4,5,6,7] made by several authors all around the world, highlighted the importance of taking into account different initial imperfections, even in case of gravitational loads and horizontal loads. The considered imperfections might be described as: column vertical deviation (in or out-of-plan), initial arc imperfections, cross sectional imperfections. Finally the following problem arises: what is more important when dealing with stability problems the type or value of imperfection?

## 2. Imperfection and tolerances for steel structures

Whether there are imperfections generated by the fabrication or the assembling process, we can say for certain that "All the structures are imperfect". Although it is an ideal of all engineers that manufacturing and assembling of steel structures shall be done without any imperfections, mistakes of any type and nature might appear. But for now this remains an aspiration of all involved in this activity, a way of raising the quality and of ensuring the serviceability of constructions, which we all must supervise.

According to [1,2] appropriate allowances should be incorporated in the structural analysis to cover the effects of imperfections, including residual stresses and geometrical imperfections such as lack of verticality, lack of straightness, lack of flatness, lack of fit and any minor eccentricities present in joints of the unloaded structure. The assumed shape of global imperfections and local imperfections may be derived from the elastic buckling mode of a structure in the plane of buckling considered. Both in and out of plane buckling including torsional buckling with symmetric and asymmetric buckling shapes should be taken into account in the most unfavorable direction and form.

The structural imperfections can be divided in two large categories, imperfections generated by the fabrication process, which include the material imperfections, the geometrical imperfections at the level of the structural elements and subassemblies and imperfections generated by the assembling process namely the global imperfections.

For reducing to minimum the structural imperfections in fabrication and assembling process the level of them is limited by quality standards and norms and in design the effect of imperfections is considered through safety coefficients and special design procedures. For frames sensitive to buckling in a sway mode the effect of imperfections should be allowed for in frame analysis by means of an equivalent imperfection in the form of an initial sway imperfection and individual bow imperfections of members [1,2].

Also the materials must always be accompanied by a quality certificate (testing of building materials) and the execution must be according to the project and the present norms.

In Fig. 1 are illustrated two types of imperfections recorded on site: a) erection imperfections (out of plane rafter displacement); b) manufacturing imperfection (local buckling of the web).



Figure 1. Imperfections recorded on site: a) erection imperfection (er); b) manufacturing imperfection (man).

### 3. Numerical analysis

#### 3.1 Analysis methods and analyzed frames

A number of frames widely used for the execution of single story buildings were analysed, they are of different spans and heights (see Fig. 2). The frames were designed to verify the ULS and SLS criteria under the gravitational loads. They have pinned column base, tapered columns, tapered

rafters and a pitch roof angle of  $8^{\circ}$ . The length of the rafter taper is 15% from the span in all the cases. The main dimensions of characteristic sections of frames are presented in Table 1. The chosen dimensions are quite common in practical applications.

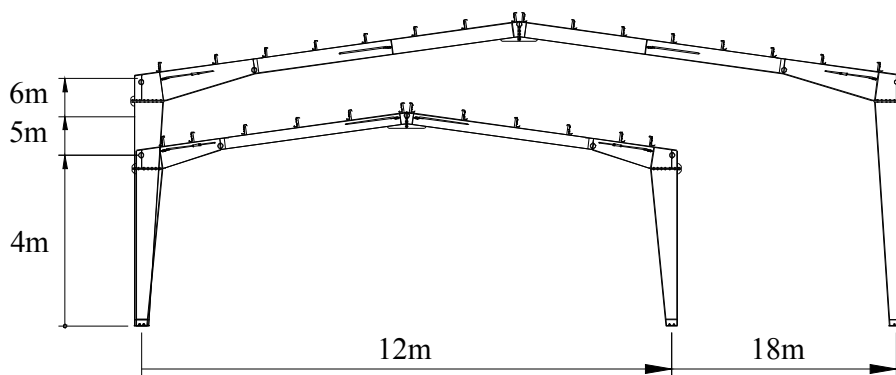


Figure 2. Geometry of the analyzed frames

Table 1. Main dimensions of the analyzed frame

Code	Frame type	H [m]	L [m]	Dimensions $h*b*t_r*t_w$ [mm]		
				tapered column	tapered rafter	rafter
4x12	var4x12pin	4	12	(250...600)*200*10*8	(260...500)*150*10*8	260*150*8*6
5x12	var5x12pin	5	12	(250...600)*220*10*8	(260...500)*150*10*8	260*150*8*6
6x12	var6x12pin	6	12	(250...600)*240*10*8	(260...500)*150*10*8	260*150*8*6
4x18	var4x18pin	4	18	(350...700)*250*12*10	(360...700)*200*12*10	360*200*10*8
5x18	var5x18pin	5	18	(350...700)*250*14*10	(360...700)*200*12*10	360*200*10*8
6x18	var6x18pin	6	18	(350...700)*260*14*10	(360...700)*200*12*10	360*200*10*8

Both eigen-buckling (LEA) and nonlinear elastic-plastic considering geometrical nonlinearities (GMNIA) analyses had been applied [8,9]. The computation was performed with Abaqus 6.4 FEM program using Shell elements enabling for large plastic deformation (see Fig. 3). Joints were modeled using contact area-to-area elements in order to simulate the real behavior of the connections in the global analysis. The material behavior was introduced by a bilinear elastic-perfectly plastic model (see Fig. 4), while S355 yield strength was considered in the analysis.

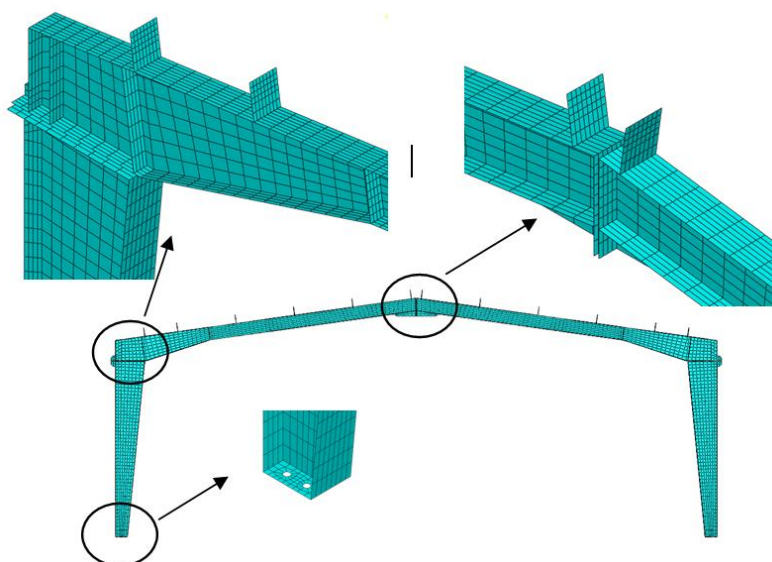


Figure 3. FEM modeling of the analyzed frames

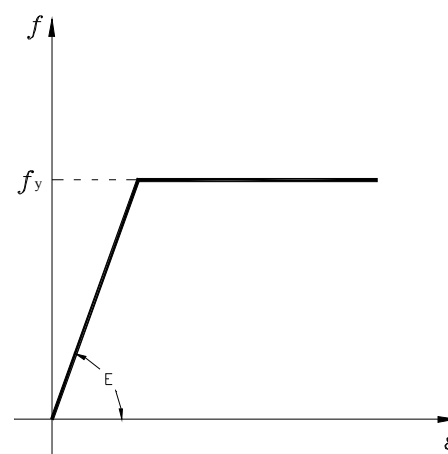


Figure 4. Elastic-perfectly plastic material behavior

Lateral restrains provided in practice by purlins were considered. Moreover, in all these cases, it was simulated the restraining effect induced by longitudinal beams located at eaves and ridges. The lateral restrains are of 4 different types, as shown in Fig. 5 [10]. Types 2 and 3 simulate the purlin/sheeting effect, when the purlin can be connected with one or two bolts, respectively. Type 4 represents type 2 with an additional fly brace. Type 1, the reference case, actually means no lateral restrains introduced by purlins. To simplify the computational model, in the analysis the lateral restrains had been considered axially rigid.

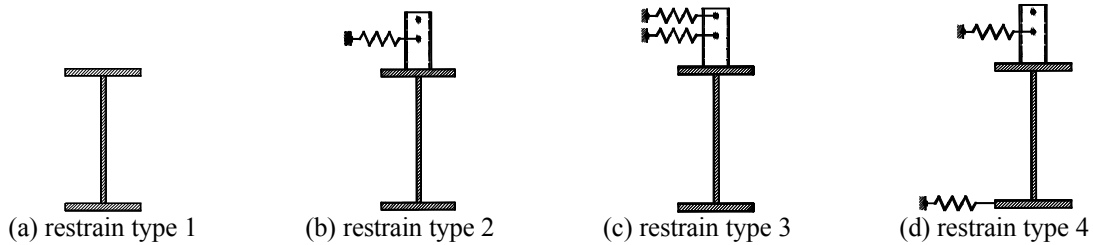


Figure 5. Types of lateral restrains

All the analyzed frames are made of elements classified as class 3 in the tapered web. Rafter-to-column and rafter-to-rafter connections are bolted with extended and plates toward exterior as shown in Fig. 2. Vertical loads from permanent and snow actions were introduced at the purlin location (e.g 1.2 m along the rafter). Both erection and manufacturing imperfections [1] were considered separately in analyses. The applied imperfections are presented in Fig 6. Using shell elements, the imperfections are slightly different from those applied on bar elements, where perfect bending or perfect inclination might be applied. Herein twisting of the element was also recorded, that represents the real shape of imperfect elements.

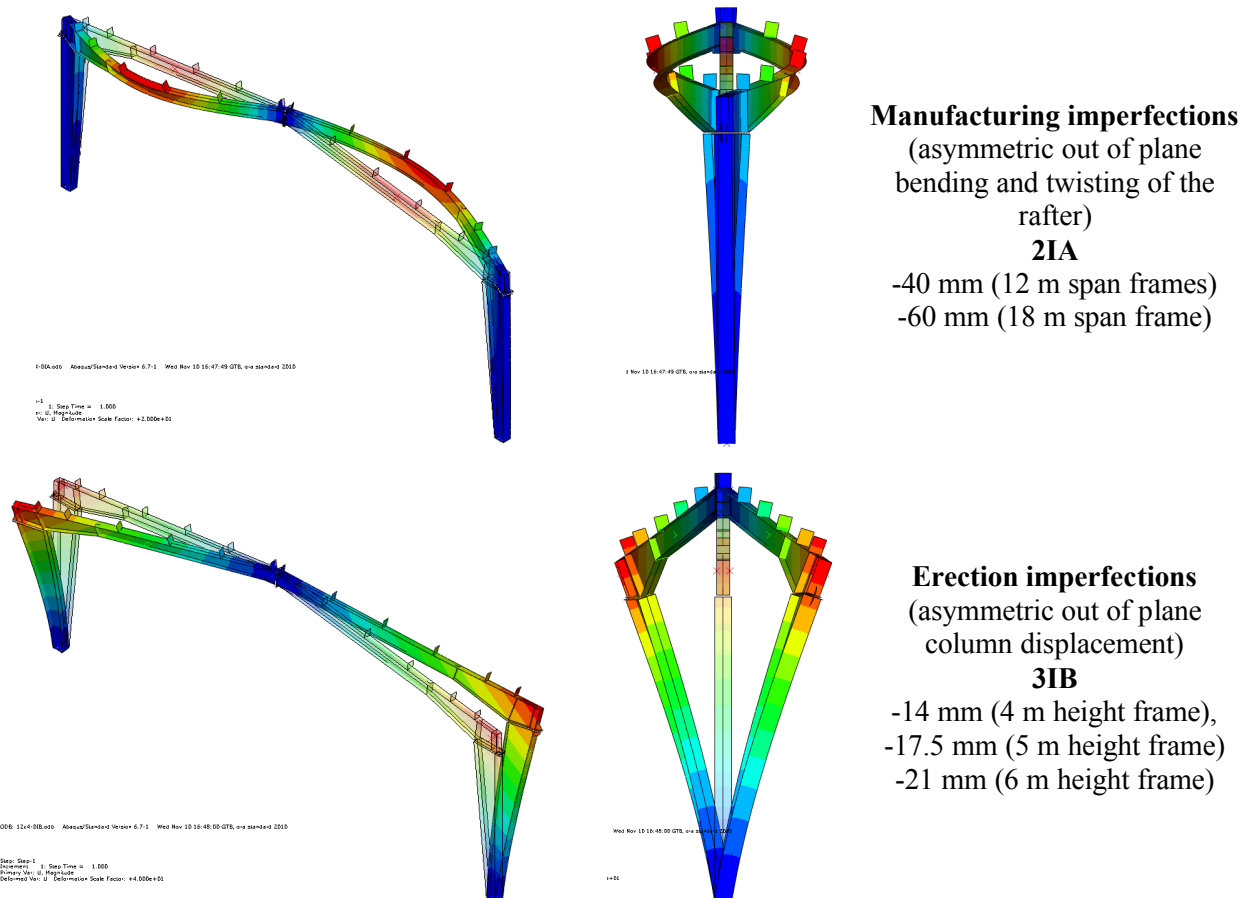


Figure 6. Imperfections considered in the FEM analyses



### 3.2. Results of the numerical analysis

Nonlinear 3D elastic-plastic analysis and 3D eigen-value analysis were performed to identify the elastic plastic-failure and critical modes of frames, respectively (Fig. 8 and Fig. 7). Correspondingly, critical and ultimate load multipliers were recorded and the results are presented, for all analyzed frames and out of plane restraining types (Fig. 9).



Figure 7. Buckling shapes of LEA analysis.

Analyzing these results one observes that lateral restraints influence the buckling shape and failure of the elements. In all of the cases both elastic and/or plastic buckling takes place out of plane. This might lead to the conclusion that out of plane instability is more likely to occur, for these types of frames, than in plane stability. When the structure is more effectively laterally restrained (case 3 and 4 restraints of Fig.3), local buckling may develop prior to lateral-torsional mode. The critical buckling load, in cases of restraints types 3 and 4, is higher than the ultimate load obtained from elastic-plastic analysis,  $l_u$  (see Fig. 7). We can say in this case that the structure may fail due to local plastic sectional buckling instead of elastic overall buckling. For case of less effective lateral restraints, type 1 and 2, elastic out of plane buckling may develop prior than plastic sectional buckling.

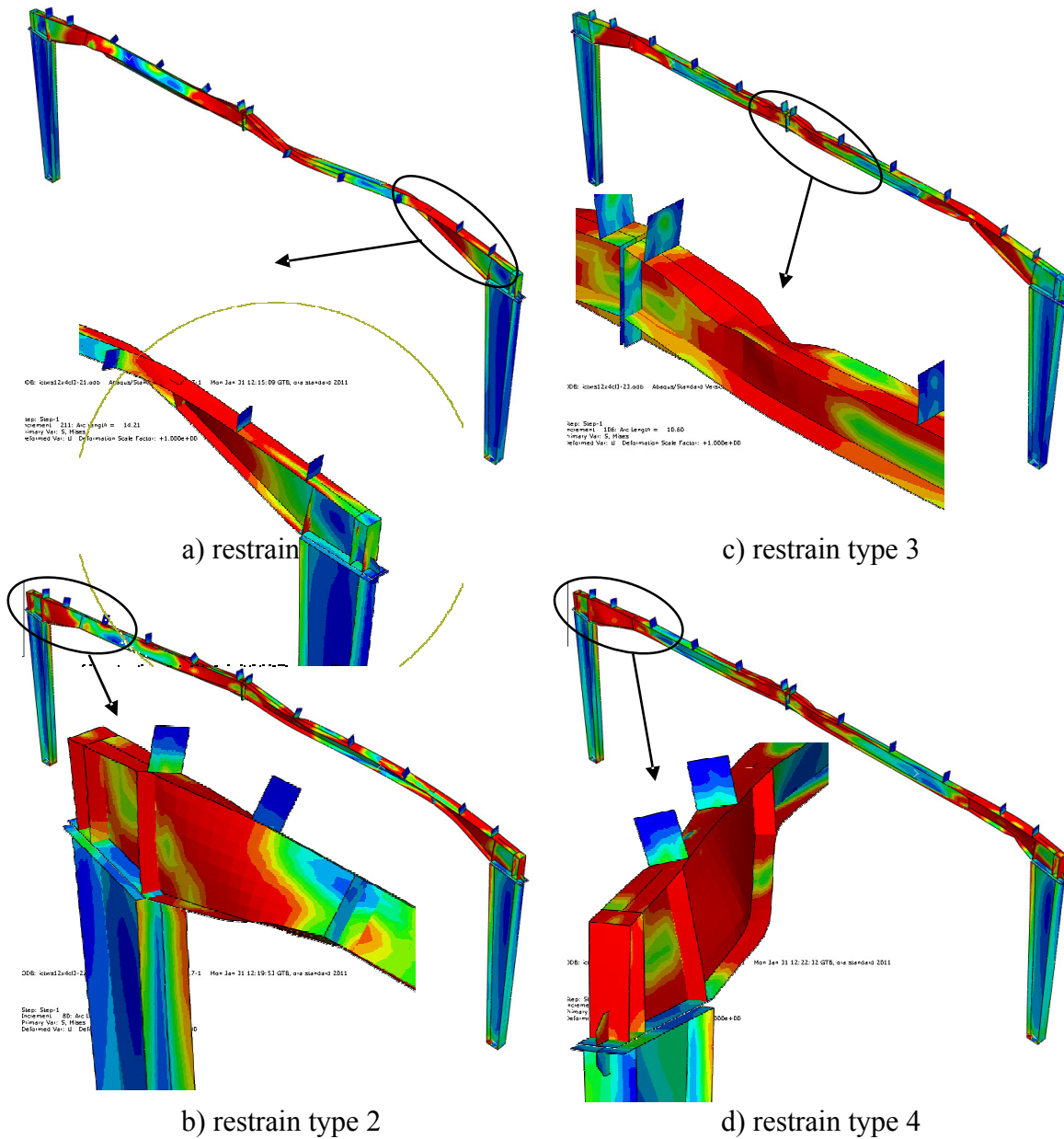


Figure 8. Plastic sectional buckling - GMNIA analysis.

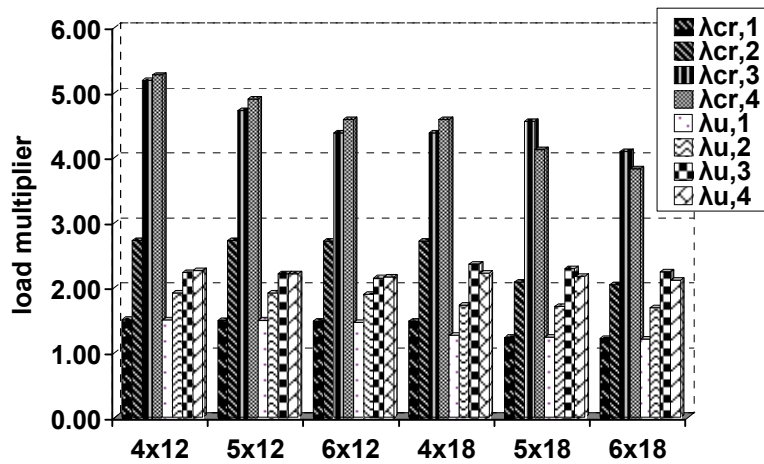


Figure 9. Load multipliers for LEA and GMNIA analyses.

For the frames described in Table 1, local and global imperfections were taken into account (Fig. 6). In Fig. 10 and Fig. 11, a comparison between perfect structure, initial bow (out of plane) imperfection and initial sway imperfection is presented. The applied lateral restraints are the ones shown in Fig. 5. The results are plotted as behavior curve i.e: load factor-vertical displacement.

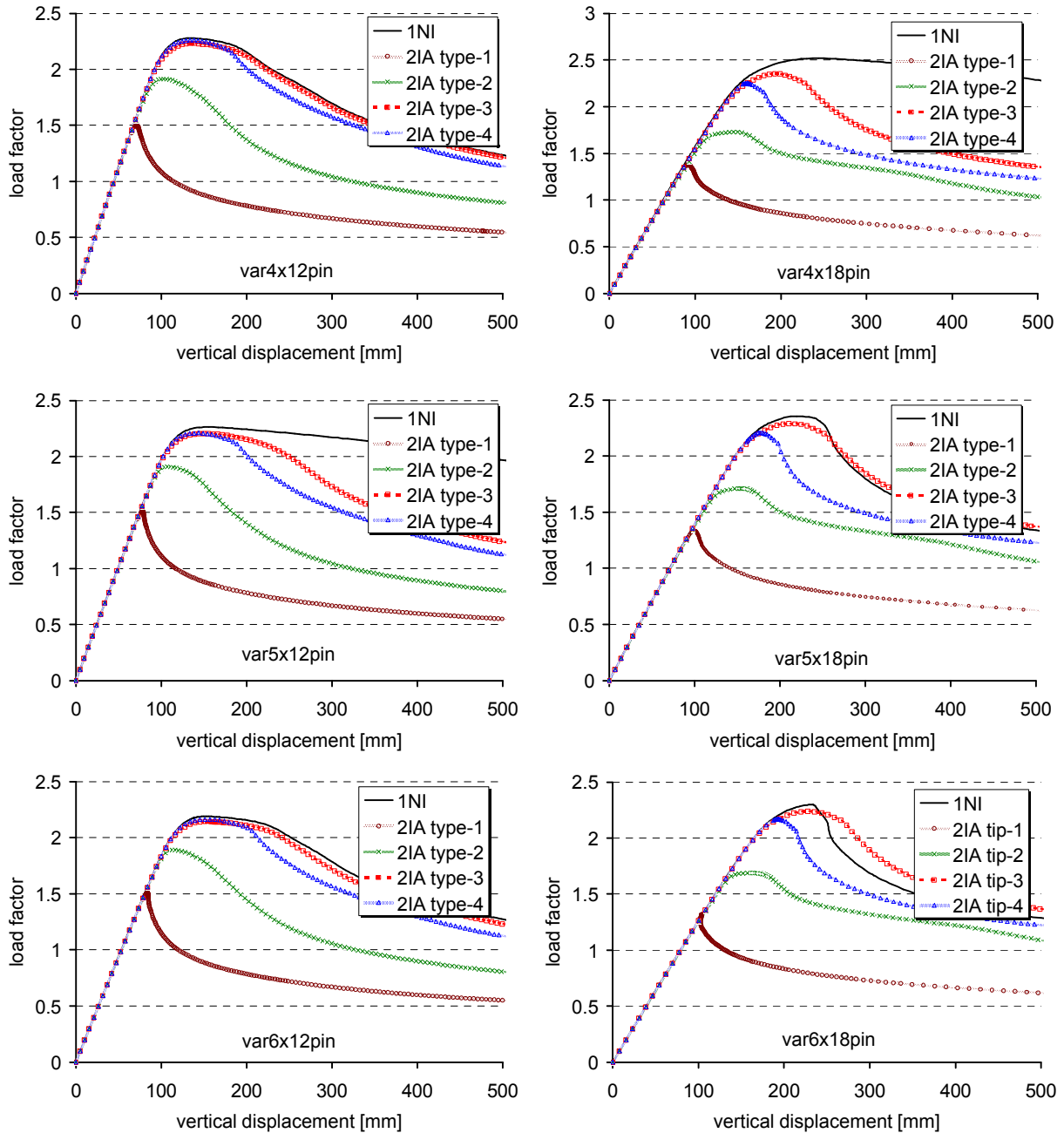


Figure 10. Load multipliers-displacement curves for 2IA-imp. GMNIA analyses.

The two types of imperfections considered in analysis influence significantly the bearing capacity of the considered structures (see Fig. 10 and Fig. 11). The considered imperfections do not influence the initial rigidity of the structure. The influence is much higher in case of low restrained structure (type 1 and 2 in Fig 5) than in the case of effective restrained ones (type 2 and 3 in Fig 5). Once more it was confirmed that in the case of lateral-torsional buckling, which represents the natural coupling between flexural and torsional modes, the actual buckling strength is characterized

by a low-to-significant erosion of theoretical one, function of the lateral restraints.

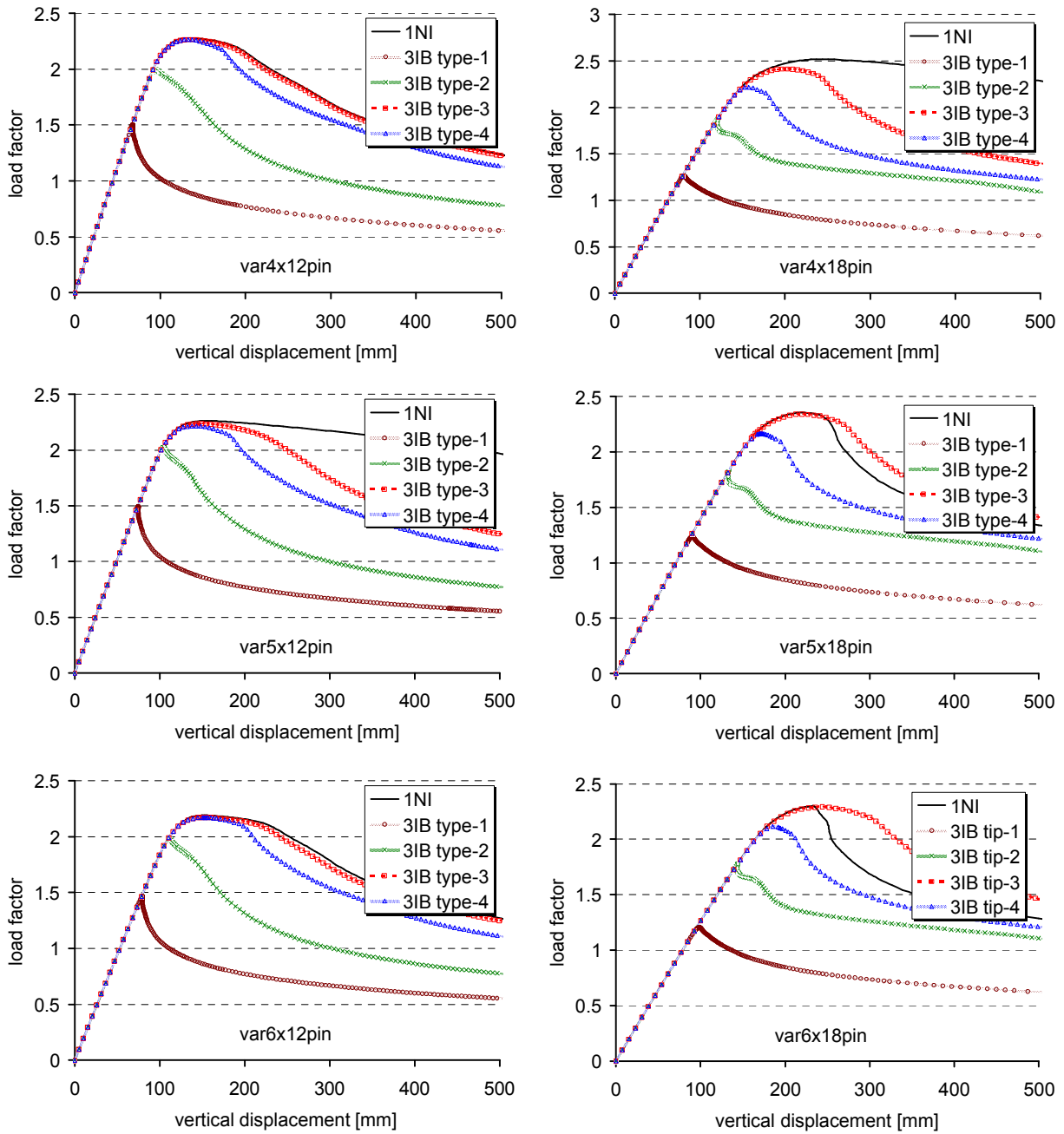


Figure 11. Load multipliers-displacement curves for 3IB-imp. GMNIA analyses.

### 5. Conclusions

A substantial parametric investigation was made in order to analyze the behavior of single storey frames made of elements with variable cross sections under the influence of both lateral restraints and imperfections. Two different types of imperfections had been considered in the study e.g.: manufacturing imperfections characterized by initial bow imperfections, and erection imperfections characterized by initial sway imperfections. The magnitude of the imperfections was considered as being equal with those prescribed in [1,2]. Within the performed analyses also lateral restraints, provided in practice by purlins, were considered.

Main failure mode of the frame was out of plane buckling for all the considered type of lateral restraints. Local buckling may also develop in case of restraint type 3 and 4, in function of web slenderness.

It was also noticed that the considered imperfections influences significantly the final capacity of the frame. The difference in the frame capacities is much higher in case of imperfect structure with less effective lateral restraint (type 1 and 2) than the imperfect structures with more effective lateral restraints (type 3 and type 4). The difference between considered imperfections 2IA and 3IB is significantly low, and the type of imperfection does not influence the failure mode of frame.

It was confirmed that in case of lateral-torsional buckling, which represents the natural coupling between flexural and torsional modes, the actual buckling strength is characterized by a low-to-significant erosion of theoretical one, function of the lateral restraints.

## Acknowledgements

The authors gratefully acknowledge the financial support of “National University Research Council – NURC-CNCSIS-Romania” through the national research grant PN-II-RU-TE-2010-1/38.

## 6. References

- [1] SR-EN1993-1-1: *Proiectarea structurilor de oțel Partea 1-1: Reguli generale și reguli pentru clădiri*, ASRO-standard roman.
- [2] EN 1993-1.1: *Eurocode 3: Design of Steel Structures. Part 1.1 : General rules and rules for buildings*, may 2005, CEN, Brussels, Belgium;
- [3] EN 1090-2:2005 *Execution of steel structures and aluminium structures - Part 2: Technical requirements for the execution of steel structures*. CEN-Brussels
- [4] Dubina D., I.M. Cristutiu (2007): *Numerical simulation of behaviour of pitched roof portal frames imperfection's sensitivity analysis and influence of joint characteristics*. TC8-2007-015 ECCS TC8 internal document.
- [5] I.G. Raftoyiannis, J.C. Ermopoulos (2005): *Stability of tapered and stepped steel columns with initial imperfections*. *Engineering Structures* 27 (2005) 1248–1257, Elsevier Science.
- [6] R. Goncalves, D. Camotim (2005): *On the incorporation of the equivalent member imperfections in the in-plane design of steel frames*. In *Journal of Constructional Steel Research*, Vol. 61 (2005), pp. 1226-1240.
- [7] J. Szalai, F. Papp (2009): *On the probabilistic evaluation of the stability resistance of steel columns and beams*. *Journal of Constructional Steel Research* Vol. 65 (2009) 569\_577. Elsevier Science.
- [8] Taras, A.; Greiner, R.:(2008): *Torsional and flexural torsional buckling — A study on laterally restrained I-sections* . - in: *Journal of constructional steel research* 64 (2008) 7-8, S. 725 – 731, Elsevier Science
- [9] Taras, A.; Greiner, R (2008) : *Development of consistent buckling curves for torsional and lateral-torsional buckling.*, *Steel construction* 1 (2008) 1, S. 42 – 50, Ernst&Son Publ.
- [10] Dubina D., Cristutiu I.M.: *Buckling strength of pitched roof portal frames of class 3 and 4 tapered members*, *Proc of EUROSTEEL 2005, 4th European Conference on Steel and Composite Structures* - Maastricht, Holland, 7-11 june. 2005

# GBT-based Analysis of Tapered Thin-Walled Members: Recent Developments

Mihai Nedelcu<sup>\*1</sup>

<sup>1</sup> Technical University of Cluj-Napoca, Faculty of Civil Engineering, 15 C Daicoviciu Str., 400020, Cluj-Napoca, Romania

Received 25 July 2011; Accepted 1 September 2011

## Abstract

*The Generalised Beam Theory (GBT) approach was proved to be a valid substitute of the Eurocode methods used for cold-formed steel member design. The conventional GBT is applied for the linear/nonlinear analysis of prismatic thin-walled members, circular and elliptical cylindrical shells and tubes. The author's new formulations extend the GBT for the special case of tapered members. This paper presents an overview of the GBT formulations recently developed by the author and also the software application GBTPower in which these theoretical developments are implemented. GBTPower performs buckling analyses of prismatic and tapered elastic thin-walled members with various types of cross-sections and boundary conditions. At the end a few numerical results are presented and briefly discussed.*

## Rezumat

*Abordările specifice Teoriei Generalizate a Grinzii (TGG) pot înlocui cu succes metodele din Eurocode în privința proiectării barelor cu pereți subțiri formate la rece. TGG este utilizată în mod convențional la analiza liniară și neliniară a barelor prismatice cu pereți subțiri și a tuburilor cilindrice și eliptice. Noile formulări ale autorului extind TGG pentru cazul special al barelor cu secțiune variabilă. Acest articol face o prezentare de ansamblu ale ultimelor formulări teoretice recent concepute de autor și de asemenea a programului de calcul GBTPower în care acestea au fost implementate. Programul efectuează analize de tip flambaj prin bifurcare în domeniul elastic pentru bare cu pereți subțiri cu diferite secțiuni și rezemări. În final câteva exemple numerice sunt pe scurt prezentate și discutate.*

**Keywords:** GBT, tapered thin-walled members, buckling, cylindrical shells

## 1. Introduction

Regarding the buckling of thin-walled members, the most complete design codes were developed for metallic members. So we have the ENV 1993-1-3 Eurocode 3 (Europe) [1], NAS 2001 (North America) [2], [3], AS/NZS 1996 (Australia and New Zealand) [5]. The design methods are generally very similar, the buckling evaluation consists of (i) computation of the elastic critical load, (ii) consideration of the degradation caused by the various kinds of imperfections as well as the possible favourable effect of post-buckling reserve. Knowing that the stability loss of thin-

---

\* Corresponding author: Tel./ Fax.: 0264/401363  
E-mail address: [mihai.nedelcu@mecon.utcluj.ro](mailto:mihai.nedelcu@mecon.utcluj.ro)

walled members may happen in the form of global, distortional and local buckling, the solving strategies generally use a reduced “effective” cross-section, avoiding in this manner the critical load computation for distortional and local buckling, more difficult to obtain. The computation of the effective cross-section is a tedious iterative process for the structural design engineer. To overcome this problem, Schafer developed the “Direct Strength Method” introduced in 2004 in NAS-Appendix 1 [4]. The method does not use effective cross-section, nor require iterations for determining effective properties, instead the method uses member elastic buckling solutions based on gross properties to determine the member strength in global, local and distortional buckling. For the evaluation of these elastic critical loads, Schafer et al. created CUFSM, free analysis software based on Finite Strip Method and Generalised Beam Theory (GBT) hypotheses [6]. Other GBT-based software applications are GBTUL [7] developed at the Technical University of Lisbon and the author’s GBTPower which will be briefly presented in this paper.

GBT is based on classical Kirchhoff-Love plate hypotheses and also Vlasov’s thin-walled hypotheses (null membrane shear strain and transverse extension.). The theory was originally developed by Schardt [8], [9] and it is a bar theory capable of describing any member deformation as a linear combination of orthogonal pre-determined pure deformation modes. Working with one-dimensional elements, GBT is computationally an extremely efficient and elegant method for the investigation of bifurcation buckling of thin-walled members. It is also capable of providing the contribution of each pure deformation mode to the final configuration and so, it helps to a better understanding of the analysed structural behaviour. Due mainly to the scientific research developed at Technical University of Lisbon, GBT provides today a general solution for the linear/nonlinear analysis of prismatic thin-walled members and frames with arbitrary cross-sections [10], [11]. Recently Silvestre [12], [13] developed a complete GBT methodology in order to analyse the buckling behaviour of circular and elliptical cylindrical shells and tubes. In two previous papers [14], [15] the author provided an extension of GBT for the analysis of isotropic members with variable cross-sections meaning tapered thin-walled bars and also conical shells. The main objective of this paper is to present the GBT extensions and then to illustrate their applicability on elastic linear and buckling analysis of tapered members with various end supports, cross-section shapes and variation laws.

## 2. Theoretical Developments

### 2.1 GBT for prismatic thin-walled members

For the arbitrary cross-section of a thin-walled member shown in Fig. 1, the stress and strain field are expressed by considering the membrane ( $M$ ) and bending ( $B$ ) behaviour of the thin-walls and also the linear ( $L$ ) and non-linear terms ( $NL$ ).

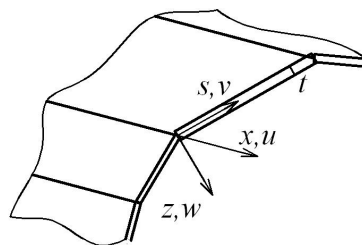


Fig. 1. Thin-walled member: local axes/displacements

The simplifying classical Kirchhoff-Love hypotheses and also Vlasov’s hypotheses ( $e_s^{M,L} = 0$ ,  $g_{xs}^{M,L} = 0$ ) are adopted for each wall. Neglecting the non-relevant strain components, the kinematic relations are written as follows:

$$\begin{aligned}
 e_x^{M,L} &= u' & e_x^{M,NL} &= (v'^2 + w'^2) / 2 & g_{xs}^{M,NL} &= \dot{w}w' \\
 e_x^B &= -zw'' & e_s^B &= -z\ddot{w} & g_{xs}^B &= -2z\dot{w}'
 \end{aligned}
 \tag{1}$$

where  $(\ )' = \frac{\partial(\ )}{\partial x}$ ,  $(\ ) = \frac{\partial(\ )}{\partial s}$ .

The constitutive relations related to the relevant stress components are written:

$$S_x^M = Ee_x^M \quad \left\{ \begin{matrix} S_x^B \\ S_s^B \\ t_{xs}^B \end{matrix} \right\} = \frac{E}{1-m^2} \begin{bmatrix} 1 & m & 0 \\ m & 1 & 0 \\ 0 & 0 & \frac{1-m}{2} \end{bmatrix} \left\{ \begin{matrix} e_x^B \\ e_s^B \\ g_{xs}^B \end{matrix} \right\}
 \tag{2}$$

The conventional GBT methodology involves (i) a modal cross-section analysis, leading to the GBT pure deformation modes, the corresponding modal mechanical properties and (ii) a member stability analysis, to obtain the critical loads and the corresponding buckling shapes [8], [9]. The final buckling shape is considered as a linear combination of  $n$  orthogonal deformation modes. The number  $n$  depends on the cross-section type, the number of the fold-lines and the considered intermediate nodes on each wall. Based on the principle of virtual work applied in its variational form, the first step will lead to the GBT system of equilibrium differential equations:

$$EC_{ik} f_k^{IV} - GD_{ik} f_k'' + B_{ik} f_k - l \left[ X_{jik} (W_j^0 f_k')' - X_{jki}^t (W_j^{0'} f_k) + X_{jik}^t W_j^{0'} f_k' \right] = 0
 \tag{3}$$

where  $E$  and  $G$  are Young's and shear moduli,  $k, i = 1..n$ . The vector  $W^0$  ( $j = 1..4$ ) contains the resultants of the applied pre-buckling stresses, namely (i) axial force ( $W_1^0 = N$ ), (ii) major and minor axis bending moments ( $W_2^0 = M_y, W_3^0 = M_z$ ), and (iii) bimoment ( $W_4^0 = B$ ).  $C, D, B$  are the mechanical stiffness matrices related with the generalized warping, twisting and transverse bending (cross-sectional distortion) respectively,  $X$  and  $X^t$  are the cross-section geometrical stiffness matrices and it is important to underline that for prismatic elements they all have constant expressions according to  $x$  [16]. Together with the appropriate end support conditions the GBT differential equations system defines the buckling eigenvalue problem. Its solution yields the buckling load parameters ( $l_b$ ) and the corresponding modal amplitude functions ( $f_k(x)$ ). Concerning single-cell closed cross-sections, the shear deformations of the cross-section mid-line induced by torsion cannot be considered using the Vlasov hypothesis of null membrane shear strain. An additional deformation mode is introduced by using the uniform shear flow hypothesis and following the Bredt formula, the term  $G \int_s t v^2 ds$  obtained from the virtual work of the shear strains, is added to the components of stiffness matrix  $D$ . Fig. 2 shows the first 10 deformation shapes of a narrow rectangular hollow section.

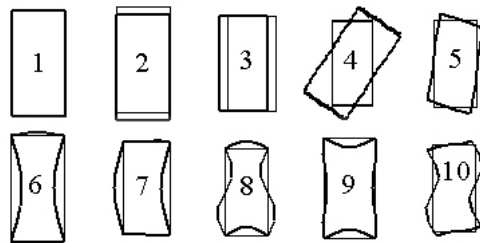


Fig. 2. First 10 deformation mode shapes



## 2.2 GBT for tapered thin-walled members

In prismatic members, the mid-plane of each cross-section wall is perpendicular to the cross-section plane. As a consequence the warping displacements are perpendicular to the cross-section plane, as in classical beam theories, an aspect which greatly simplifies the GBT cross-section analysis. It is well known that tapered members don't have this characteristic. The author extended the theory by using the approximation that the warping displacements are still perpendicular to the cross-sectional plane. In this approach the tapered member is replaced with a succession of prismatic elements as shown in Fig. 3. This approximation gives good results for tapered members with small tapering slope, which is a structural characteristic largely used in practice. There are no restrictions regarding the type of cross-section (branched or unbranched) or the variation law of each wall width or thickness. Approximating the annular cross-section with a polygonal one, this approach can also analyse conical elements, hyperbolic cooling towers, etc. Of course, this new extended formulation will also accept members with constant cross-section.

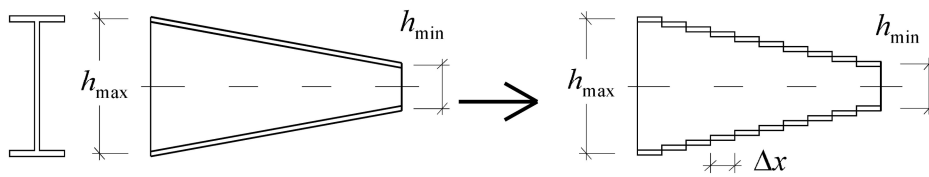


Fig. 3. Geometry idealization of the tapered member

To determine the equilibrium equations we follow the same path explained in the previous chapter using the principle of virtual work. Taking into account that the components of the cross-section linear and geometrical stiffness matrices ( $C$ ,  $D$ ,  $B$ ,  $X$  and  $X^t$ ) are no longer constant according to  $x$ , new terms are added to the system of equilibrium differential equations. In the case of buckling analysis, the differential equations system becomes:

$$E \left( C_{ik} \mathbf{f}_k'' \right)'' - G \left( D_{ik} \mathbf{f}_k' \right)' + B_{ik} \mathbf{f}_k - \left[ \left( X_{jik} W_j^0 \mathbf{f}_k' \right)' - \left( X_{jki}^t W_j^{0'} \mathbf{f}_k \right)' + X_{jik}^t W_j^{0'} \mathbf{f}_k' \right] = 0 \quad (4)$$

To determine the variable components of the stiffness matrices, two ways are suggested: (i) an analytical approach developed for the special bar type for which all the section walls have constant thickness and the same variation law in width (see Nedelcu [14]). For arbitrary variable cross-section the author used a simple numerical approach. A mesh is defined along the bar length and in each mesh point the stiffness matrices are computed in the GBT conventional manner specific to prismatic members. Knowing that the stiffness matrices are continuous functions of  $x$ , the intermediate values are computed by interpolation.

## 2.3 GBT for conical shells

Consider the conical shell depicted in Fig. 4, with length  $L$ , constant thickness  $t$  and semi-vertex angle  $\alpha$ . Next we have the global coordinate system  $x_g, y_g, z_g$  and the local coordinate system  $x, \varphi, z$ , (meridional coordinate  $x \in [a, L / \cos \alpha]$ , circumferential coordinate  $\varphi \in [0, 2\pi]$  and normal coordinate  $z \in [-t/2, +t/2]$ ). According to the local coordinate system we have the  $u$  (warping - meridional),  $v$  (transverse - circumferential) and  $w$  (flexural - normal) displacements.

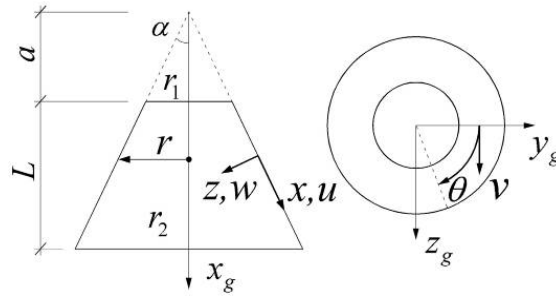


Fig. 4. The geometry of the conical shell

The strain-displacement (kinematic) relation has the following form:

$$\{e\} = \{\epsilon^M\} + \{\epsilon^B\} = \{\epsilon^M\} + z\{C\} \quad (5)$$

where  $\{\epsilon^M\}$  and  $\{C\}$  are, respectively, the membrane strain (having linear and non-linear components) and change-of-curvature (bending) vectors of the reference surface, given as follows (Goldfeld [18]):

$$\begin{aligned} e_{xx}^M &= e_{xx}^{M,L} + e_{xx}^{M,NL} = (u') + \left( \frac{w'^2}{2} + d_2 \frac{v'^2}{2} \right) \\ e_{qq}^M &= e_{qq}^{M,L} + e_{qq}^{M,NL} = \left( \frac{\dot{v}}{r} + \frac{wc}{r} + \frac{us}{r} \right) + \left( \frac{1}{2} \left( \frac{d_1 vc - \dot{w}}{r} \right)^2 + \frac{d_2}{2} \left( \frac{\dot{v} + wc}{r} \right)^2 \right) \\ g_{xq}^M &= g_{xq}^{M,L} + g_{xq}^{M,NL} = \left( \frac{\dot{u}}{r} + v' - \frac{vs}{r} \right) + \left( \frac{w'\dot{w}}{r} - d_1 \frac{vw'c}{r} + d_2 \frac{v'\dot{v}}{r} \right) \\ C_{xx} &= -w'' \\ C_{qq} &= -\frac{\ddot{w}}{r^2} - \frac{w's}{r} + d_1 \frac{\dot{v}c}{r^2} \\ C_{xq} &= 2 \left[ -\frac{\dot{w}'}{r} + \frac{\dot{w}s}{r^2} + d_1 \frac{c}{r} \left( \frac{v'}{2} - \frac{vs}{r} \right) \right] \end{aligned} \quad (6)$$

where  $c = \cos(a)$ ,  $s = \sin(a)$ ,  $(\cdot)' = \frac{\partial(\cdot)}{\partial x}$ ,  $(\cdot) = \frac{\partial(\cdot)}{\partial x}$ .

The coefficients  $d_1$  and  $d_2$  represent specific shell theories ( $d_1 = d_2 = 0$  for Donnell's [19],  $d_1 = 1$  and  $d_2 = 0$  for Sanders' [20],  $d_1 = d_2 = 1$  for Love- Timoshenko [21]). Being the most exact theory, the last one was adopted by the author. Using the Vlasov's null membrane shear strain and transverse extension hypotheses ( $g_{xq}^{M,L} = 0$ ,  $e_{qq}^{M,L} = 0$ ) and the geometry idealization described in the previous section (see Fig. 5) the author obtained the following GBT differential equations system for the buckling analysis:

$$\begin{aligned} C_{kk} f_k^{IV} + 2C_{kk}' f_k''' + (C_{kk}'' - D_{kk}^1 + 2D_{kk}^2 - X_{jkk}^{Sx}) f_k'' + (-D_{kk}^{1'} + 2D_{kk}^{2'} - X_{jkk}^{Sx'}) f_k' \\ + (D_{kk}^{2''} + B_{kk} - G_{kk}' + X_{jkk}^{Sq} - X_{jkk}^t) f_k = 0 \end{aligned} \quad (7)$$

where  $k, i = 1..n$ .  $C$ ,  $D^1$ ,  $D^2$ ,  $G$  and  $B$  are the cross-section linear stiffness matrices,  $X_j^{Sx}$ ,  $X_j^{Sq}$ ,  $X_j^t$  are the elements of the geometric stiffness matrices taking into account the 2<sup>nd</sup> order effect of the pre-buckling meridional, circumferential and shear stresses ( $S_{xx}^o$ ,  $S_{qq}^o$ ,  $t_{xq}^o$ ) respectively, associated with the 1<sup>st</sup> order deformation mode  $j$ . These have to be calculated by a previous 1<sup>st</sup> order analysis and normally they introduce the bifurcation stress coefficient  $l_b$ . It is important to underline that the

elements of the stiffness matrices are not constant along the member longitudinal axis as long as they depending on the variable radius  $r$  but they can be analytically and efficiently computed [15].

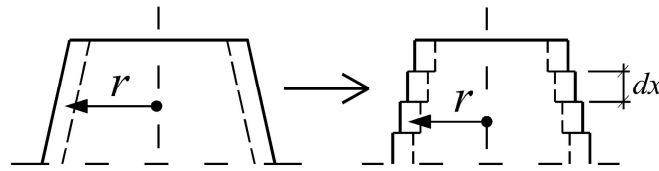


Fig. 5. Geometry idealization of the conical shell

The critical shape is either described by a combination of “shell-type” deformation modes characterized by a specific number of sine waves along the member cross-section (see Fig. 6), or by one of “special” buckling modes: extension, axisymmetric and torsion modes (see Fig. 7).

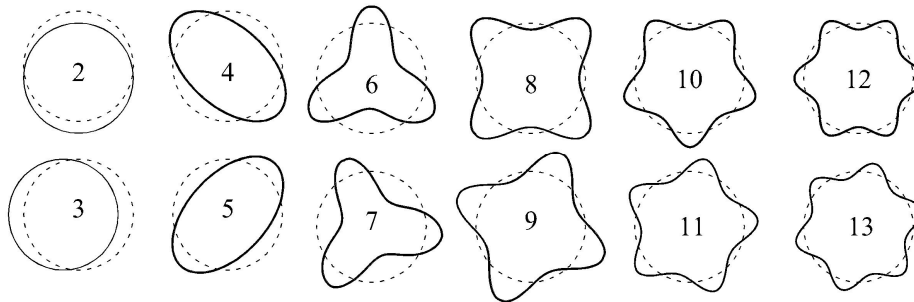


Fig. 6. First 12 shell-type deformation modes

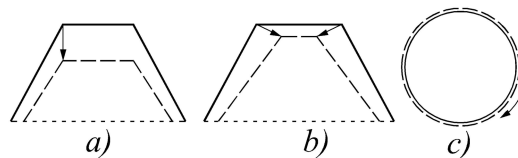


Fig. 7. Displacement field for a) extension mode, b) axisymmetric mode, c) torsion mode

The GBT differential equation systems described by Eq. (4) and (7) can be solved by different numerical methods like finite difference method [8], FEM [11], Galerkin method, etc. The results presented in this paper were obtained through the application of a Runge-Kutta numerical method, namely the collocation method Lobatto IIIA of fourth order [17]. This method uses a finite-dimensional space of candidate solutions for  $f_k(x)$  (usually, polynomials up to a certain degree) and a mesh of points ( $0 < x_1 < x_2 < \dots < L$ ) in the domain (the collocation points), and then selects the solution which satisfies the given differential equation at the collocation points.

### 3. Illustrative Examples

#### 3.1 The GBTPower software application

In order to implement the theoretical developments described above, the author created a software application called GBTPower using the *Matlab* programming language [22] (version *R2006b*). GBTPower is able to compute the 1<sup>st</sup> order and elastic buckling response for isotropic thin-walled members with various types of cross-sections: opened branched, opened unbranched, single-cell closed, constant and variable with different variation laws.

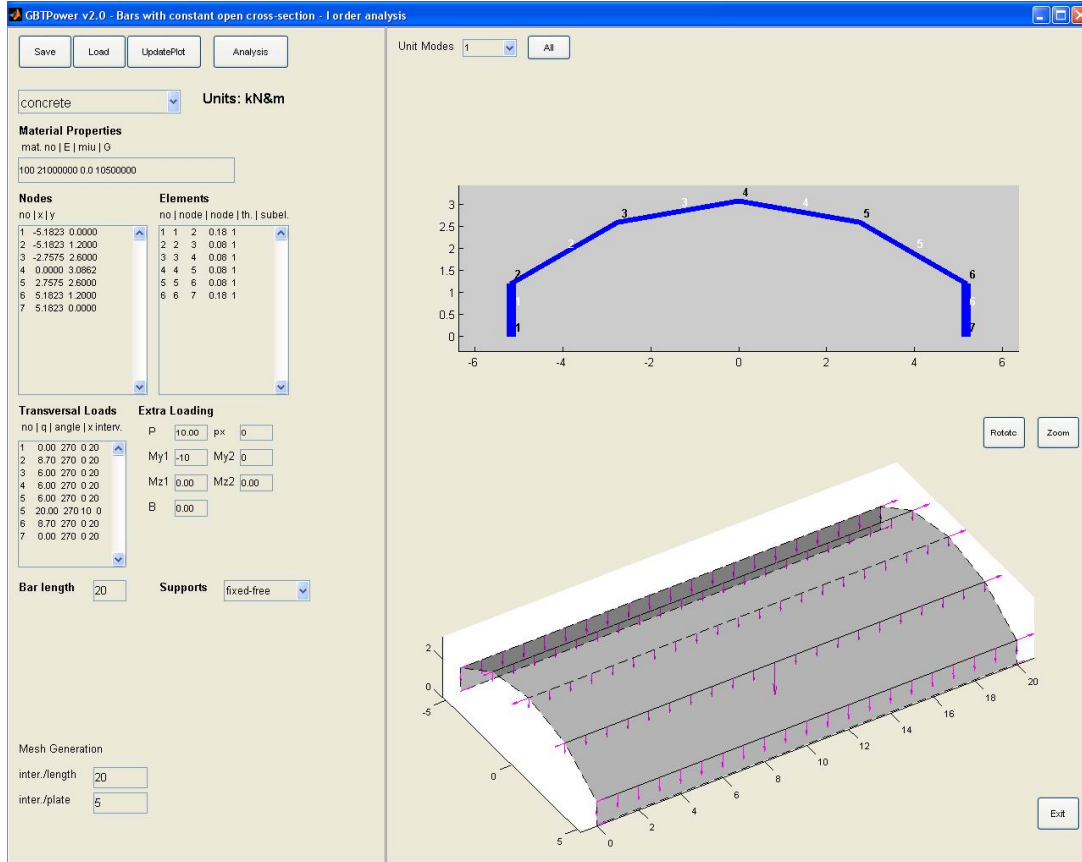


Fig. 8. GBTPower input interface

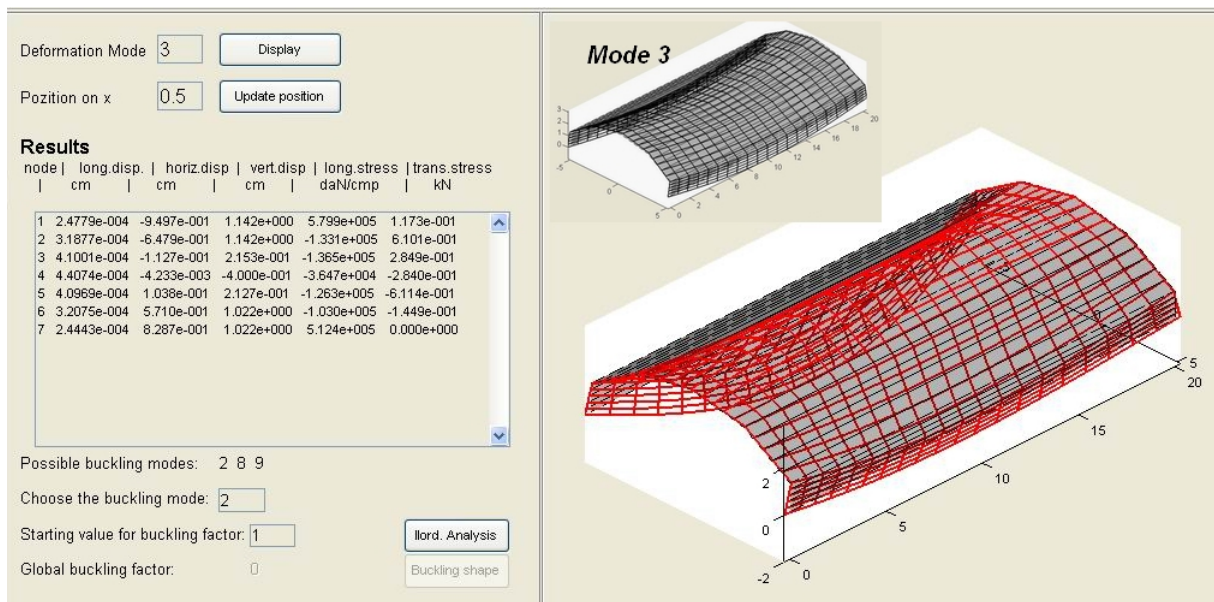


Fig.9. GBTPower output interface

Each cross-section type and variation law is handled in a different module. GBTPower also accepts different boundary conditions: cantilevers, simple supported, double fixed or fixed-simple-supported members. The latest developed module deals with the buckling analysis of conical shells. The input interface for opened and constant cross-section is shown in Fig. 8. The output interface displays for 1<sup>st</sup> order analysis the displacement and stress field, the shape for each pure deformation

mode and for the total deformation Inside Figure 9 the image of the third mode deformation (simple bending around the minor axis) was graphically inserted. For buckling analysis the deformation shapes are presented together with the critical load factor and the contribution of each mode to the final solution.

### 3.2 Tapered thin-walled members

#### 3.2.1 Open cross-section

Fig. 10 presents a tapered I-section cantilevered column investigated by Ronagh et al [23] using a different theory and a finite element approach. Fig.10 b) shows the good agreement between the GBT values and the estimates of Ronagh et al. The buckling deformation of Fig. 10.c) was obtained for a bar length  $L = 100mm$  and a tapering ratio of  $b = 0.2$ .

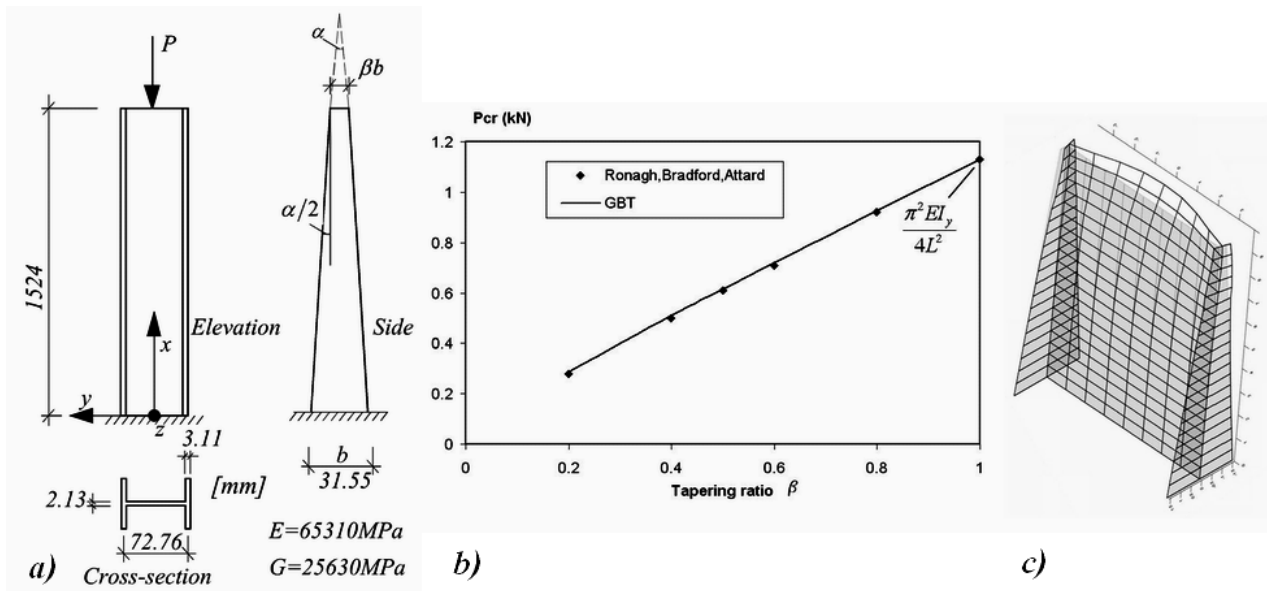


Fig. 10: a) Tapered I-section cantilevered column, b) buckling load and c) shape

#### 3.2.2 Rectangular hollow cross-section

The author analysed the buckling of a tapered column with both ends fixed, rectangular hollow cross-section  $b \times h$  and variable length for two tapering ratios applied to the cross-sectional height (see Fig. 11). Table 1 presents the critical loads obtained by means of (i) GBT formulation, (ii) two-dimensional shell FEA using ABAQUS S4R finite shell elements [24]. Fig. 12 shows the buckling shape obtained by FEA with  $L = 200mm$  and tapered ratio  $b = 0.5$ .

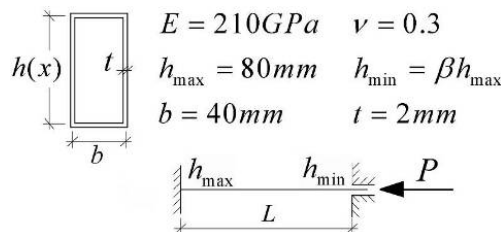


Fig. 11. End fixed column

Table 1: FEA vs. GBT results for fixed members

L (mm)	b	$P_{cr}^{FEA}$ (KN)	$P_{cr}^{GBT}$ (KN)	$\Delta$ (%)
100	1	385,30	406,60	5,53
	0,5	493,15	516,40	4,71
200	1	321,50	326,77	1,63
	0,5	410,53	416,55	1,47
500	1	300,77	301,06	0,10
	0,5	362,18	368,80	1,83
1000	1	301,73	301,09	0,22
	0,5	351,41	358,96	2,15

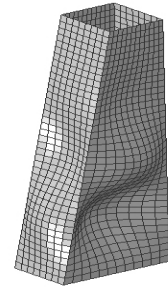


Fig. 12. Buckling shape

### 3.2.3 Regular polygonal cross-section

This formulation can be used to analyse truncated – conical and hyperbolic towers if their annular cross-section is approximated by a regular polygonal one. For this example a concrete hyperbolic cooling tower was chosen, namely the Trojan tower, Portland Oregon USA, extensively analysed by Cole et al [25] and presented in Fig. 13.a). For the GBT approach, the annular cross-section was approximated by a regular dodecagon and each side had an intermediate node in its middle. Starting with a unit weight of  $24\text{ kN} / \text{cbm}$ , the author searched the concrete critical dead load for which the tower exhibits the bifurcation stability loss. Using ABAQUS S4R finite shell elements, the FEA of the Trojan Tower showed that the buckling deformation is described by 6 sine waves for a critical factor of  $\lambda = 26.7$  (see Fig. 13.b)). Using the formulation described in this paper, a critical factor of  $\lambda = 27.4$  emerged for the GBT mode 14 presented in Fig. 13.c).

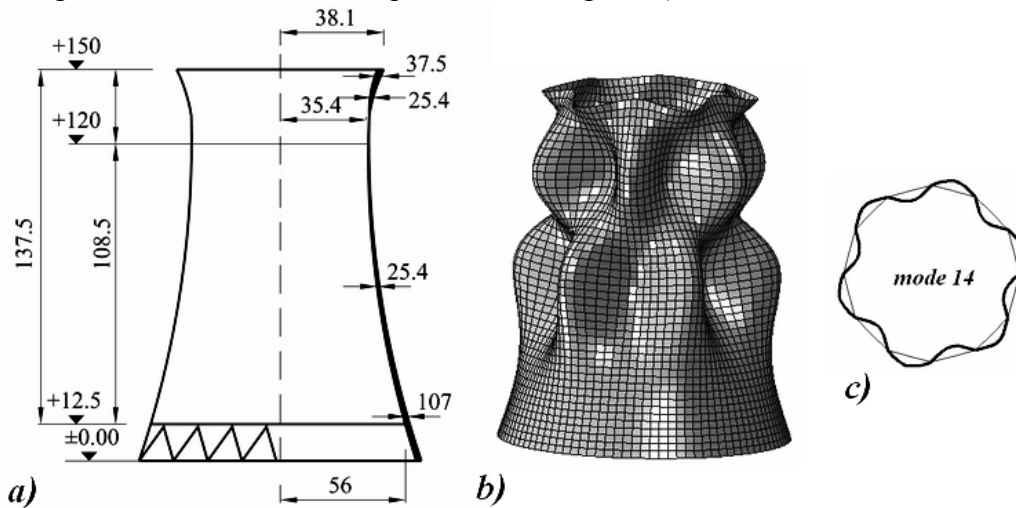


Fig. 13. a) Trojan Tower, b) buckling shape and c) GBT mode 14

### 3.3 Conical shells

The author studied the buckling behaviour of conical columns with different end conditions. Consider the steel conical shell depicted in Fig. 14,  $E = 210\text{GPa}$ ,  $\nu = 0.3$ , wall thickness  $t = 1\text{ mm}$  and length  $L = 1200\text{mm}$ . The starting radius is taken  $r_1 = 50\text{mm}$  and the end radius  $r_2$  is variable. The pre-buckling meridional stress is calculated in the classic manner  $\sigma_{xx}^0 = P / (2\pi r t c)$ , with  $P = \lambda_b P_0$ . The minimum bifurcation load coefficient is introduced as  $\lambda_c = \lambda_{b,\min}$  or critical load coefficient. The initial value of the axial load was taken as  $P_0 = 2\pi r_1 \cdot 1\text{kNmm}^{-1} = 314.16\text{kN}$ .

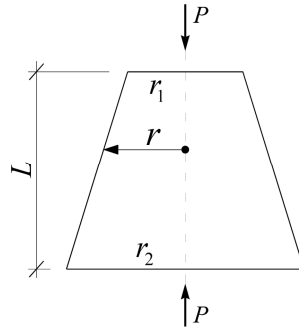


Fig. 14. Conical shell under axial compression

The critical load coefficient ( $l_{c,FEM}$ ) for several values of  $r_2$  were obtained using ABAQUS S4R finite shell elements. These values are compared with the GBT critical load coefficients ( $l_{c,GBT}$ ) and the results are presented in Fig. 15, 16 and 17 for different end supports: simply supported, fixed and cantilever members, respectively. Fig. 18 presents the critical buckling shapes and the corresponding load coefficients for simply supported members, results obtained using shell FEA, for several values of  $r_2$ .

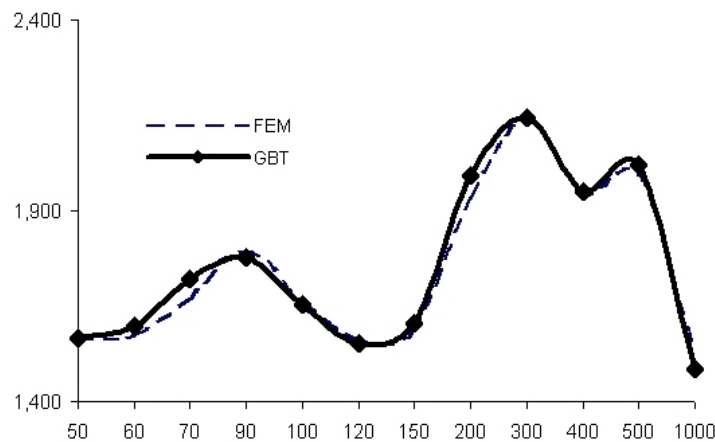


Fig. 15. FEM vs. GBT results for simply supported members

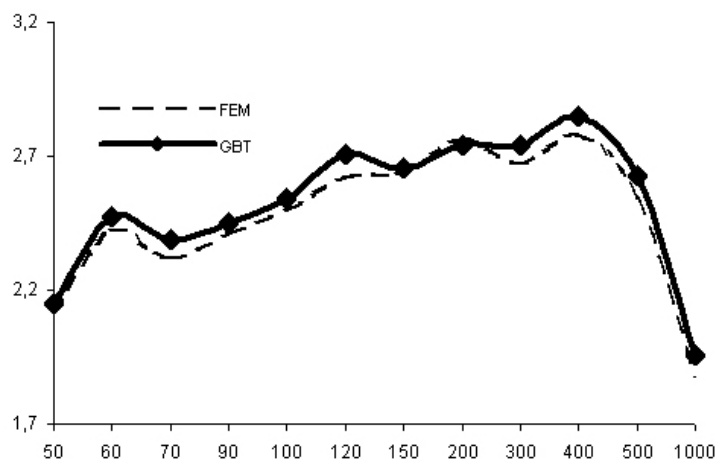


Fig. 16. FEM vs. GBT results for fixed members

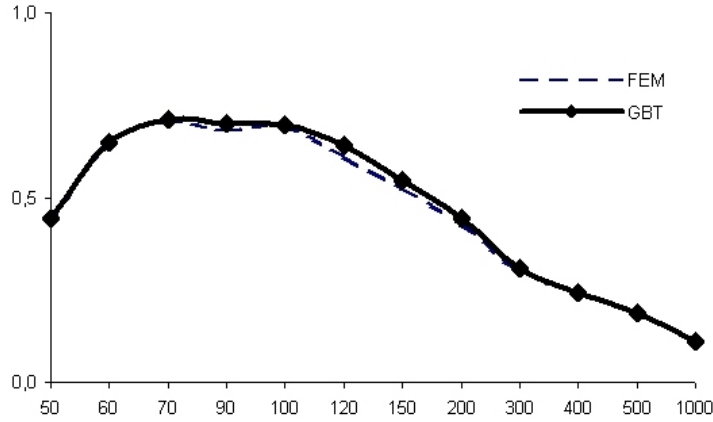


Fig. 17. FEM vs. GBT results for cantilever members

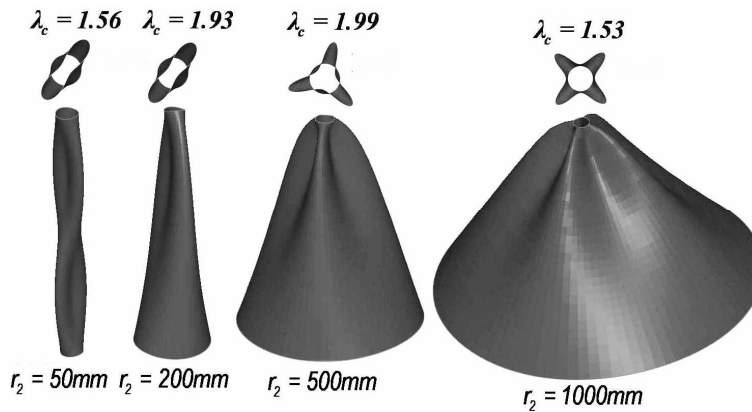


Fig. 18 Simply supported members: critical buckling shapes and load coefficients  $\lambda_{c,FEM}$

### 5. Conclusions

As a beam theory, GBT is an elegant and computationally very efficient method for the investigation of thin-walled members buckling behaviour. The GBT approach could be a valid substitute of the Eurocode methods used for cold-formed steel member design. This paper presented the latest GBT formulations developed by the author regarding the tapered thin-walled members and conical shells. The stiffness matrices have no longer constant elements along the bar length and because of that, the equilibrium differential equations gained new terms. GBT was successfully applied for the buckling analysis of tapered isotropic open and single-cell closed thin-walled members with constant or variable thickness and also for isotropic conical shells with constant thickness. To illustrate the potential of the GBT extensions, a few numerical results were presented in connection with the software application GBTPower in which the latest theoretical formulations were implemented.

### 6. References

- [1] *EUROCODE 3, EN 1993-1.1*. Design of steel structures. Part 1.1: General rules and rules for buildings, European Committee for Standardisation, Final Draft, 2001.
- [2] *AISI – American Iron and Steel Institute: Cold-formed steel design manual*, Washington, DC, 1996.
- [3] *AISI – American Iron and Steel Institute: North American Specification for the Design of Cold-Formed Steel Structural Members with Commentary*, Washington, DC, 2001.
- [4] *AISI – American Iron and Steel Institute: Supplement 2004 to the North American Specification for the Design of Cold-Formed Steel Structural Members*, 2001 Edition: Appendix 1, Design of Cold-Formed



- Steel Structural Members Using Direct Strength Method, Washington, D.C., 2004.
- [5] *AS/NZS 4600* – Australian Standards / New Zealand Standards. Cold-formed Steel Structures, Sydney, 1996.
- [6] *CUFSM: Elastic Buckling Analysis of Thin-Walled Members by Finite Strip Analysis*, CUFSM v2.6, <http://www.ce.jhu.edu/bschafer/cufsm/>
- [7] *GBTUL Buckling and Vibration Analysis of Thin-Walled Members*, <http://www.civil.ist.utl.pt/gbt/>
- [8] Schardt R. *Verallgemeinerte Technische Biegetheorie*. Springer Verlag, Berlin, (in German), 1989.
- [9] Schardt R. Generalized beam theory – An adequate method for coupled stability problems. *Journal of Thin-Walled Structures*, Vol.19, pp.161-180, 1994.
- [10] Gonçalves R, Dinis P, Camotim D. GBT formulation to analyze the first-order and buckling behaviour of thin-walled members with arbitrary cross-sections. *Journal of Thin-Walled Structures*, Vol.47, No. 5, pp. 583-600, 2009.
- [11] Camotim D, Basaglia C, Silvestre N. GBT buckling analysis of thin-walled steel frames: A state-of-the-art report, *Journal of Thin-Walled Structures*, Vol. 48; No 10-11, pp. 726-743, 2010.
- [12] Silvestre N. Generalised beam theory to analyse the buckling behaviour of circular cylindrical shells and tubes. *Journal of Thin-Walled Structures*, Vol. 45, No 2, pp. 185-198, 2007.
- [13] Silvestre N. Buckling behaviour of elliptical cylindrical shells and tubes under compression. *International Journal of Solids and Structures*, Vol. 45, No 16, pp. 4427-4447, 2008.
- [14] Nedelcu M. GBT formulation to analyse the behaviour of thin-walled members with variable cross-section. *Journal of Thin-Walled Structures*, Vol. 48, No. 8, pp. 629-638, 2010.
- [15] Nedelcu M. GBT formulation to analyse the buckling behaviour of isotropic conical shells. *Journal of Thin-Walled Structures*, Article in Press, 2011, [doi:10.1016/j.tws.2011.02.006](https://doi.org/10.1016/j.tws.2011.02.006).
- [16] Bebiano R, Silvestre N, Camotim D. GBT formulation to analyze the buckling behaviour of thin-walled members subjected to non-uniform bending. *International Journal of Structural Stability and Dynamics*, Vol. 7, No. 1, pp. 23-54, 2007.
- [17] Ascher U, Mattheij R, Russell R. *Numerical Solution of Boundary Value Problems for Ordinary Differential Equations*, SIAM, Philadelphia, PA, 1995.
- [18] Goldfeld Y, Sheinman I, Baruch M. Imperfection sensitivity of conical shell. *AIAA Journal*, Vol. 4, No. 3, pp. 517–524, 2003.
- [19] Donnell LH. *Stability of thin-walled tubes under torsion*. NACA TR-479, 1933.
- [20] Sanders JL. Nonlinear theories for thin shells. *Quarterly Journal of Applied Mathematics*, Vol. 21, No. 1, pp. 21–36, 1963.
- [21] Timoshenko S, Woinowsky-Krieger S. *Theory of Plates and Shells*, McGraw-Hill, New York, 1959.
- [22] *MathWorks*. MATLAB R2006b. 2009. (last visited 1 Aprilie 2012), [www.mathworks.com](http://www.mathworks.com)
- [23] Ronagh HR, Bradford MA, Attard MM. Nonlinear analysis of thin-walled members of variable cross-section. Part II: Application, *Journal of Computers and Structures*, Vol. 77, pp. 301-313, 2000.
- [24] Hibbit, Karlsson and Sorensen Inc. *ABAQUS Standard (Version 6.3)*, 2002.
- [25] Cole PP, Abel JF, Billington DP. Buckling of cooling tower shells: Bifurcation results. *Journal of the Structural Division*, ASCE, Vol. 101, No. ST6, pp. 1205-1222, 1975.

# Full Scale Test of a Prestressed Concrete T-Beam

Mircea I. PĂSTRĂV\*<sup>1</sup>

<sup>1</sup> The National Institute for Research and Development in Building, Urbanism and Sustainable Territorial Development – URBAN-INCERC - NIRD “URBAN-INCERC” Cluj-Napoca Branch, 117 Calea Florești, 400524 Cluj-Napoca, Romania

Received 21 March 2011; Accepted 5 June 2011

## Abstract

*The paper presents aspects from the strength test of a full scale prestressed concrete T-beam, performed at the Transylvania Motorway site. The test was done at the request of Bechtel International Inc Reno Nevada Cluj Branch, general contractor of the project. The paper presents the testing procedure, equipment, load history and emphasizes the behavior under loading of a 24m span girder used at the bridges superstructure, including deflection, strains, cracking and failure mechanism. The paper ends with conclusions and commentaries.*

## Rezumat

*Lucrarea prezintă aspecte ale încercării de rezistență efectuate pe o grindă de beton precomprimat, la scară naturală, efectuată la șantierul Autostrada Transilvania. Testul a fost efectuat la solicitarea Bechtel International Inc Reno Nevada Sucursala Cluj, contractorul general al proiectului. Lucrarea prezintă modul de încercare, echipamentele, istoria încercării și descrie modul de comportare sub încărcări a grinzii de 24 m deschidere utilizată la tablurile podurilor, incluzând deplasările, deformațiile specifice, fisurarea și mecanismul de cedare. Lucrarea se încheie cu concluzii și comentarii.*

**Keywords:** Prestressed concrete, beam, bridge, testing, cracking, strain, deflection, failure

## 1. Introduction

This paper deals with the destructive test performed on the 24 m span, precast prestressed concrete T beam, to be certified for use at Transylvania motorway bridges and viaducts [1], [2] and [3].

The girder was manufactured by Bechtel International Inc. Reno Nevada Cluj-Napoca Subsidiary, in accordance with the design drawn up by IPTANA SA Bucharest [4].

The full scale test was performed in a stand, at the site of the production plant in Săvădisla Camp, in October 2009.

The T-beam was made of C 50/60 concrete.

Prestressing was made by 30 strands, T 12.9 mm positioned on the tensioned area and 2 strands T 12.9 mm in the tensioned area of the girder (EN 10138-3-Y1860 S7-12.9-F1-C1); as passive reinforcement, OB 37 and PC 52 mild steel were used.

The total weight of the T beam was 193 kN.

---

\* Corresponding author: Mircea I. Păstrav, Tel. 0720 026 642/ Fax.: 0264 425 462  
E-mail address: [mircea.pastrav@incerc-cluj.ro](mailto:mircea.pastrav@incerc-cluj.ro)



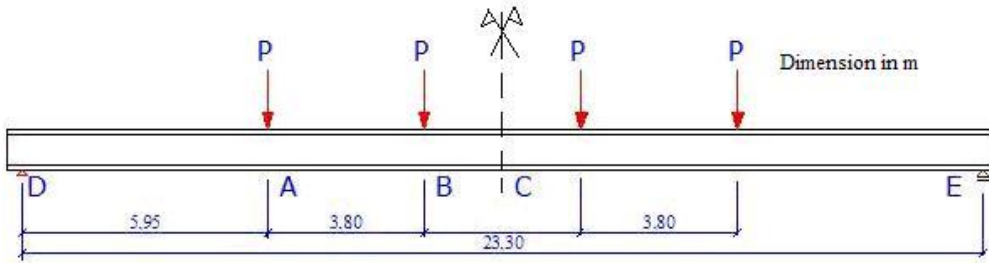


Figure 3. Statically scheme

The actual set-up is presented in Fig. 4.



Figure 4. T- 24m beam in the test stand in Săvădisla Camp

The load was applied by a hydraulic jack of a 1200 kN capacity connected to an electric pump. For force and displacement measurements, a Hottinger-Baldwin Messtechnik data acquisition system was used. The Spider 8 was connected at a C6A/2000 kN load cell and to 5 displacement transducers HBM-WA/300 mm and the data were stored on a PC using the Catman Easy soft. The displacements were also measured by 5 mechanical flexmeters, having 0.1 mm precision. Strains at the mid span of the beam were measured using dial coparators with 0.01 mm precision. Cracks width has been monitored using a crack magnifying glass. The equipment layout is shown in Fig. 5.

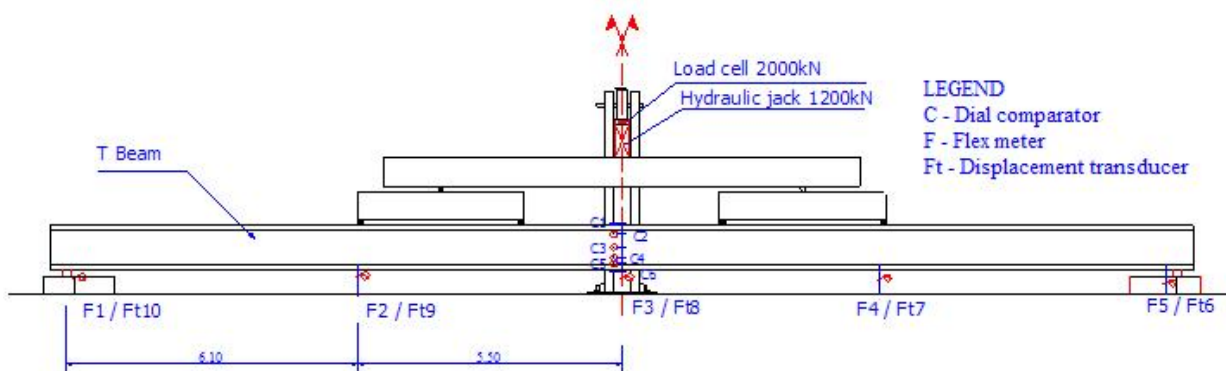


Figure 5. Layout of the load system and measuring devices

### 3. Calculated control values

The design bending moment was  $M_D = 1303$  kNm. This moment could not be used directly for the test, due to a different loading system applied to the beam when part of the bridges superstructures is missing and when the specimen is tested under 4 equivalent forces  $P$  (Fig. 3). The control values of the equivalent forces, stress, deflection, cracking and ultimate moment were computed by the designer IPTANA S.A. and are briefly presented in Table 1.

Table 1. Control values

Stage	M	4 P	$\Delta$	$\sigma_{cP}^U$	$\sigma_{cP}^L$	$\sigma_c^U$	$\sigma_c^L$
	kNm	kN	mm	MPa	MPa	MPa	MPa
SLEN	1501.2	382.4	62.1	+15.60	-20.58	+18.30	+1.23
Initiation of cracking	1793.0	456.8	74.2	+18.64	-24.59	+21.34	-2.78
Ultimate	3526.9	898.4	146.0	-	-	-	-

SLEN - normal exploitation service state;

M - bending moment;

P - equivalent force acting as in Fig. 5;

$\Delta$  - deflection;

$\sigma_{cP}^U$  - stress in concrete upper fiber of the T- beam due to P forces;

$\sigma_{cP}^L$  - stress in concrete lower fiber of the T- beam due to P forces;

$\sigma_c^U$  - total stress in concrete upper fiber of the T- beam;

$\sigma_c^L$  - total stress in concrete lower fiber of the T- beam;

Note: Values of M,  $\Delta$  and  $\sigma$  are calculated in the mid-span of the girder.

### 4. Test results

Before test, a visual survey has been done, and no cracks, segregation of the concrete mix or surface defects have been observed.

#### 4.1 Deflections

The measured camber of the beam, under the load of the test devices ( $P = 35$  kN), was 30 mm.

The deflections of the T-beam under the hydraulically applied forces, along the girder axis, are presented in Fig. 6 to Fig. 10, at all 3 steps, respectively for all five loading cycles.

In the graphical representations, the initial position of the beam is considered horizontal under self weight loading and total force  $4P = 140$  kN.

The deflection at the mid-span of the T-beam under the loading is shown in Fig. 11

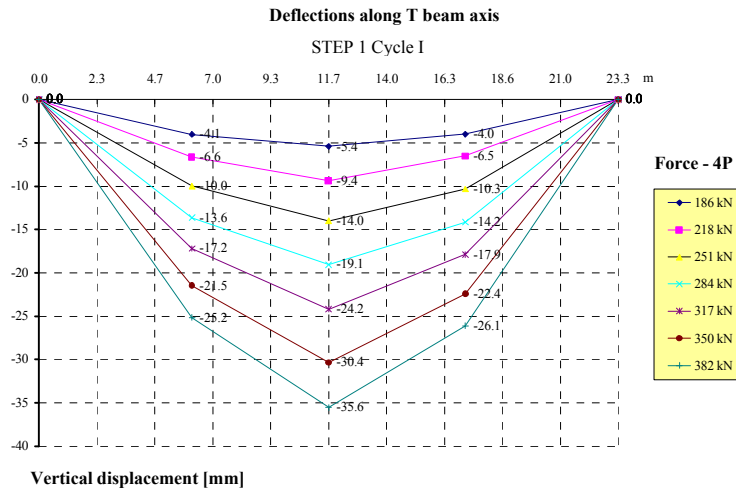


Figure 6. Deflections at first cycle of loading

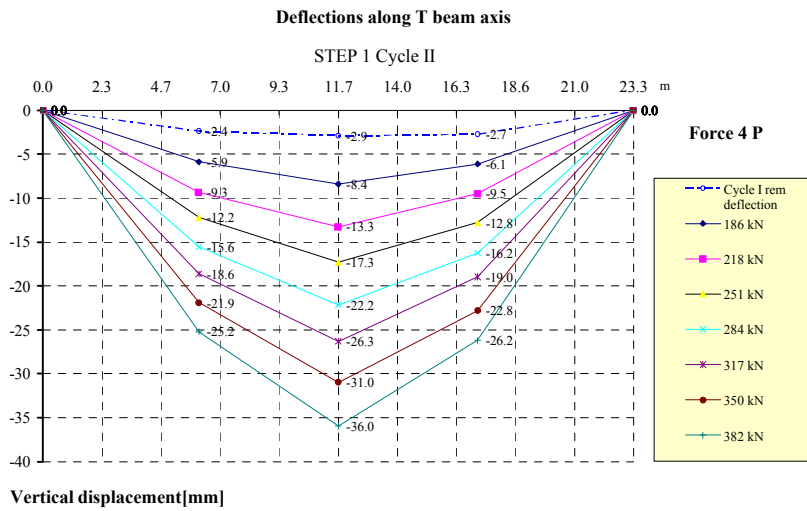


Figure 7. Deflections at second cycle of loading

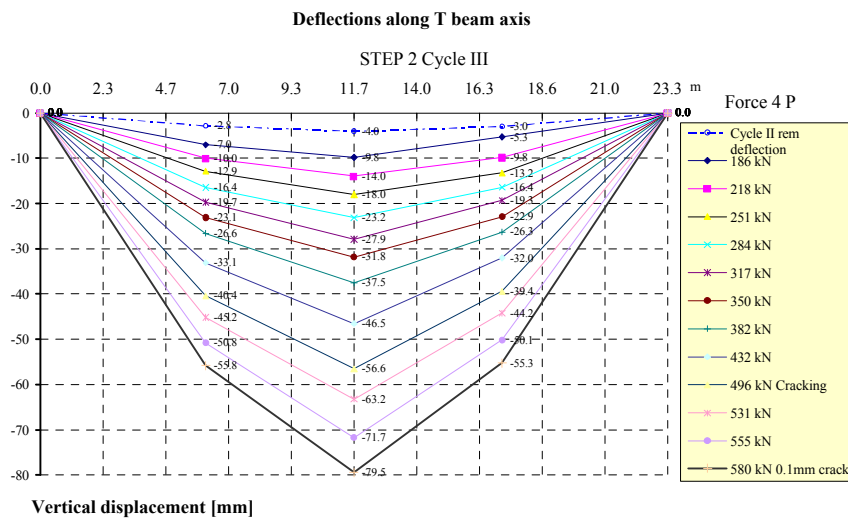


Figure 8. Deflections up to the load corresponding to a maximum 0.1 mm crack width

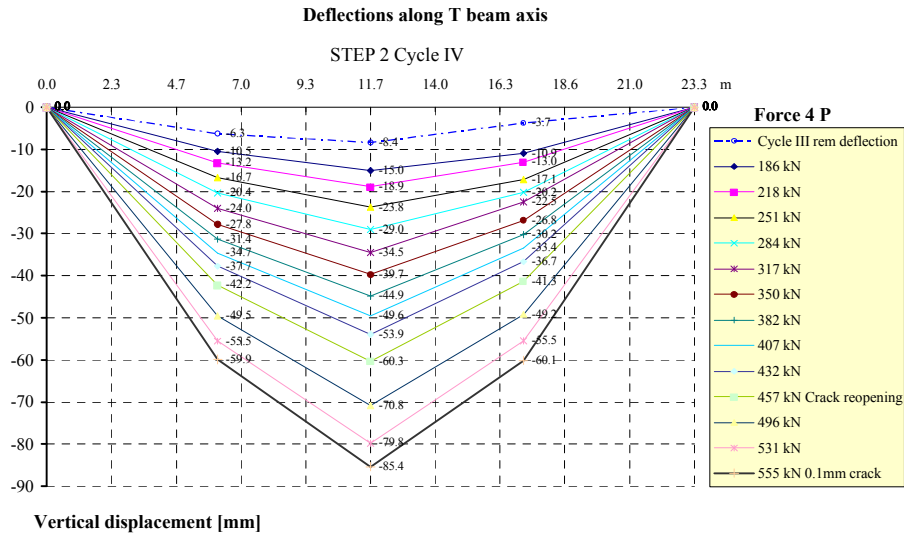


Figure 9. Deflections up to the load corresponding to a maximum 0.1 mm crack width, 2<sup>nd</sup> loading

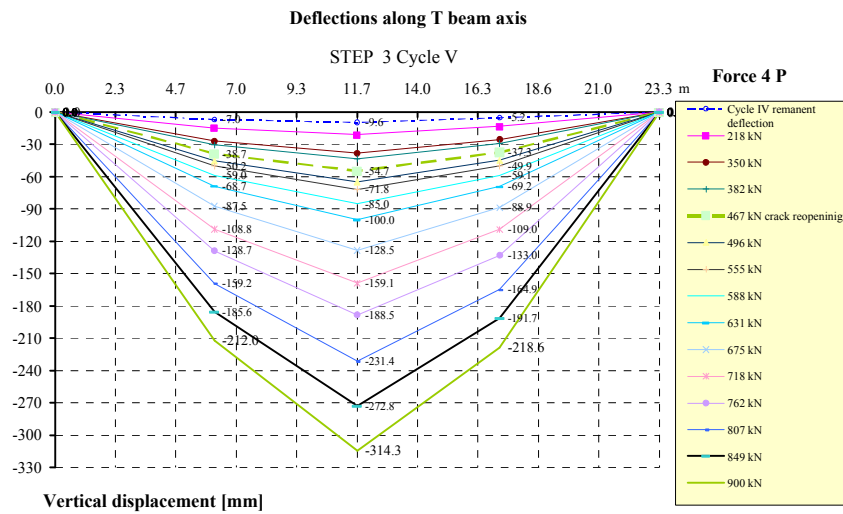


Figure 10. Deflections at Step 3 of loading

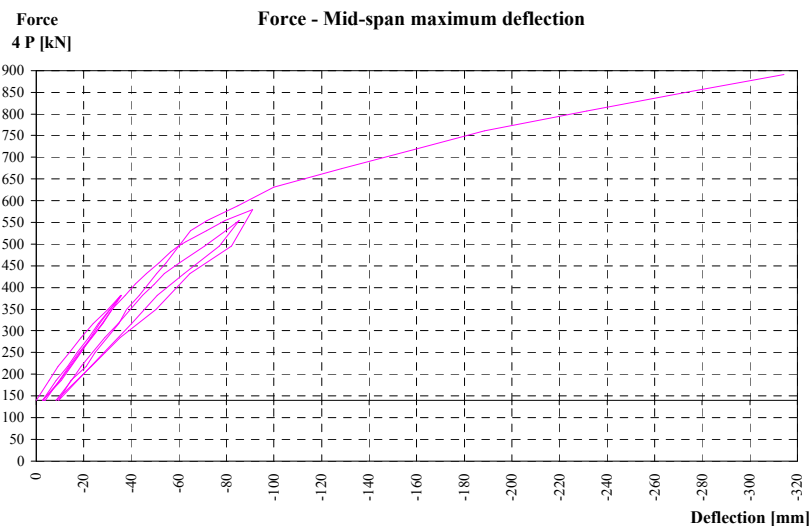


Figure 11. Force-Deflection diagram at the mid-span of the T- beam

### 4.2 Strains

The strain development under loading, in the mid-span cross section of the tested member, is shown in Fig. 12.

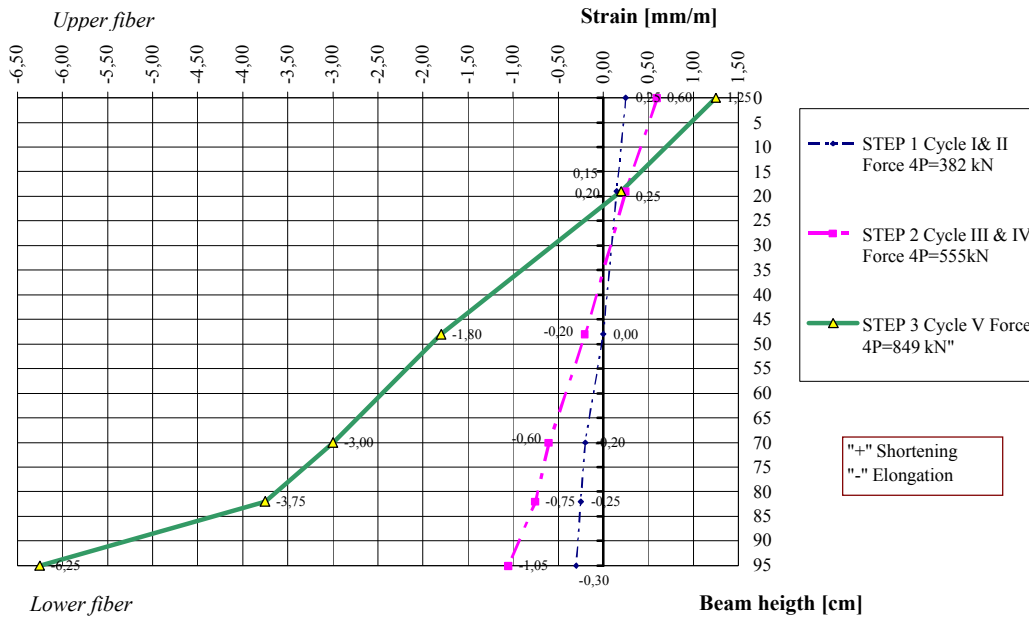


Figure 12. Strains in the mid-span of the T-beam

### 4.3 Cracking

Cracking pattern and details are shown in Fig. 13 to Fig. 15. Ends of the beam remained un-cracked up to 4.0 m measured from the supports at all loading levels. First, cracks initiated in the middle of the beam and then they developed toward the endings. Dens cracking pattern was observed with a relatively even distribution, with vertical directions of cracks till 6 meters from edges. The cracks direction in the span from 4 to 6 meters to the both ends was inclined to angles up to 45° to horizontal line.

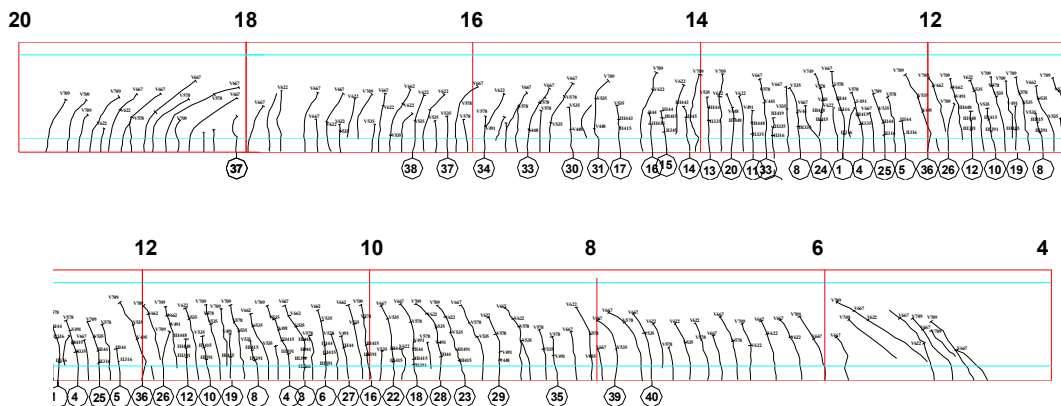


Figure 13. Cracking pattern (Section 12 is the mid-span of the T- beam)





a) The maximum experimental deflection  $\Delta_{exp}$  should be less than 1.1 times the calculated control value,  $\Delta_{cal}$ :

$$\Delta_{exp} = 6.0 \text{ mm} < \Delta_{cal} 1.1 * 62.1 \text{ mm} = 68.3 \text{ mm}$$

b) The maximum experimental deflection should be less than  $L / 800$ :

$$\Delta_{exp} = 6.0 \text{ mm} < 23300 \text{ mm} / 800 = 29.1 \text{ mm}$$

c) The partial remanence factor could not be determined due to the fact that the unloading was not complete, but even so, at the equivalent loading of 140 kN, a camber of 26.0 mm was registered.

The T-beam met the requirements, from the deflection point of view.

## 5.2 Strains and stresses

A comparison between estimated stress in upper and lower concrete fiber was done after the calculated values were revised in order to fit the actually measurements after the loading devices were put on the beam. So the control values were named as  $\delta\sigma_{cP}^U$  - stress variation in concrete upper fiber of the T-beam due to P forces respectively,  $\delta\sigma_{cP}^L$  - stress variation in concrete lower fiber of the T-beam due to P forces were re-evaluated, and for the initiation of cracking moment the actual value was used. The strains were multiplied by the concrete elasticity modulus. The results are presented in Table 2.

Table 2. Re-evaluated control values

Stage	M	4 P	Calculated		Measured	
			$\sigma_{cP}^U$	$\sigma_{cP}^L$	$\sigma_{cP}^U$	$\sigma_{cP}^L$
	kNm	kN	MPa	MPa	MPa	MPa
SLEN	951.4	382	+9.87	-13.03	9.25	-11.10
Estimated initiation of cracking	1792.9	456.8	+14.57	-19.21	13.00	-18.50

No explicit conformity criterion is given, but good correspondence between calculated and measured values of stress at the upper and the lower mid-span section was found.

## 5.3 Cracking

No cracks have been registered at the step 1 of loading, so the tested member met the requirement of working un-cracked at normal exploitation limit state.

At cycle III of loading, the initiation of cracking was observed at a loading equal to 496.0 kN exceeding the estimated one, of 456.8 kN;

At cycle IV of loading, the re-opening of the cracks occurred at a load of 456.8 kN.

## 5.4 Failure

The maximum load was 900 kN, equal to the estimated one, so the T-24 m span beam met this last requirement without actually breaking, as the failure criterion used was an arbitrary one, as previously mentioned.

The failure mechanism could not actually be revealed, but it is more likely that the failure mechanism is a bending ductile one, based on large recorded deflection, cracking pattern and the large L/h ratio of the T-beam.

## 6. Final remarks

The prestressed concrete T-beam of 24 m span, tested in the stand, met all the conformity requirements. More, it had a uniform cracking pattern up to the maximum load, no crack width exceeded 0.4 mm and a quasi-elastic behavior has been observed after the unloading. The maximum residual deflection was equal to the camber under the test devices loading, respectively 30 mm and the cracks width reduced to 0.1...0.2 mm or even closed.

This good behavior of the tested T-beam assures the durability for the designed service life of the girders of the same type, used at the superstructures of bridges and viaducts of Transylvania motorway.

## Acknowledgements

To Bechtel International Inc. Cluj Branch, Săvădisla Camp team, for preparing the test and to my researcher colleagues who helped me performing the test.

## 7. References

- [1] INCERC Cluj Branch, Test report No. 977, Cluj Napoca, 2009 (in Romanian)
- [2] INCERC Cluj Branch, T 24m Bridge Beam Test Review, Cluj Napoca, 2009 (in Romanian)
- [3] Mircea C., Ioani A. & Kiss Z., Test on a bridge PC girder. In: *Shell and Spatial Structures: New Materials and Technologies, New Designs and Innovations - A Sustainable Approach to Architectural and Structural Design, IASS Symposium Acapulco, Extended abstracts*, Mexico, pp 179-180, 2008
- [4] IPTANA SA., Bridges on Motorway, "T" Beam Testing, Revision A, Bucharest, 2009
- [5] Păstrav M., Stand for Testing 37 m Span Prestressd Beams, Revista "Urbanism, arhitectură, construcții", **Vol. 2**, Nr. 1 / 2011, pp. 21-24 (in Romanian)
- [6] STAS 12313-85 Railway and Road Bridges. Stand Testing of Concrete, Reinforced Concrete and Prestressed Concrete Members (in Romanian)

## SEMIRIGIDITY. PAST AND PRESENT

Moldovan Corina  
Technical College "A. Saligny", Cluj-Napoca, Romania

Received 23 June 2011; Accepted 20 August 2011

### Abstract

*The present contribution is intended to be a state of the art review of semirigidity problem associated to steel multi-storey skeletal structures. It has been a long time since semirigidity is no longer regarded as an erection fault. Today, the semirigidity has achieved a design code status. A decisive role in this development of semirigidity has been played by Northridge 1994 earthquake. This unfortunate event triggered the signal that welded (rigid) beam – column connections of frame type structures miss a vital mechanical property: the ductility.*

*Starting at this stage, the present paper reviews the analytical results regarding the constitutive bending moment – relative rotation relations. Several such relations are presented together numerical examples associated to beam to column connections of engineering practice in the field of steel skeletal structures. Also, numerical studies are conducted to several planar semirigid steel frames including the reference case of a rigidly connected (end plate type beam – column connection) structure. After a short presentation of seismic performances of structures and the principles of performance based design, several numerical studies (geometrically nonlinear analyses) on semirigidly connected structures are conducted.*

*The results of these numerical studies are presented in the manner of performance based analysis focusing on force (lateral top) displacement constitutive relationship. The obtained numerical results are presented in a graphical comparative manner that exhibits the influence of semirigidity at beam – column connection level on general lateral rigidity of the structure.*

### Rezumat

*Lucrarea constituie o trecere în revista a problematicei structurilor multietajate din oțel cu conexiuni semirigide la nivelul rigle – stâlpi. După o scurtă revedere a problemei semirigidității, este evocat momentul decisiv al intrării semirigidității „pe ușa din față” în proiectarea structurilor de tip cadre multietajate din oțel amplasate în regiuni seismice – cutremurul Northridge 1994. Sunt subliniate câteva avantaje ale considerării semirigidității evidențiindu-se cel adus de conferirea de ductilitate în comportarea la acțiuni seismice. Încadrarea semirigidității în codurile de proiectare – în primul rând în EUROCODE 3 este, de asemenea, evocată și prezentată grafic. Referirile teoretice sunt însoțite de studii numerice constituite din analize geometrice neliniare ale unor structuri cu conexiuni semirigide la nivelul rigla – stâlp. Analizele sunt precedate de o succintă prezentare a proiectării pe baze de performanțe seismice. Aceasta prezentare deschide posibilitatea focalizării rezultatelor numerice ale analizelor pe parametrii asociați performanțelor seismice.*

*Studiile numerice sunt conduse pe structuri având diferite tipuri de îmbinări semirigide rigle – stâlpi selectate din setul restrâns de tipuri mecanice de îmbinări folosite în practica ingineriască. Rezultatele numerice obținute sunt focalizate pe relația constitutivă forța laterală – deplasare*

---

<sup>1</sup> \* Corresponding author: Tel.: 0040723193962  
E-mail address: corina\_mold2003@yahoo.com

*laterală a ultimului nivel, constituind, astfel, o analiză de tip „pushover”. Curbele de tip „pushover” obținute sunt prezentate într-o manieră comparativă între diferitele tipuri de conexiuni rigla – stâlp. În același timp, curbele evidențiază efectul semirigidității de la acest nivel asupra rigidității laterale a structurii.*

**Keywords:** semirigid connections, relative beam – column rotations, constitutive bending moment – relative rotation relation, nonlinear performance based analysis

## 1. Introduction

According to the past and – on a large extent – to the present tradition - the steel frame analysis and design processes assume that beam-to-column connections exhibit either a rigid or a pinned behaviour. Rigid connections, where no relative beam – column rotations occur between the connected members, transfer great amounts of stress resultants (bending moments, shear forces, axial forces, and torsion moments) between structural members connected in the respective joint. Opposite to rigid connections, the pinned connections may be characterized by almost free rotation movement between the connected elements that prevents the bending moment transfer. In spite of this old and present belief, observations on real behaviour of steel frame type structures lead to the conclusion that the great majority of joints does not exhibit either of such idealized behaviour. These are the flexible or semirigid connections (Fig.1), and it is a common place that their design should be performed according to their actual (flexible) structural behaviour.

The approach of scientists to the semirigidity followed two ways: a laboratory extensive research and a theoretical approach to the computation (analysis / design) of these types of steel structures. The experimental / laboratory research focused on the behaviour of beam to column zone behaviour (Fig.2) under both, monotonic and cyclic loadings (Fig.3). The target of experimental work has been the constitutive relation bending moment – relative rotation in semirigid connections (Fig.2). The experimental work extended over more than 30 years and resulted in important results concerning the assessment of the actual behaviour of such joints. Numerous studies were made on composite and steel semi-rigid connections including: state of the art reports [1], [2], numerical studies and experiments [2], [3], [4]. The fundamental results of these experimental investigations led to code specifications that provided structural designers with adequate procedures to evaluate the semi-rigid connections structural capacity. A good example of this new design trend is currently found in Eurocode 3 [5].

The theoretical component of research on semirigidity focused on analytical models of – mainly – bending moment – relative rotation constitutive relationship. This relationship has been modelled by several analytical relations depending on the mechanical making up of beam – column connections of engineering practice (Fig.1). The proposed analytical models have been (mathematically) adapted to match experimental results and, it may be concluded, that at present the proposed models not only exhibit an acceptable accurate behaviour of beam to column connection, but, also, are they undisputed and accepted in what concerns the semirigid behaviour of steel frames with bolted beam – column joints.

The most important victory on the “semirigidity front” is, by no means, the introduction of semirigid connectivity in code design provisions regulating the design activity in a large number of countries. Also, a relevant development in the field of semirigidity has been achieved in what concerns the computational means. Strong algorithms have been developed [6] that deal with advanced analysis including the flexible connexions. Present contribution focuses on the most important results and aspects of semirigid behaviour of planar steel multi-storey frames acted upon by static and dynamic loadings.

## 2. Why semirigid connectivity?

For a long time, seismic design of steel structures followed the fully welded connections solution. Welded connections are mainly used in moment resisting frames. More economical types of bolted connections were not utilized mainly due to their relative flexibility (semirigidity) as compared to fully welded connections, which may lead larger deformations (both, rotations and lateral and vertical displacements / deflections) under the same forces. Whereas this consequence applies for static conditions, the response under dynamic loading may be substantially different. Due to the period elongation of the frame as well as the higher energy dissipation in the connection, semirigid frames are associated to lower loads and possess higher structural damping. Consequently, the displacements associated with bolted frames may be not only be allowed, but they may be lower than those associated to the welded frames.

The significance of examining the behaviour of semirigid frames under earthquake loads has been initiated and soon got an urgency feature immediately after reported failures in welded connections (of steel multi-storey structures) during the Northridge earthquake of 1994 [3]. The conclusions inferred from Northridge earthquake damages were sustained by further evidence from the Hyogo-ken Nanbu (Kobe) earthquake of 1995. These repeated observations of failure and damages in welded steel structures lead to further effort to and research regarding the behaviour of flexibly connected steel frames. A great deal of laboratory research has been dedicated to the utilization of non - welded forms of connection.

In spite of the substantial increase in the knowledge of structural design of steel structures, the semi-rigid connection solution is still facing lack of confidence from many structural engineers. The opposition to semirigidity may be explained by:

1. Lack of detailed information on the advantages of semi-rigid design philosophy. This may be concluded not only among the structural designers, but among the university education as well. In this matter, it has to be noted that semi-rigid steel frame design has certain advantages. Among these, one may include:

- *Material economy*. Investigations showed that for a four story semi-rigid floor system up to 15% economy in terms of steel weight was reached even when compared to the traditional most economical solution. As these structures are used in large scale construction the achieved 15% weight reduction can generate an even greater economy [3], [4].

- *Ductility*. The components of partial strength joints can deform in a ductile manner in the case of strong earthquake. In the common case where beam sizes are governed by drift or alike design criteria, rather than flexural strength requirements, ductile partial strength connections allow the formation of a desirable beam hinging global frame mechanism. The possibility of using partial strength connections as the main energy dissipative mechanism for the seismic resistance of frames has now been recognized in modern design codes [2].

2. Complexity and difficulty of effective tools (soft products) for global analysis of semi-rigid frames. The non linear characteristics of a steel beam-to-column connection play a very important role for frame global analysis. Although modern structural steel and composite codes [5], [7] include procedures and formulas to define both the stiffness and resistance of semi rigid connections there is no explicit method to model and analyze frames with these connections.

3. The necessity of applying specific analytical models (Fig.4) for each type of beam to column connection used in engineering practice. [8]. This specificity of analytical model is imposed by the results of a very large experimental data base.

The design and construction of steel, as compared to others, is not yet at its outset in our country which leads to lack of experience. Besides the behaviour of semi rigid connections is very dependent on experimental investigations which is not possible in our country due to the cost associated. Hence structural engineers usually face the problem of experimentally validated

connection data bases which, in consequence, hinders the planning of structural steel frames of semi rigid nature.

### 3. Modelling of semirigidity at beam – column connection level

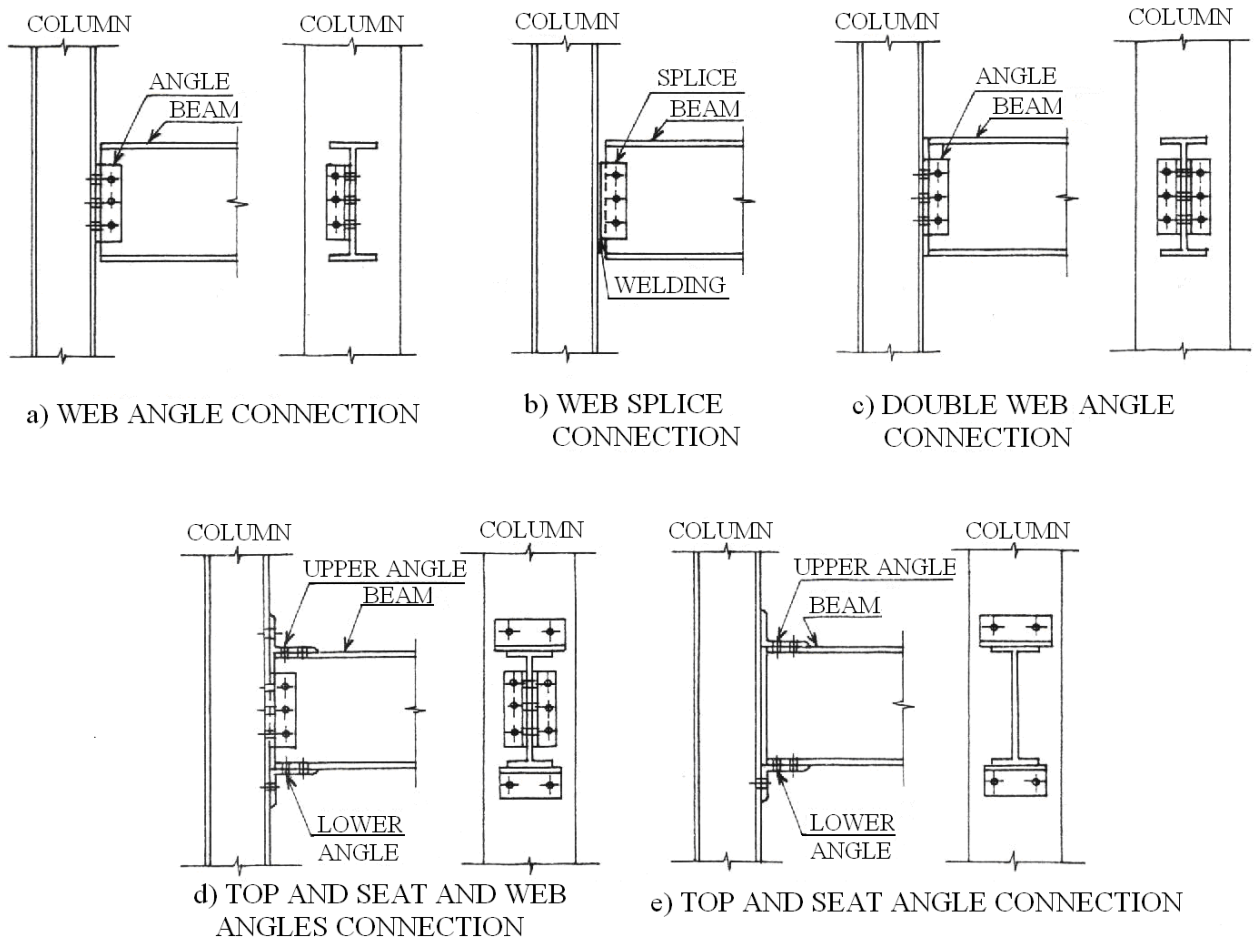


Fig. 1. Beam – column connections of engineering practice

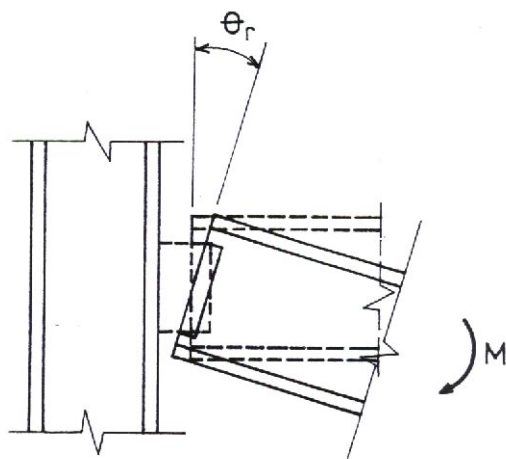


Fig.2. Classical relative rotation of the beam in a semirigid connection

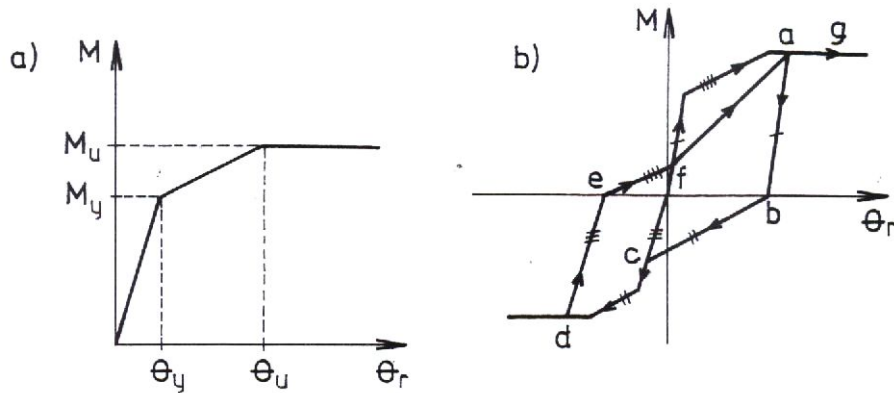


Fig. 3. Monotonically and cyclical bending moment – relative rotation curves

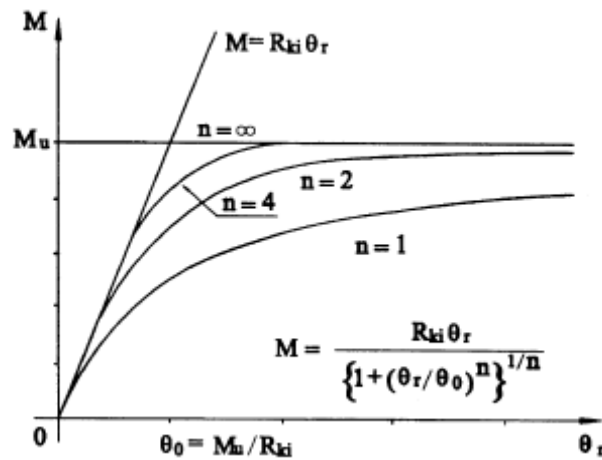


Fig.4 – Bending moment – relative rotation curve. Three parameter power model

The generalized form of this model is:

$$M = R_{ki} \cdot \theta_r / [1 + (\theta_r / \theta_0)^n]^{1/n}$$

where:

$R_{ki}$  = initial connection stiffness

$M_u$  = ultimate bending capacity

$\theta_0 = M_u / R_{ki}$

$n$  = shape parameter

Classification of beam-column connections was, among others, a target of different researches (Fig.5, [9]).



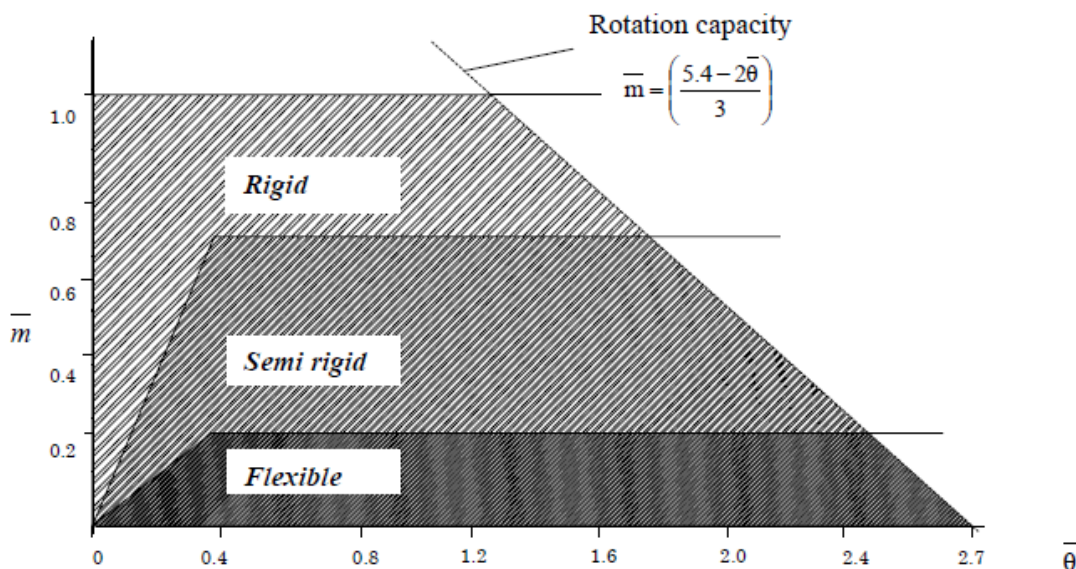


Fig.5 Classification of beam – column connection according to Bjorhovde et al. (1990)

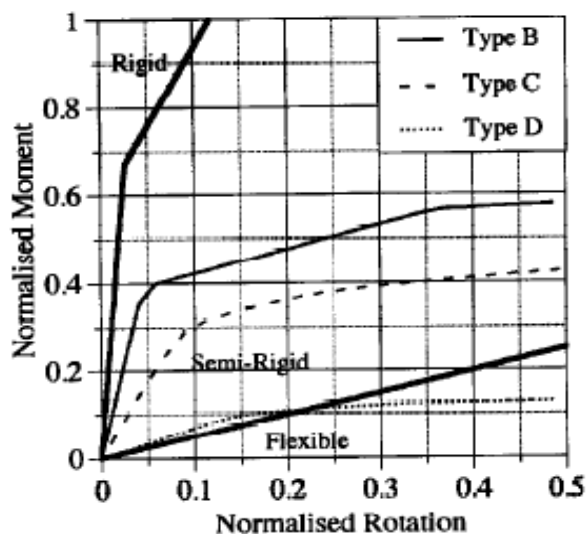


Fig.6. Classification of connection according to EUROCODE 3

The EC3 classification of beam to column connections (Fig. 6) highlights several types of semirigid beam to column connections. Out of the engineering practice types of connections, the following four types are presented from the point of view of normalized moment ( $M/M_u$ ) – normalized relative rotation ( $\theta_r/\theta_u$ ) relationship:

- Type A - Fully rigid connections. They are fully welded and no shear panel deformation is taken into account;
- Type B - Fully rigid connections. They are fully welded but the shear panel deformation is taken into account;
- Type C - Semirigid connections: top angle, seat angle and two web angle connections;
- Type D – Semirigid connections. Top and web angles

## 4. SEISMIC PERFORMANCE BASED DESIGN

At the beginning of 20<sup>th</sup> century, most of the steel building design had been based on the use of linear analysis methods. Although an elastic analysis gives a good indication of the elastic capacity of structures and indicates where first yielding will occur, it cannot predict failure mechanisms and account for the redistribution of forces during progressive yielding. The use of inelastic procedures for design and evaluation is attempts to help engineers better understand how structures behave when subjected major earthquakes, where the elastic capacity of structures is exceeded.

Recently, the direction of building design in seismic regions has been towards Performance Based Seismic Design. The purpose of this design method is to accurately predict the performance of a building during any intensity of earthquake ground motion that may occur at the building site during the design life of the building. In most of the analysis, the effects of semi-rigid connections are not taken into consideration. However, these effects considerably affect the response and seismic performance of the steel frame.

Design and evaluation procedure following the Performance Based Seismic Design Methodology enables the structural engineer to quantify the probability that a building design satisfies specified seismic performance objectives. Also, as can be seen in the preceding chapter, a good performance based analysis can result in optimum frame sections. Two other key terms, demand and capacity, come into scene with the matter of performance.

In short demand is a representation of the earthquake ground motion. This motion produces complex horizontal displacement patterns in structures that may vary with time. For a given structure and ground motion, the displacement demand is an estimate of the maximum expected response of the structure during the ground motion [10].

On the other hand, capacity is a representation of structure's ability to resist seismic demand. The overall capacity of a structure depends on the strength and deformation capacities of the individual components of the structure. In order to determine capacities beyond the elastic limits some form of nonlinear analysis, such as Pushover Procedure, is required [10]. The detail of this procedure is given in the following pages but in short this procedure uses series of sequential elastic analysis each contributes to reflect the nonlinear response of the structure.

The performance is dependent on the manner that the capacity is able to handle the demand. In other words, the structure must have the capacity to resist the demands of the earthquake such that the performance of the structure is compatible with the objectives of the design. Once capacity curve and demand displacement are defined, a performance check can be done. This check verifies that structural and non-structural components are not damaged beyond the acceptable limits of the performance objective for the forces and displacements implied by the displacement demand.

Nonlinear analysis methods are the fundamental tools for accurately evaluating building performance objectives. As stated earlier, nonlinear static "pushover" analysis methods are accepted as convenient methods for estimating building response quantities and predicting building performance in a Performance Based Seismic Design. The documents related with Performance Based Seismic

Design Methodology are ATC-40 and FEMA 273. ATC-40 was published in 1996 by Applied Technology Council [10], as a report entitled "Seismic Evaluation of Retrofit of Concrete Buildings" ATC-40 [10] and FEMA 273 was published in 1997 by Federal Emergency Management Agency, as a report entitled "NEHRP Guidelines for the Seismic Rehabilitation of Buildings".

### 4.1 Performance Levels

Both ATC-40 [10] and FEMA 273 propose different performance levels for the seismic rehabilitation of building structures. Different performance levels according to FEMA 273 are described as follows:

**Immediate Occupancy Performance Level (S-1):** Structural Performance Level S-1, immediate occupancy, means the post-earthquake damage state in which only very limited structural damage has occurred. The basic vertical - and lateral force- resisting systems of the building retain nearly all of their pre-earthquake strength and stiffness. The risk of life-threatening injury as a result of structural damage is very low, and although some minor structural repairs may be appropriate, these would generally not be required prior to re-occupancy.

**Life Safety Performance Level (S-3):** Structural Performance Level S-3, Life Safety, means the post-earthquake damage state in which significant damage to the structure has occurred, but some margin against either partial or total structural collapse remains. Some structural elements and components are severely damaged, but this has not resulted in large falling debris hazards, either within or outside the building. Injuries may occur during the earthquake; however, it is expected that the overall risk of life-threatening injury as a result of structural damage is low. It should be possible to repair the structure; however, for economic reasons this may not be practical. While the damaged structure is not an imminent collapse risk, it would be prudent to implement structural repairs or install temporary bracing prior to re-occupancy.

**Collapse Prevention Performance Level (S-5):** Structural Performance Level S-5, Collapse Prevention, means the building is on the verge of experiencing partial or total collapse. Substantial damage to the structure has occurred, potentially including significant degradation in the stiffness and strength of the lateral-force resisting system, large permanent lateral deformation of the structure, and—to a more limited extent—degradation in vertical-load-carrying capacity. However, all significant components of the gravity-load- resisting system must continue to carry their gravity load demands. Significant risk of injury due to falling hazards from structural debris may exist. The structure may not be technically practical to repair and is not safe for re-occupancy, as aftershock activity could induce collapse.

**Damage Control Performance Range (S-2):** Structural Performance Range S-2, Damage control, means the continuous range of damage states that entail less damage than that defined for the Life Safety level, but more than that defined for the Immediate Occupancy level. Design for Damage Control performance may be desirable to minimize repair time and operation interruption; as a partial means of protecting valuable equipment and contents; or to preserve important historic features when the cost of design for Immediate Occupancy is excessive. Acceptance criteria for this range may be obtained by interpolating between the values provided for the Immediate Occupancy (S-1) and Life Safety (S-3) levels.

**Limited Safety Performance Range (S-4):** Structural Performance Range S- 4, Limited Safety, means the continuous range of damage states between the Life Safety and Collapse Prevention levels. Design parameters for this range may be obtained by interpolating between the values provided for the Life Safety (S-3) and Collapse Prevention (S-5) levels.

## 5. Methods of analysis

Rigid frames are analyzed by conventional matrix structural analysis. This analysis assumes that the deformations are relatively small, and the equilibrium equations can be formulated with respect to initial geometry. For this linear elastic analysis, the following structural level constitutive relation (applied forces – associated displacements) holds:

$$[P] = [K][d] \quad (1)$$

where:

[P] = applied force matrix

[K] = global stiffness matrix

[d] = displacement matrix

The applied force vectors [P] and resulted displacements [d] are associated (i.e., they are defined in the same sections of the structure and along the same directions).

At the element level, the first order frame element stiffness matrix  $[k]_e$  has to be defined. It takes the following form [1], [2]:

$$\mathbf{K}_e = \begin{bmatrix} \frac{4EI}{L} & \frac{6EI}{L^2} & 0 & \frac{2EI}{L} & -\frac{6EI}{L^2} & 0 \\ & \frac{12EI}{L^3} & 0 & \frac{6EI}{L^2} & -\frac{12EI}{L^3} & 0 \\ & & \frac{EA}{L} & 0 & 0 & -\frac{EA}{L} \\ & & & \frac{4EI}{L} & \frac{6EI}{L^2} & 0 \\ & & & & \frac{12EI}{L^3} & 0 \\ & & & & & \frac{EA}{L} \end{bmatrix} \quad (2)$$

By proper transformation, the element level relations associated to FEM technique, reaches the structural level *elementary* form [1], [2]:

$$\mathbf{R}^T dr = \mathbf{X}^T dx \quad (3)$$

Where,  $\mathbf{R}$  is the general force matrix,  $\mathbf{X}$  is the structural stress resultants vector and  $dr$  and  $dx$  are the increments in structural displacements  $\mathbf{r}$  and associated member end deformations  $\mathbf{x}$ . More popular, above expression is known as P –  $\Delta$  relation. A graphical representation of above nonlinear constitutive relation and its step – by – step solution is given in Fig. 7.

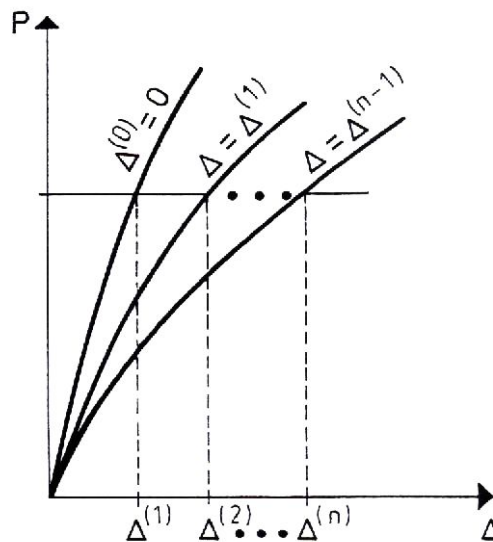


Fig.7. Incremental step – by step P –  $\Delta$  technique

## 6. Algorithm. Case studies

The computer algorithm has been developed for the analysis of steel semirigid skeletal structures and it is adapted for a step - by - step incremental analysis. The semirigid connectivity refers to beam – column connection only. For a reference basis, the rigid connection is, also, considered. The finite dimensions of connection zones are not taken into account. The iterative incremental analysis follows bellow step – by – step technique:

1. The load is applied with its given (total) value considering a homogeneous displacement state and an initial stiffness  $R_{ki}$  for each elastic connection. A displacement state  $S_D^{(1)}$  and a deformation state  $S_d^{(1)}$  are obtained. By their use, a new stiffness matrix is computed using that takes into account the existing deformed state of the structure;
2. The total; load is, again, applied and via deformed state and associated stiffness matrix new displacements and deformation states  $S_D^{(2)}$  and, respectively  $S_d^{(2)}$  are computed
3. The procedure is repeated till the convergence criterion (4) is fulfilled [2]. In a two-dimensional P - D state, the procedure is schematically presented in Fig. 9.

Convergence criterion reads:

$$\frac{\sum_{i=1}^n |D d_k^i|}{\sum_{i=1}^n |d_k^i|} \leq e \quad (4)$$

where:

$n$  is the no of elements

$d_k^i$  is the  $k$  element of displacement vector associated to iteration “i”

$D d_k^i = d_k^i - d_k^{i-1}$

$e = 10^{-3}$

## 7. Case studies

Geometrical nonlinear analyses have been performed for a six level frame with semirigid beam – column connections (Fig. 8). The connections have been considered in several analytical models. Performed analyses are associated to gravitational loads, to lateral (monolithically increasing) load and to a general loading (gravitational + top lateral) (Tables 1,2,3).

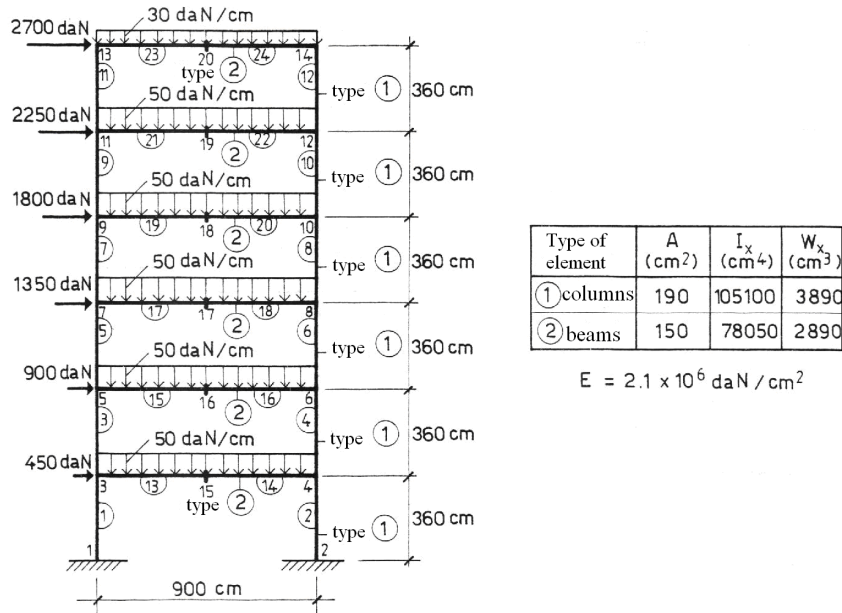


Fig.8. Six level frame

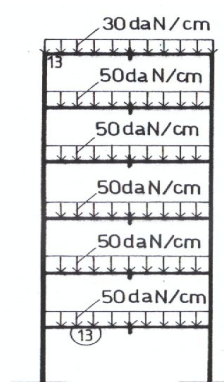
**Case study 1. Six level frame - Total loading case**

Table 1.

$D_{x13}$ [cm]	$M_{I3}^{st}$ [daN·cm]	$M_{I3}^{drt}$ [daN·cm]	<b>Type of connection</b>	<b>Polynomial model</b>			<b>Three parameter model</b>		
				$D_{x13}$ [cm]	$M_{I3}^{st}$ [daN·cm]	$M_{I3}^{drt}$ [daN·cm]	$D_{x13}$ [cm]	$M_{I3}^{st}$ [daN·cm]	$M_{I3}^{drt}$ [daN·cm]
2,41	$0,200 \times 10^7$	$0,189 \times 10^7$	1. Two web angles connection	15,93	$0,747 \times 10^6$	$0,410 \times 10^7$	55,41	$0,214 \times 10^6$	$0,505 \times 10^7$
			2. Top and seat angle connection	27,65	$0,215 \times 10^6$	$0,463 \times 10^7$	55,28	$0,231 \times 10^6$	$0,506 \times 10^7$
			3. Top and seat and web angle connection	3,95	$0,188 \times 10^7$	$0,220 \times 10^7$	37,40	$0,338 \times 10^6$	$0,500 \times 10^7$
			4. End plate connection	11,54	$0,141 \times 10^7$	$0,334 \times 10^7$			

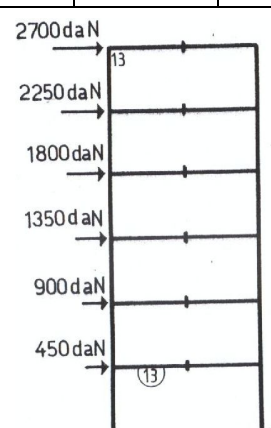
**Case study 2. Six level frame - The case of gravitational loading**

Table 2

Rigid geometrical analysis			Semirigid geometrically nonlinear analysis						
$D_{x13}$ [cm]	$M_{13}^s$ [daN·cm]	$M_{13}^{drt}$ [daN·cm]	Type of connection	Polynomial model			Three parameter model		
				$D_{x13}$ [cm]	$M_{13}^s$ [daN·cm]	$M_{13}^{drt}$ [daN·cm]	$D_{x13}$ [cm]	$M_{13}^s$ [daN·cm]	$M_{13}^{drt}$ [daN·cm]
0,001	$0,318 \times 10^7$	$0,188 \times 10^7$	1. Two web angles connection	0,005	$0,104 \times 10^7$	$0,402 \times 10^7$	0,0013	$0,226 \times 10^6$	$0,484 \times 10^7$
			2. Top and seat angle connection	0,003	$0,538 \times 10^6$	$0,452 \times 10^7$	0,0014	$0,232 \times 10^6$	$0,483 \times 10^7$
			3. Top and seat and web angle connection	0,013	$0,299 \times 10^7$	$0,207 \times 10^7$	0,03	$0,472 \times 10^6$	$0,459 \times 10^7$
			4. End plate connection	0,013	$0,184 \times 10^7$	$0,319 \times 10^7$			

**Case study 3. Six level frame - The case of lateral loading**

Table 3

Rigid geometrical analysis			Semirigid geometrically nonlinear analysis						
$D_{x13}$ [cm]	$M_{13}^s$ [daN·cm]	$M_{13}^{drt}$ [daN·cm]	Type of connection	Polynomial model			Three parameter model		
				$D_{x13}$ [cm]	$M_{13}^s$ [daN·cm]	$M_{13}^{drt}$ [daN·cm]	$D_{x13}$ [cm]	$M_{13}^s$ [daN·cm]	$M_{13}^{drt}$ [daN·cm]
2,34	$-0,144 \times 10^6$	$0,372 \times 10^3$	1. Two web angles connection	6,28	$-0,812 \times 10^6$	$0,214 \times 10^3$	33,97	$-0,225 \times 10^6$	$0,274 \times 10^2$
			2. Top and seat angle connection	18,25	$-0,465 \times 10^6$	$0,828 \times 10^2$	33,85	$-0,232 \times 10^6$	$0,400 \times 10^2$
			3. Top and seat and web angle connection	2,36	$-0,114 \times 10^7$	$0,387 \times 10^3$	22,55	$-0,472 \times 10^6$	$0,142 \times 10^3$
			4. End plate connection	2,35	$0,114 \times 10^7$	$0,152 \times 10^3$			

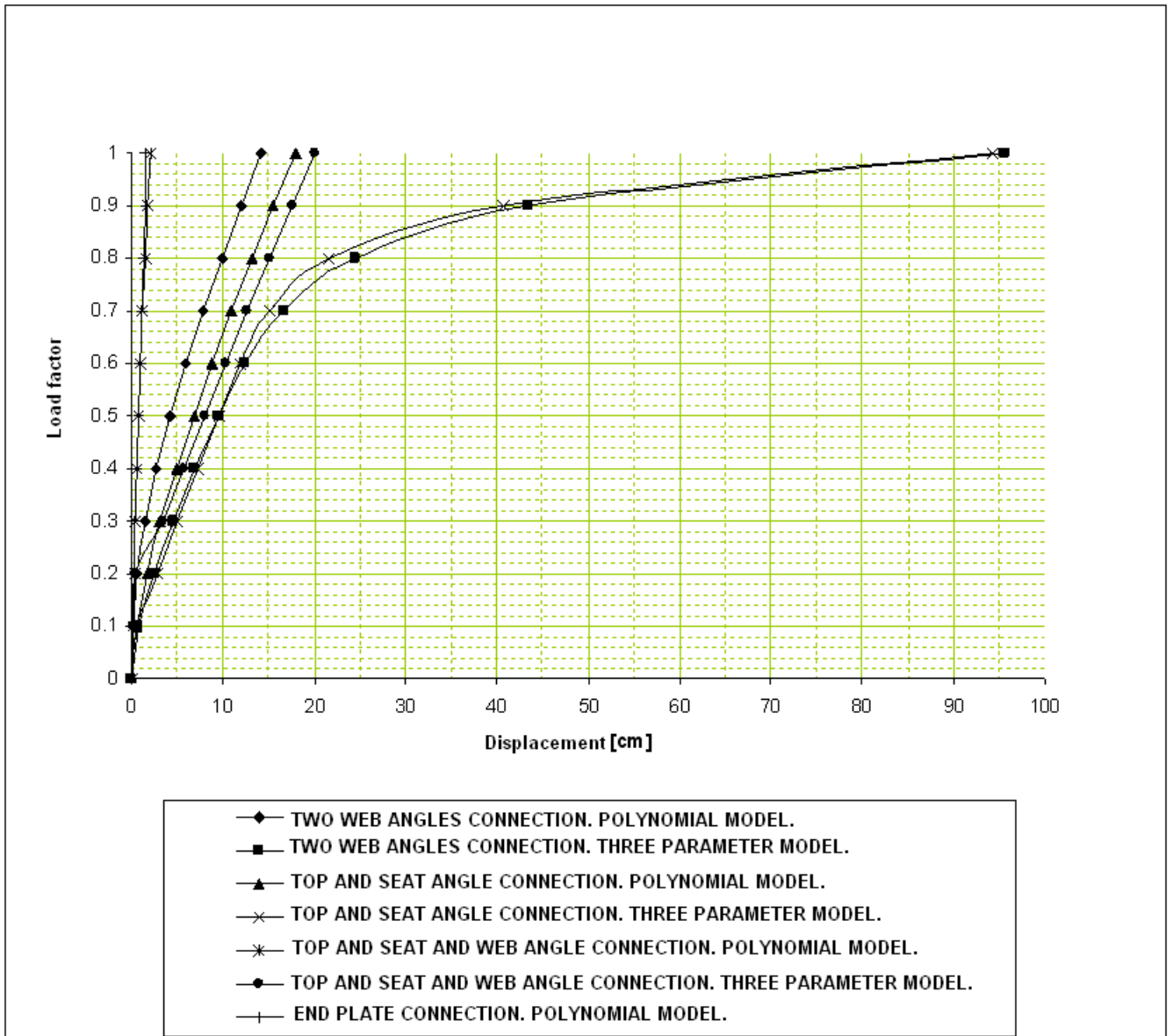


Fig. 9. Top lateral load – top lateral displacement curves

## 8. Conclusions

This article aims at illustrating some of the computational details necessary for the nonlinear analysis of steel structured frames with semi-rigid connections. Computational aspects related to an approach of incremental-iterative solution, connection stiffness and moment-rotation curves are presented.

Based on a comparison of the results, it can be concluded that nonlinear analysis procedures of semi-rigid structural systems were implemented with success in the methodology of nonlinear equations system solution. The modification of stiffness matrix of semi-rigidly connected elements subjected to a nonlinear analysis produces accurate results when compared with those found in the literature. The results demonstrate not only the validity of the applied procedure, but also the computational implementation for connections with linear behaviors, as well as those that behave in a nonlinear way. This last observation emphasized that the adopted form to update the connection



stiffness for each load step produced quite accurate results as well. The use of an incremental procedure for the computation of a new, updated stiffness whose value is inserted in the mathematical equation that models the behavior of the connection, supplying a new stiffness, is, actually, the classical way of geometrically nonlinear structural analysis.

The obtained results prove that there is a significant difference between the results obtained from frames with ideal (rigid) connections and those with semi-rigid connections.

Still, it is noted that in the elastic analysis the behavior of an unbracing frame is strongly controlled by the flexibility effect of the connection, as can be observed in the results of solved and presented case studies.

However, the effect of the joint nonlinearity does make such connection reaches out very inferior load when compared with a constant semi-rigid situation. For small displacements the considerations for linear and nonlinear semi-rigid connections, mainly for more rigid connections, are almost indistinguishable.

## 9. References

- [1] Moldovan C., *Modele mecanice și analitice în analiza structurilor metalice alcătuite din bare cu conexiuni elastice*, Teză de doctorat, Cluj-Napoca, 1997.
- [2] Alexa P., Moldovan C., *Structuri metalice alcătuite din bare cu conexiuni elastice*, Editura Risoprint, Cluj-Napoca, 2005.
- [3] Jaspart J.P., General report: Session on connections, *Journal of Constructional Steel Research* 55 pp. 69–89., 2000.
- [4] Piluso V., Faella C. and Rizzano G., *Structural Semi-Rigid Connections — Theory, Design and Software*, CRC Press, Boca Raton, USA, 2000.
- [5] EUROCODE 3 European Committee for Standardisation, Eurocode 3. ENV-1993-1-1. Revised Annex J. *Design of Steel Structures*. Doc. CEN/TC250/SC3-N419E; 1997.
- [6] Bârsan G.M. and Chiorean C.G., Computer program for large deflection elasto-plastic analysis of semi-rigid steel frameworks, *Computers & Structures* 72, pp. 699–711, 1999.
- [7] EUROCODE 4 Eurocode 4: *Design of composite steel and concrete structure*.
- [8] Chen W.F., Goto Y., and Liew J.Y.R., *Stability design of semi-rigid frames*, John Wiley & Sons, 1996.
- [9] Bjorhovde R., Brozzetti J. & Colson A., A Classification System for Beam to column Connections, *Journal of Structural Engineering*, ASCE, 116 (11) 1990, p. 3059-76.
- [10] ATC-40 Seismic Evaluation and Retrofit of Concrete Buildings, Vol. 1 by *Applied Technology Council*, California.

# Composite Steel-Concrete Columns with High Strength Concrete versus Normal Strength Concrete

Sav Vladut<sup>\*1</sup>, Campian Cristina<sup>2</sup>, Senila Mihai<sup>3</sup>, Constantinescu Horia<sup>4</sup>

<sup>1,2,3,4</sup> Technical University of Cluj-Napoca, Faculty of Civil Engineering, 15 C Daicoviciu Str., 400020, Cluj-Napoca, Romania

Received 29 May 2011; Accepted 15 August 2011

## Abstract

*In this paper a comparative study between composite columns with High Strength Concrete (HSC) versus similar specimens with Normal Strength Concrete (NSC) is provide. The study is drawn up on experimental results obtained from recent test on columns with HSC, respectively earlier tests on columns with NS. All those tests were made in CBACM's department laboratory. The specimens were loaded with axial force and bending moment. The experimental tests analyze was focused on several parameters: increasing bearing capacity, failure mode, ductility ratios, resistance ratios, rigidity ratios, absorbed energy ratios. The conclusions marks strong point and weak points of using HSC revealed during the tests.*

## Rezumat

*În această lucrare este prezentat un studiu comparativ între stâlpi micști având în componență Beton de Înaltă Rezistență (BIR) și stâlpi similari având în componență Beton Obișnuit (BO). Studiul se bazează pe rezultate experimentale provenite din încercări recent realizat (cazul stâlpilor cu BIR), respectiv experimente din trecut realizate pe stâlpi cu BO. Teste au fost făcute în laboratorul catedrei CBACM. Specimenele au fost supuse la solicitări de compresiune și moment încovoietor. Analiza rezultatelor experimentale se axează pe evaluarea următorilor parametrii: creșterea capacității portante a secțiunii, moduri de cedare, variația rigidității, variația ductilității, gradul de disipare a energiei. Concluziile marchează punctele forte și punctele vulnerabile ale utilizării BIR în componența stâlpilor micști.*

**Keywords:** composite column, high strength concrete, bending moment, axial loading

## 1. Introduction

Composite columns are designed using various combinations of steel and concrete in a manner that both materials provide the highest performances. Therefore increasing the concrete class is a natural act intended to improve composite columns behavior to various external action, especially seismic action. Using High Strength Concrete (HSC), which generally implies primarily higher strength, has been used successfully in reinforced concrete columns. However, HSC tends to be stiffer and more brittle than normal strength concrete (NSC).

The comparison between composite columns using HSC and composite columns using NSC take

---

\* Corresponding author: Tel./ Fax.:

E-mail address: [vladut.sav@bmt.utcluj.ro](mailto:vladut.sav@bmt.utcluj.ro); [ccampian@bmt.utcluj.ro](mailto:ccampian@bmt.utcluj.ro)

into account the advantages and disadvantages provided by using HSC.

The developments related to high-strength concrete and seismic design motivate the review of composite column behavior and current design provisions. Using the composite leads to larger openings, reduces the height levels and provides better lateral stiffness. Under large-magnitude seismic events, concrete shells crack and lower the flexural stiffness of composite beam-columns. Nevertheless, the steel core acts as a back-up system in providing the shear strength and the required ductility to prevent brittle failure modes.

Eurocode 4 [1] provides a relative simple method to design composite columns. The EC4 Simplify Method has some restrictions related to cross section; it applies only for bi-symmetric forms of the cross sections of the steel shape, and for the concrete class, restricted to maximum C50/60.

## 2. Experimental Tests

### 2.1. Test procedure and devices

The tests were carried out in Technical University of Cluj Napoca laboratories, and they were focused on the increasing the concrete class effects. Therefore, the mechanical behavior and seismic resistance of the 8 specimens of concrete encased composite columns Figure 2 were observed. Seismic resistance of columns was tested on full-scale specimens subjected to cyclic loading and a constant axial force. The cross-sectional area of composite columns was 220 mm×170 mm and height varying from 2 m long, for 4 specimens to 3 m long for the rest of them, resulting different slenderness.

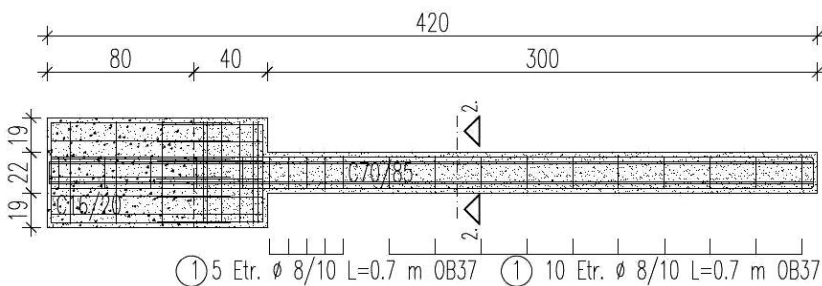


Figure 1. Arrangement of reinforcing bars

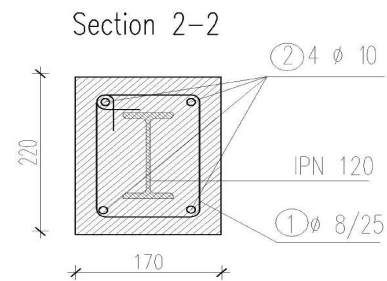


Figure 2. Specific cross section

The used steel profile was an IPN 120, having yield  $f_y=380\text{N/mm}^2$ . These values have been obtained in traction test. The profile was encased in high strength concrete (HSC) C70/85. The longitudinal reinforced are 4 PC52 (BST500) bars of  $\phi 10$  diameter. The confining hoops have  $\phi 8$  diameters with spacing of 100 mm on the critical zone (600 mm) and 200 mm spacing on the rest of the column length, Figure 1.

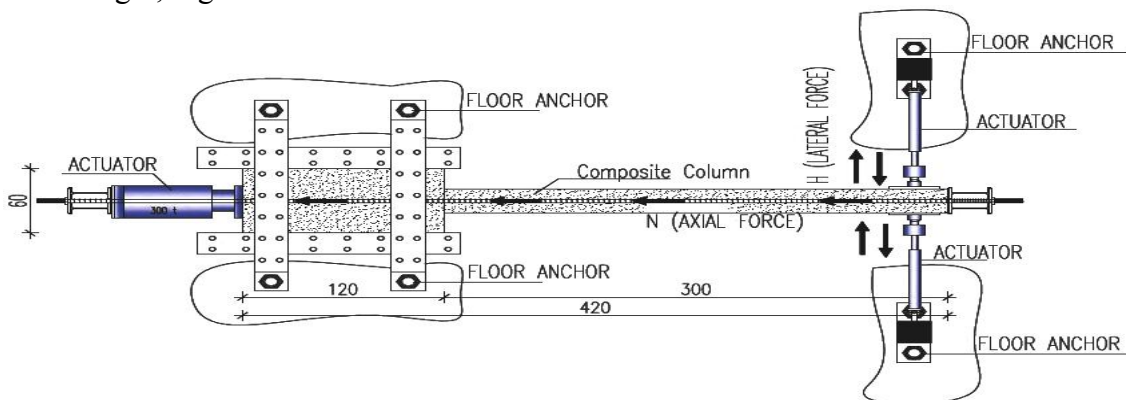


Figure 3. The setup for the cyclic loading test

The specimens were tested combining several parameters as magnitude of axial force  $N$ , which was chosen to correspond to a design compression rate of 10% from  $N_{pl,Rd}$ , respectively 20% from  $N_{pl,Rd}$ , to simulate static load on the column, where  $N_{pl,Rd}$  was the nominal compressive strength of the composite column. The  $N_{pl,Rd}$  value was calculated in accordance with the design rules of EC4 Simplified Method except the concrete provisions.

The horizontal load was applied on the column at the distance representing the middle height of the storey. This load was cyclically applied in positive and negative range of value by two 80 kN actuators placed in the right and in the left side of the free end to simulate the horizontal seismic force on the column Figure 3. The column was considered embedded on the base and free of restraints on the other side. To ensure a suitable full restraining at the column base, the elements were ended by a sudden cross-section enlargement acting as a foundation (the flexural stiffness ratio between the element and the so-realized foundation was about 1/5).

Similar experimental tests have been held in our department in 2000 [2] but the used concrete was a normal concrete (NC) C20/25. This was the start point for furthermore researches in order to be able to make a full comparison and parameters analysis. The testing procedure in both cases was the one recommended by ECCS for characterizing the behavior of steel elements assessing to seismic action (ECCS-TWG 1.3, 1986 – using a monotonic test to calibrate the cyclic tests) [3].

### 3. Comparative analysis

#### 3.1 Monotonic loading test analysis

The monotonic test according to ECCS Procedure was meant to be done for deduction of the value of conventional limit of elastic displacement  $e_y^+$  from the recorded  $F$ - $e$  curve, and the corresponding loading  $F_y^+$  used in calibration of the cyclic tests series.

The comparison includes evaluation of failure values, displacements values, elastic limits, failure modes and energy dissipation rates. It has to be mentioned that geometric characteristics as well as the other materials used in the composition of the columns with HSC and the columns with NSC are similar. The exception is made only on the concrete class. The loadings are also similar.

In Figures 4 and 5 a comparison was made by superposition the lateral force – displacement graphics of the two types of columns analyzed [4]. On the one hand the brittle characteristics of columns with HSC conducts to a sharply failure mode, on the other hand the rigidity obtained from the curve slope is higher. Elastic limit as we aspect is lower in comparison with columns using NSC.

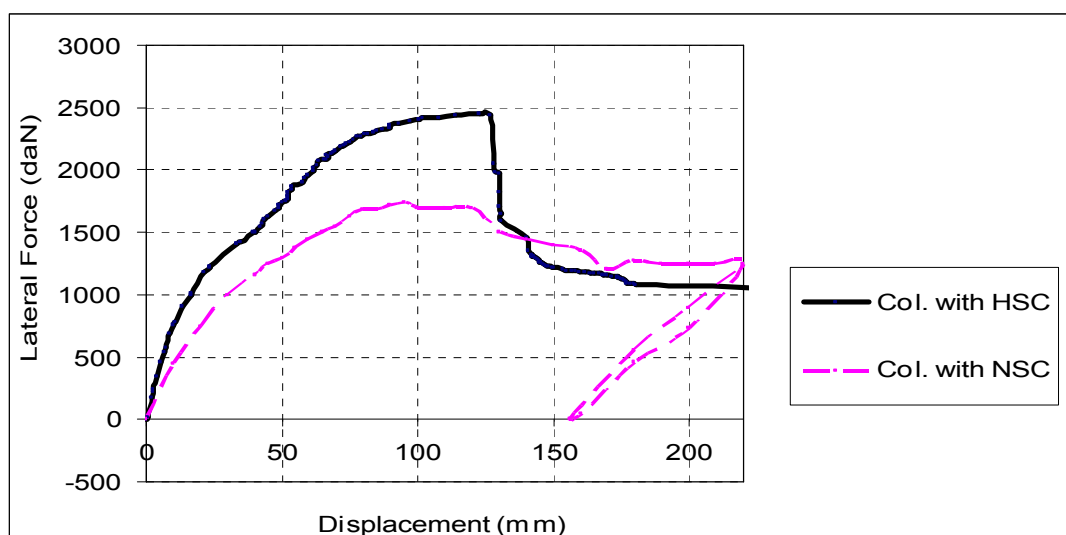


Figure 4. Columns with HSC vs. Columns with NSC – Specimens having 3 m length

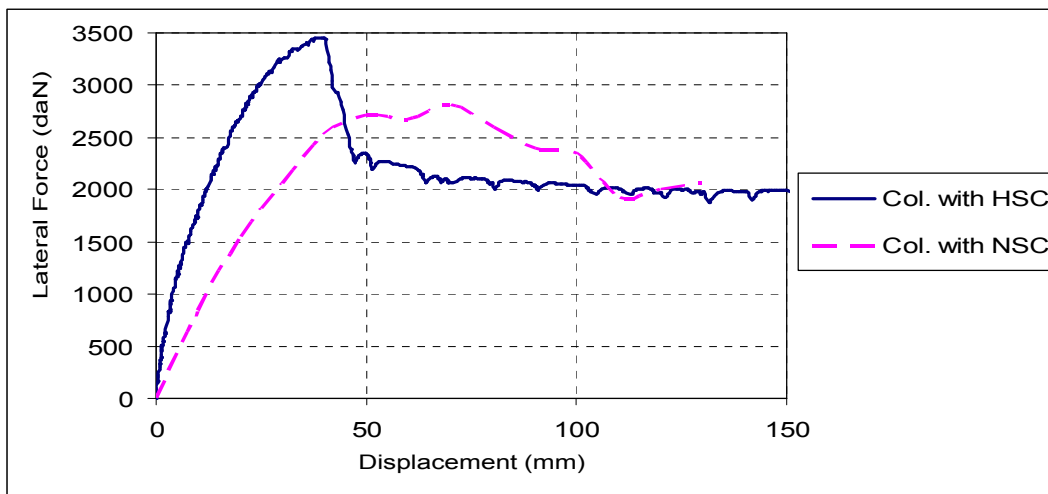


Figure 5. Columns with HSC vs. Columns with NSC – Specimens having 2 m length

The values of the obtained elastic displacement are presented in Table 1.

Table 1: Various values obtained from monotonic loading test

Specimen	Length (m)	Axial load (kN)	Elastic displacement (mm)	Lateral loading $F_y$ (kN)	Displacement related to value $F_{max}$ (mm)	Maximum laterl force $F_{max}$ (kN)
HSC	2	20,00	25	34,10	40,21	34,49
NSC	2	20,00	34	22,10	70,00	28,10
HSC	3	20,00	30	22,90	126,60	24,45
NSC	3	20,00	35	12,50	95,00	17,20

### 3.1 Cyclic loading test analysis

Evaluation of composite column was made according with ECCS Procedures, so an analysis of parameters stipulated in procedure was made. From the hysteresis diagram we observe that composite columns have an unstable behavior due to permanent increasing displacement during loading process. Also, as much as we increase the cycles number, as fast the rigidity ratios of the element drop. The cycles analysis was made in relation with elastic displacement and with the ideal cycle, considering a behavior of a perfect elastic-plastic material type.

In the graphics, the variation of the parameters afferent to a group of 3 cycles of equal displacement is presented.

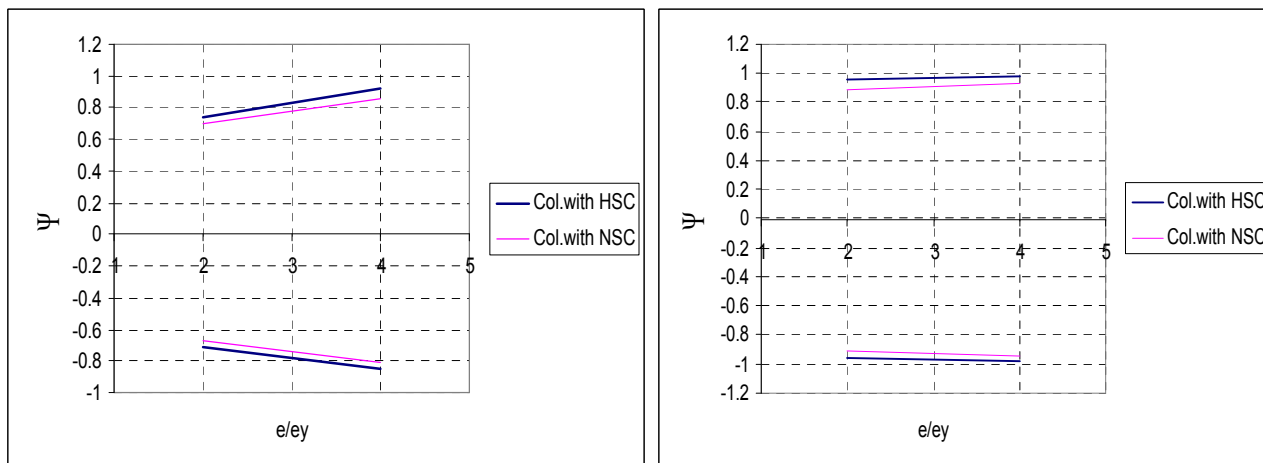


Figure 6. Full ductility ratios –a) Specimens of 3 m length; b) Specimens of 2 m length

The ductility ratios of the two types of columns maintain an ascending slope and the equidistance between the graphics indicates relative similar behavior.

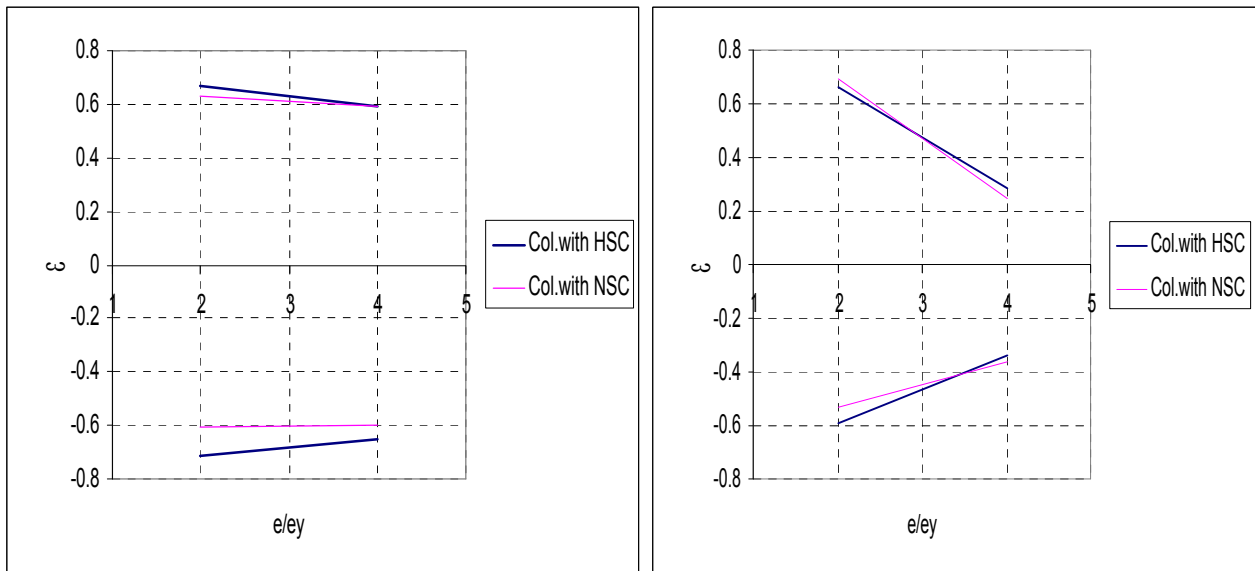


Figure 7. Resistance ratios a) Specimens having 3 m length; b) Specimens having 2 m length

Progressive decrease of resistance is more pronounced in columns with HSC case due to brittle failure mode. It is obvious that the columns having 2 m in length have a rate of resistance ratio decrease higher than columns having 3 m in length and the values are nearer between the two type of columns.

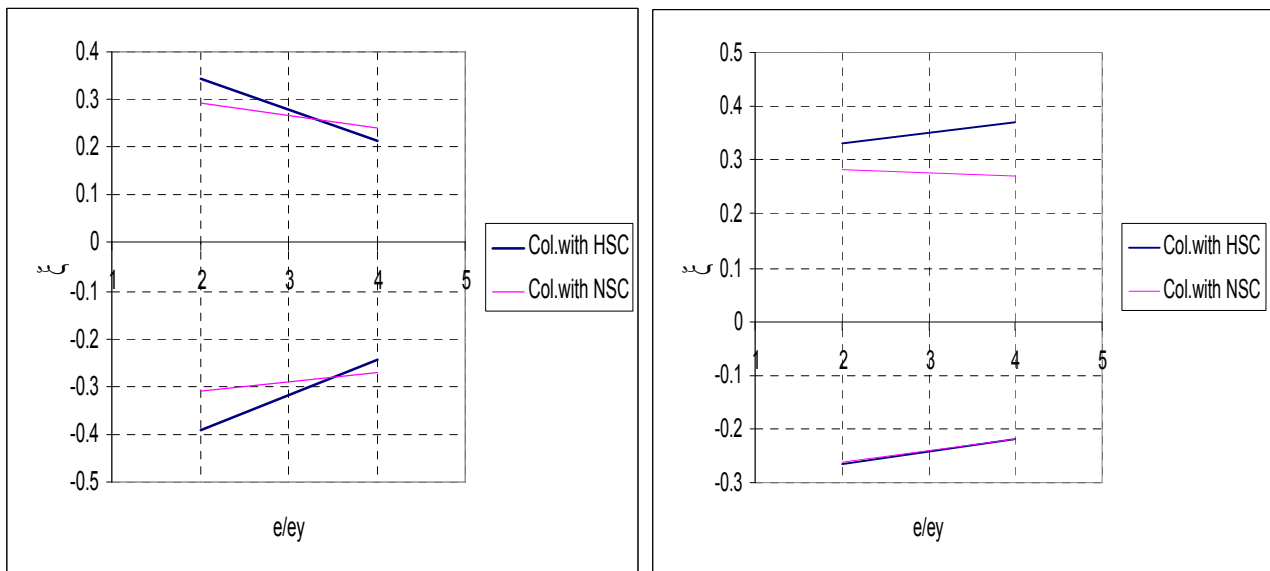


Figure 8. Rigidity ratios – a) Specimens having 3 m length; b) Specimens having 2 m length

On the one hand the specimens having 3 m length with HSC reveal higher rigidity ratios for low displacements, on the other hand the rigidity ratios decrease dramatically when the displacement value grows. Variations of rigidity ratios deduction in columns with NSC case were lower. The specimens having 2 m in length with HSC proves higher rigidity ratios on positive domain. The tangent angle  $\alpha$  made by the graphic with abscissa dictate a rigidity ratios values appreciation, but this was directly influenced by the fact that the compressed concrete area is lower on that side of the column (specimen S8-2C). Implicit, the decreasing of bearing capacity of this specimen was faster and all the loading were carried by the steel shape. At this point the residual displacements have a high level and this leads to even higher values for the tangent of angle  $\alpha$ .

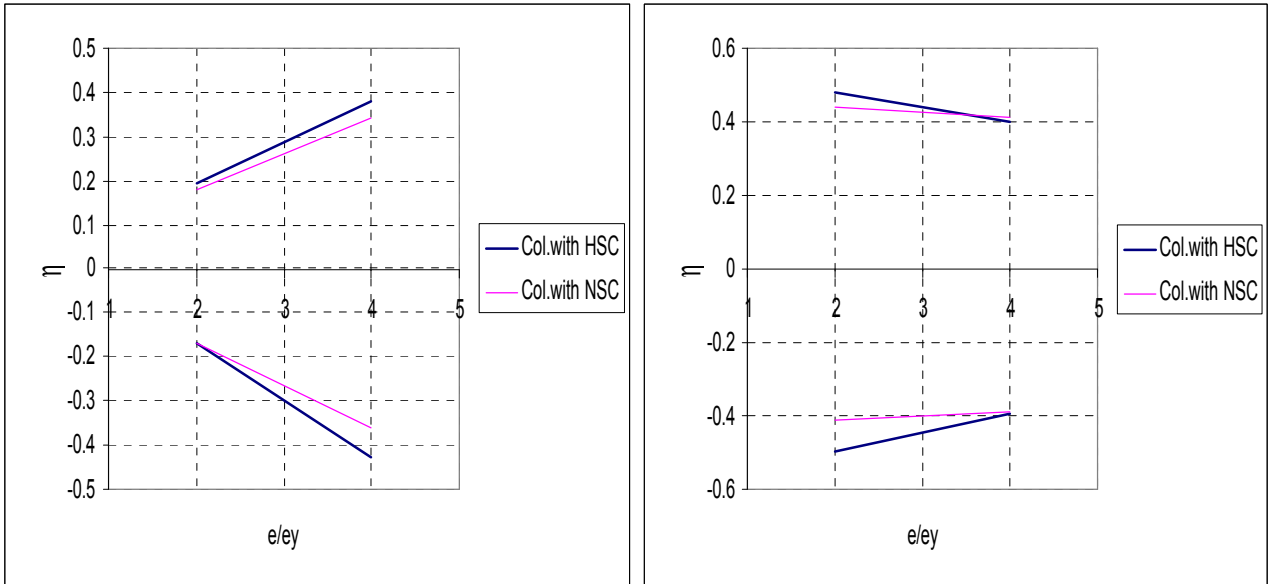
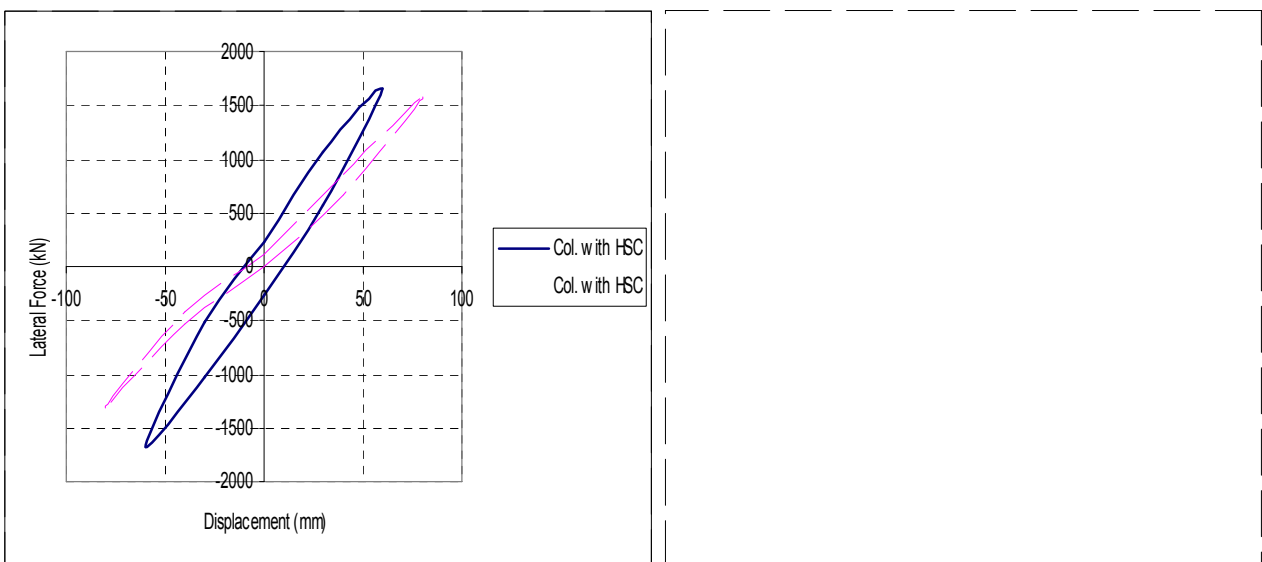


Figure 9. Absorbed energy ratios – a) Specimens having 3 m length; b) Specimens having 2 m length

The variation of this parameter indicates the absorbed energy ratios, and it is different depending on the length of the specimen. For 3m length case, the dissipated energy compared to the ideal elasto-plastic cycle is lower for low displacements. The specimen of 2 m long behave totally in a different manner – for displacement equal to 2e<sub>y</sub> the absorbed energy ratio was higher, and for displacement equal to 4e<sub>y</sub> the absorbed energy ratio was lower.

In order to make a full comparison, in Figures 10, 11, 12 a superposition of lateral force-displacement graphics for a cyclic loading, having the displacements values of 2e<sub>y</sub> and 4e<sub>y</sub> for both specimens, was made. A percentage analysis reveals that the composite columns with HSC having 3 m length absorbed with 140 % more energy than the one with NSC, for a displacement of 2e<sub>y</sub>. When the displacement increased to 4e<sub>y</sub> the absorbed energy value is higher with 29%.

Higher levels of absorbed energy were maintained in composite columns with HSC having 2 m length, too. The percentages increase with 208% for a displacement of 2e<sub>y</sub>, respectively with 24 % for a displacement of 4e<sub>y</sub>.



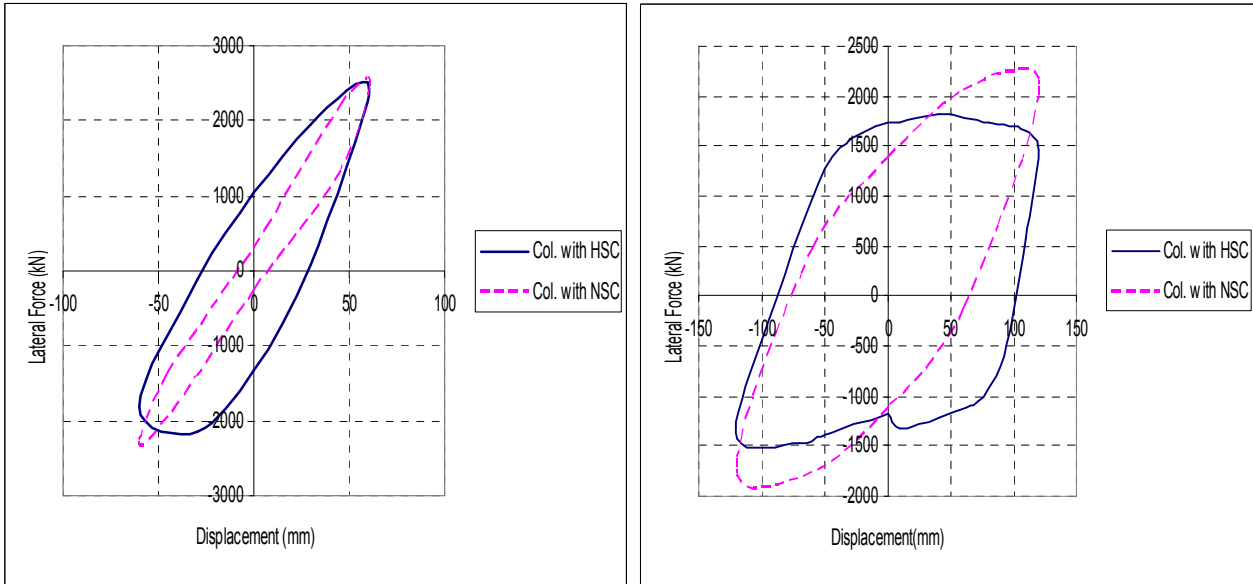


Figure 11. Comparative graphics between absorbed energy in 3 cycles- Specimens having 2 m length – a)  $2e_y$  displacement; b)  $4e_y$  displacement

The analysis above was made in relation with elastic displacement  $e_y$ , but to have a complete comparison criterion, a graphic superposition of the envelope of cycles was made, Figure 12. We could compare in this way the absorbed energy for equal displacements. The value of displacements where upon we considered that the concrete provides bearing. Beyond this level, the bearing capacity of the element is represented only by the steel shape, issue which is not included in our interests.

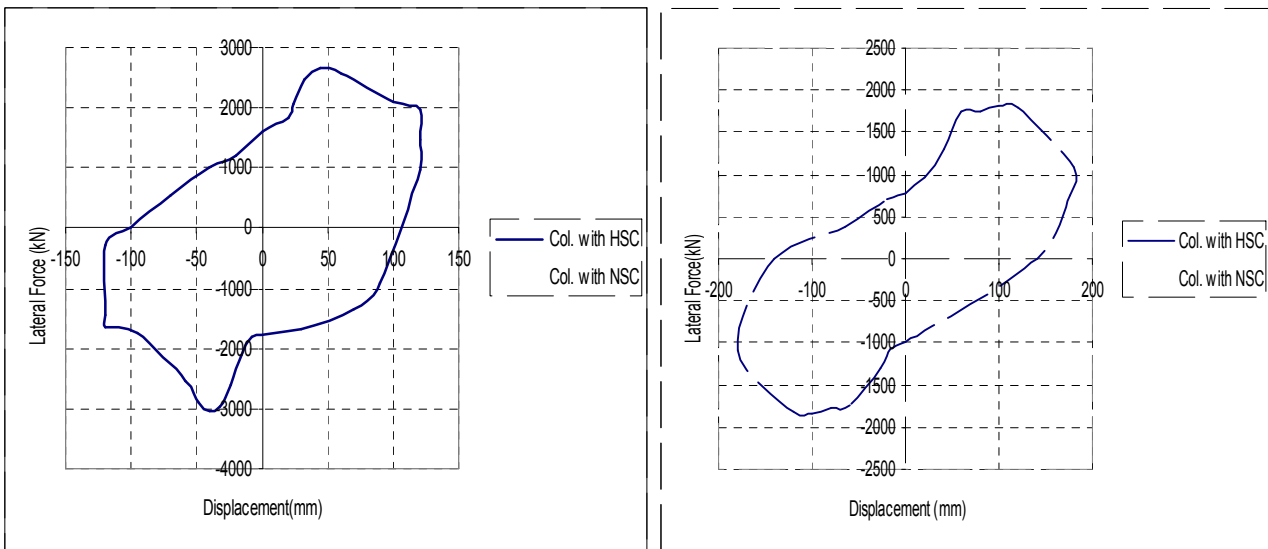


Figure 12. Comparative envelope graphics for equal displacement a) Specimens having 3 m length; b) Specimens having 2 m length

The ratios between absorbed energy for equal displacements reveal a growth of 48% in the 2m length specimens' case and of 30% for the 3m long specimens.

#### 4. Conclusions

In composite columns with HSC case, even if elastic displacement  $e_y$  decreases, the value of the



lateral force  $F_y$  corresponding to the  $e_y$  displacement and the maximum lateral loading  $F_{max}$  indicates a significant increase.

Failure modes were different, characterized by sudden and violent concessions due to cracking developments through aggregate in columns with HSC, while columns with NSC shows a “slow” failure mode characterized by gradual decline of bearing capacity with the growth of displacements.

From the graphics and parameters analysis we can conclude that the columns with HSC have a higher energy absorption capacity.

In structural terms, composite columns with concrete class C70/85 provide obvious better performances to structures, having significant increases to almost all analyzed parameters

## 6. References

- [1] *Eurocode 4: Design of composite steel and concrete structures. Part 1-1 ; General rules and rules for buildings ENV 1994-1-1,2004.*
- [2] M., Aribert, C., Campian, V., Pacurar(2003), “Monotonic and cyclic behavior of fully encased Composite columns and dissipative interpretation for seismic design”, Swets&Zeitlinger B.V., Lise, The Netherlands, *Proc. of STESSA 2003*, pp.115-122
- [3] ECCS (1986): Recommended testing procedure for assessing the behavior of structural steel elements under cyclic loads, *Doc. no 45 of European Convention for Constructional Steelwork*, TWG 1.3, 1986.
- [4] C., Campian, N. Chira ,V. Sav, ”Strength and ductility of concrete encased composite Columns”, Turkish Constructional Steelwork Association (TUCSA), Istanbul, Turkey, *Proc. of Steel Structures: Culture & Sustainability 2010*, pp. 485-493, ISBN 978-97592461-2-9.
- [5] C.Campian :” *Considerations sur le comportement et le calcul des poteaux mixtes acier-beton soumis a des charges de type sismique*”, These de doctorat, INSA Rennes, France, 2001

# STRUCTURAL SYSTEMS AND THE QUALITY OF DAYLIGHT IN BUILDINGS

Dana Opincariu<sup>1</sup>

<sup>1</sup> Technical University of Cluj-Napoca, Faculty of Architecture and Urbanism, 34-36 Observatorului Str.,  
400500, Cluj-Napoca, Romania

Received 12 May 2011; Accepted 20 August 2011

## Abstract

*Structure has a manifold role in architecture. First is that of stability and strength, then is the role of sustaining the architectural aesthetic concept on the level of the facades; another important role is regarding the quality of the interior space, through the capacity to give a rhythm, to distribute, to liberate and to offer a maximum of flexibility to the configuration of the interior space and also to allow for a good relationship with the natural light, on the level of the covering. The natural light is tapped into the interior space of the buildings through hollows in the facades: windows, panoramic openings of different types, skylights, etc. Among the other factors that control the level of comfort of a building (heat, air, sound and water), natural lighting has a big contribution to the quality of built space, its contribution depending on the purpose of the building, the spacial typology, the surface and the complexity of the functional scheme. The structure of the building supports the opening system of the facade, it optimizes the distribution of natural lighting in the architectural space and it contributes to the helioplasic effects in the ambiance of the architectural space.*

## Rezumat

*Rolul structurii în arhitectura actuală este multiplu. În primul rând este acela de a oferi stabilitate și rezistență, apoi are rolul de a susține conceptul arhitectural estetic la nivelul fațadelor, un alt rol important îl are în calitatea spațiului interior, prin capacitatea de a ritma, distribui, elibera și oferi maximă flexibilitate configurației spațiului interior și de asemenea de a permite la nivelul anvelopei o bună relație cu lumina naturală. Lumina naturală este captată în spațiul interior al clădirilor prin intermediul golurilor fațadelor: ferestre, deschideri panoramice de diferite tipuri, luminatoare, etc. Pe lângă ceilalți factori care controlează gradul de confort al unei clădiri (căldura, aerul, zgomotul și apa), lumina naturală are un aport foarte mare în calitatea spațiului construit, aportul acesteia fiind necesar în mod diferit în funcție de destinația clădirii, tipologia spațială, suprafața și complexitatea schemei funcționale. Structura construcției susține sistemul de deschidere la nivelul fațadei, optimizează distribuția luminii naturale în spațiul arhitectural și contribuie la efectele helioplastice în ambianța spațiului arhitectural.*

**Keywords:** natural lighting, structure, architectural space, function, flexibility, construction material, technology

## 1. Introduction

Besides its role of stability and strength, structure is also involved in aspects regarding the closing of the space, the typology of the facades and their solid-hollow relation, from a functional point of view, their subdivision, articulation of circulations and functional separation. The choice of the structural system that supports the architectural form or it determines volumetric composition characteristics, is involved in its flexibility, configuration of space that needs natural lighting, as a factor of ambiance. As a ratio between the lighting of the image of an object and the glow of that object in the case of architectural spaces, luminosity is variable, so the norms for the hollows in the facade to be  $1/5 - 1/6$  of the floor surface of a room, have to be reconsidered and interpreted according to some equally important factors, that come from the qualities of the environment and from the furnishings of the interior space. Along with the factors of luminosity that pertain to the exterior environment (climate zone, built environment, time of day, weather, seasonal luminosity), the factors of luminosity that pertain to the micro ambiance are essential to the quality of natural lighting in the architectural space.

These factors refer to the influence of shape and size of the windows inspired by the constructive system, the orientation of the lit space according to the cardinal points and the morphological luminosity of spaces, that refers to the organization and subdivision of space in relation to the constructive system of the facades, by means of type of closing and the solid-hollow ratio. The shadow and half-shadow effect in the built space is also determined by the way in which the facade is built, its relation to the structural system and the closing systems.

The nuances of the shadows and half-shadows are determined by the type of floor and ceiling finish, surfaces that reflect the interior light. The spacial configuration, the shape of the rooms and also the structural elements (beams, pillars, jutties, the geometry of the ceiling, pockets, niches, free columns, different types of internal stairs), the length of the window recesses that are resulted from the distribution of windows in the external walls, the height of the lintel and the window breast, all create more pronounced or soft shadows, half-shadows on different zones, that contribute to the quality of the interior space if they are correctly guided and controlled.

The structure's implication in the quality of the natural lighting of the built space can be studied according to the three distinct roles it has, namely:

- A. Sustaining the type of natural lighting source in the facade constructive system
- B. Optimizing natural lighting in the interior space
- C. Contribution to the plastic effects determined by shadows and lights (helioplastics) (fig.1).

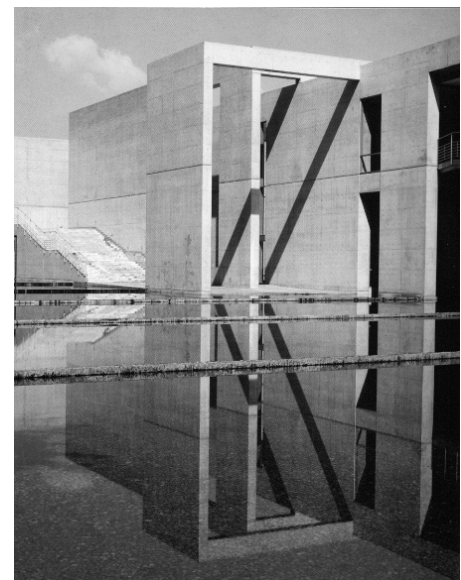


Figure 1. Church of Light, Ibaraki, Osaka Prefecture, Japan, Tadao Ando, 1999

## 2. Daylight and the shape of the openings

The form and size of windows, the main channels for natural lighting in the built space have to be adapted to contemporary design, to the needs determined by the activities that take place a particular space, to the constructive system of the architecture, to the architectural style of the facade. The building interiors constantly need air and light, an extra role of the openings in the facade is that of ensuring the constant interior conditions, despite the fluctuation of the exterior environment. Thus openings have the role of creating a connection between the exterior and the interior, by controlling the climate, the exchange of climate between exterior and interior. Light, together with individual parameters such as temperature, sound and humidity are associated under the domain called “the control of permeability” in the study of building facades. Usual windows control the permeability of light through their structure and the materials used even when closed, but do not have the performance to make the exchange of air through ventilation, except for when they are open. Modern architecture brings the possibility to achieve the two functions of windows, lighting and ventilation, at the same time, without the surface of the window opening, but by using a separate opening for ventilation, on the level of the facade<sup>1</sup>. The advent of the first facades with large glass openings in the 18th Century and the erection of buildings such as The Crystal Palace in London, in 1851 or the glass palace in Munchen in 1854 mark a new transition in architecture. The window goes from the concept of transparent element integrated in the solid, opaque surface of the walls to the concept of “glass wall”. The position and geometry of the openings is also important to the geometry and spatiality of the interior that has to be lit, having a definite effect on the permeability of light, on the space ventilation and on the visual relation between exterior and interior. There also has to be a relation between the utility of the space and the shape of the windows and the proportion of their horizontal and vertical dimensions. The visual relation between exterior – interior is an important aspect of integrating openings in the plane of the facade, in so that we can distinguish the following average heights for different postures (table 1), and both the position and the subdivision of the opening must match to type of utilization and position of the occupants<sup>2</sup>.

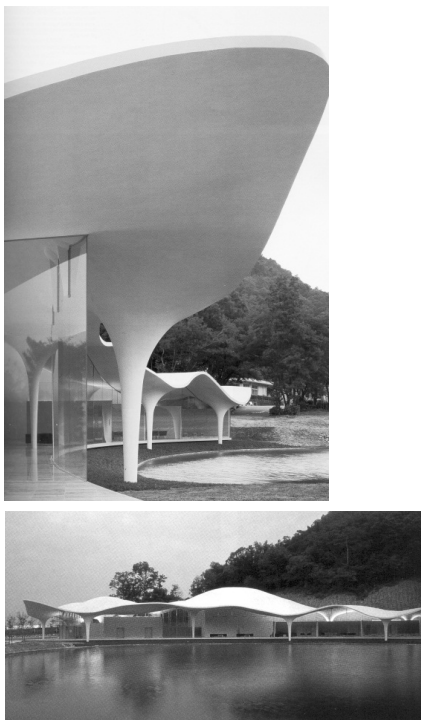
*Table nr. 1. Average heights for different postures.*

STANDING	Approx. 1750 mm
SEATED AND WORKING	Approx. 1300 mm
SEATED AND RELAXING	Approx. 800 mm
LYING DOWN(300mm above floor level)	Approx. 700 mm

The daylight factor (df)<sup>3</sup>, time of day, local environment factors (climate conditions, shading determined by the built vicinity and vegetation). Besides the degree of light reflection of the finished surfaces with different textures and colours, the plane of the façade, the position and the geometry of the openings, the way in which the constructive system relates with the elements of the bearing structure, with the closing elements, is crucial for the quality of the natural lighting in the interior space (table 2).

The shape and geometry of openings are determined by the position of the closing elements in relation to the structural system of the building, of the horizontal, vertical and oblique elements that are implicated in the project, a system that is responsible for the performances and the appearance of the building's facades. The structure – window relationship can be of two types:

- 1) A façade independent of the structural system (fig. 2a)
- 2) A loadbearing façade (fig. 2b)



1. Sealant,  
3 mm polyurethane  
coating  
Leveling layer,  
10 mm mortar  
200 mm reinforced  
concrete slab  
20 mm insulating mortar  
3 mm coating
2. 5 mm stainless-steel sheet
3. Glazing, 19 mm,  
toughened glass
4. Integrated drainage: Ø  
216 mm steel tube
5. 20 mm marble  
10 mm mortar bed  
20 mm thermal insulation  
200 mm reinforced  
concrete
6. Condensation channel,  
stainless-steel
7. 165/12 mm steel flat
8. 165/9 mm steel flat

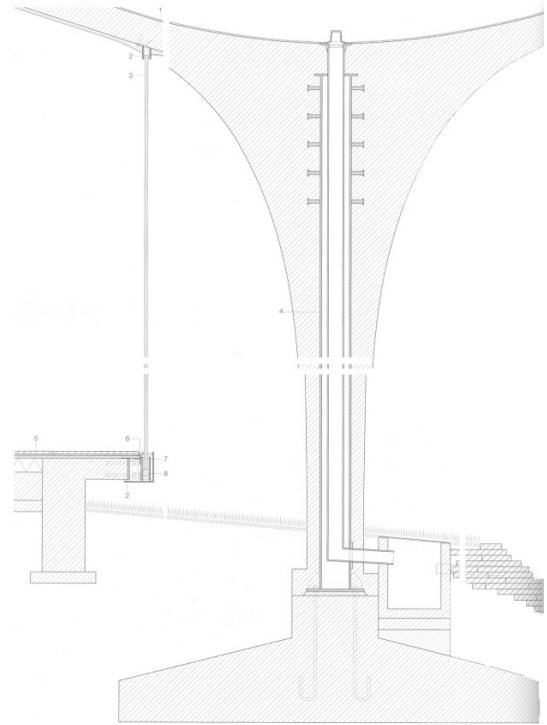
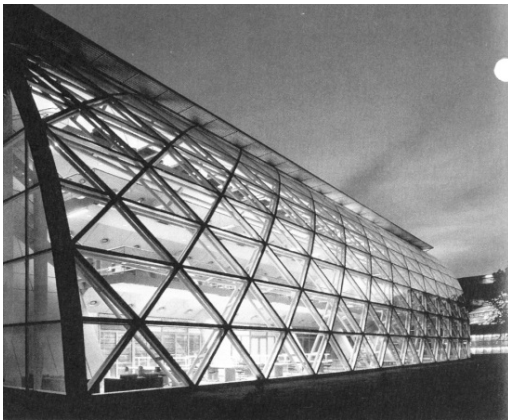


Figure 2a. Municipal Funeral Hall, Kakamigahara, Japan, Toyo Ito & Associates



1. Primary loadbearing  
framework of steel circular  
hollow sections, 140 mm  
dia., welded nodes, painted  
white
2. Horizontal bracing, steel  
circular hollow sections,  
140 mm dia., painted  
white
3. Stepped insulation glass,  
10 mm toughened safety  
glass + cavity + 2 No. 8  
mm laminated safety glass,  
projecting outer pane  
bonded to aluminium  
frame
4. Specially formed framing  
member
5. Inspection opening for  
district heating duct
6. Silicone seal

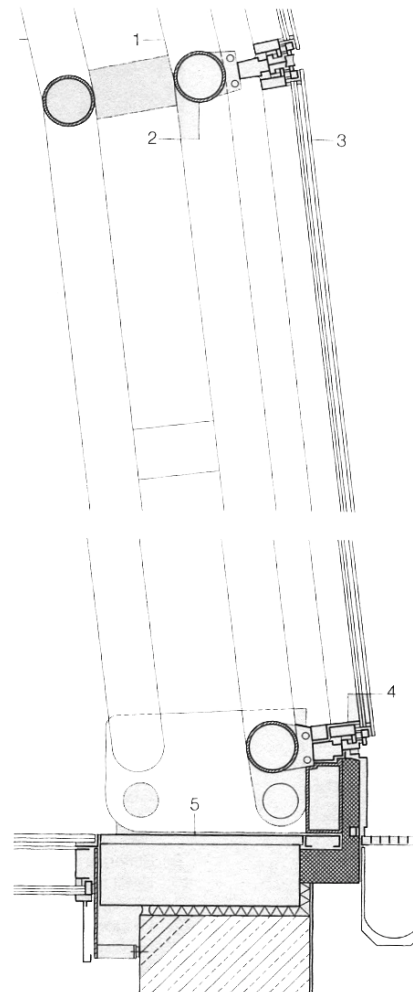
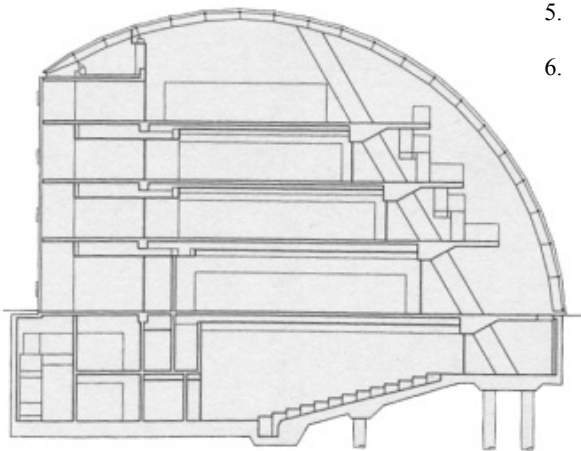


Figure 2b. Faculty of Law, Cambridge, U.K., Sir Norman Foster and Partners, 1995

In the case of facades that are independent form the structural system, in principle, we can distinguish between the following positions, considered from outside to inside in the case of a non-loadbearing façade

- 1) in front of the columns
- 2) on the front face of the columns
- 3) between the columns
- 4) on the rear face of the columns
- 5) behind the columns

Table 2. Factors that influence the daylight penetration according to the window geometry (fig. 2c).

The vertical position of the opening	High level window Eye level window Low level window
The vertical dimension of the opening	Middle Lower higher
Shape of the reveal	Parallel Tapering inwards Tapering outwards Parallelogram sloping inwards Parallelogram sloping outwards
The thickness of the facade	Thick wall construction Thin wall construction

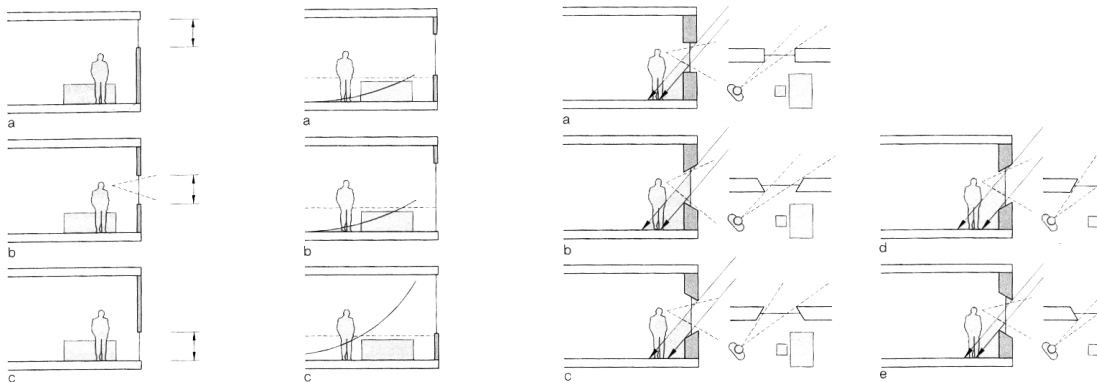


Figure 2c.

The shape of windows can be classified in the following categories:

1) CLASSIC WINDOWS correspond to traditional constructive systems, such as brick, stone, wood masonry, the width of which depends on the way in which the opening in the façade was built, with stone lintels, metal or wood lintels, all types of arches with the hopper and the depth of the embrasure determined by the thickness of the walls. The tall openings and rooms in this case, generated an elongated beam of light that lit limited portions of the space, the shadows and lights alternating in the interior space according to the window sequence. These type of windows are found at restoration interventions, when the reproduction or continuation of the existent façade architecture is necessary or in situations when a new building, in a new architectural style, because of its position among historical buildings, it respects the rhythm and window proportion of the adjacent facades through its composition.

2) STANDARD WINDOWS (rectangle, round, arched, triangular). This type of window that is a component of a façade, has an opening surface smaller than the adjacent solid surface, and the daylight enters laterally or with a dormer, component of the roof, integrated in the structure of the roof as an added volume or with a folding dormer window in the plane of the roof that lights a mansard type of space, a modern architecture, modular. With the typification and the standardizing

of modern architecture of the '50s, the prefabrication of façade elements, also came standard windows.

3) SKYLIGHTS are transparent volumes in the architecture of buildings that distribute zenith light and are from a functional point of view are used in spaces where the walls don't allow for openings or in spaces where the surface of the walls has a concentric configuration with connecting spaces, such as bridges and interior circulations or central hallways on multiple levels. Also in the situation of some industrial architecture programs where the depth of the space is too large there is the necessity of a zenith daylight source that complements the lateral windows. Zenith daylight is also used when covering interior courtyards of historical buildings and also as covering for wide open spaces in contemporary architecture (fig. 3).

4) GLASSHOUSE TYPE. This category presumes an unequal total transparency of the room's volume, the relationship of the structure with the glass facets is visible. It is among metal, wood or plastic structures, pneumatic structures that allow full daylight into a space. The destination of glasshouse buildings is horticulture, botanical, bio climate and the constructive system has a well-defined technological and functional role. This model was brought to civilian architecture as well. This type of opening is used in ecological facades, where the glazing acts as a solar energy collector. The architectural elements for glazing are buffer zones such as winter gardens, glasshouses, inclined glazing or double facades, the functioning principle of which is that of an exterior glazed covering placed at a 50 cm distance from the glazed insulated wall, determining an intermediary space that in wintertime serves as a solar collector. Multiple glass facades are called "epiderms"<sup>4</sup>, due to their behaviour that is similar to that of live organisms.

5) BOW WINDOWS are volumes that come out from the building façade of a polygon shape, that through their shape can bring more daylight into the interior space and have a better visual relationship with the exterior. (Throughout history in the Medieval Period, Colonial Period, English Georgian architecture, contemporary manifestation manner, etc.)

6) HORIZONTAL BAND WINDOWS create an alternation between solid and hollow with horizontal bands. These windows are characteristic to reinforced concrete slabs with cantilevers on the façade level.

7) SLIT WINDOWS (horizontal, vertical, oblique) – narrow vertical or oblique in the façade are specific to contemporary concrete architecture, massive and sculptural, with exposed concrete facades with a raw unfinished aspect, with formwork markings.

8) PANORAMIC WINDOWS, of the hollow type, large opening that is integrated between structural elements such as columns and beams. They appeared when modern architecture promotes the open plan, large openings determined by the reinforced concrete frame structures, visual communication with the outside. The structure composes the façade, it creates the composition rhythm, composing the solid façade, the opaque part, the shape of the hollow and its dimensions are determined by the structural shape.

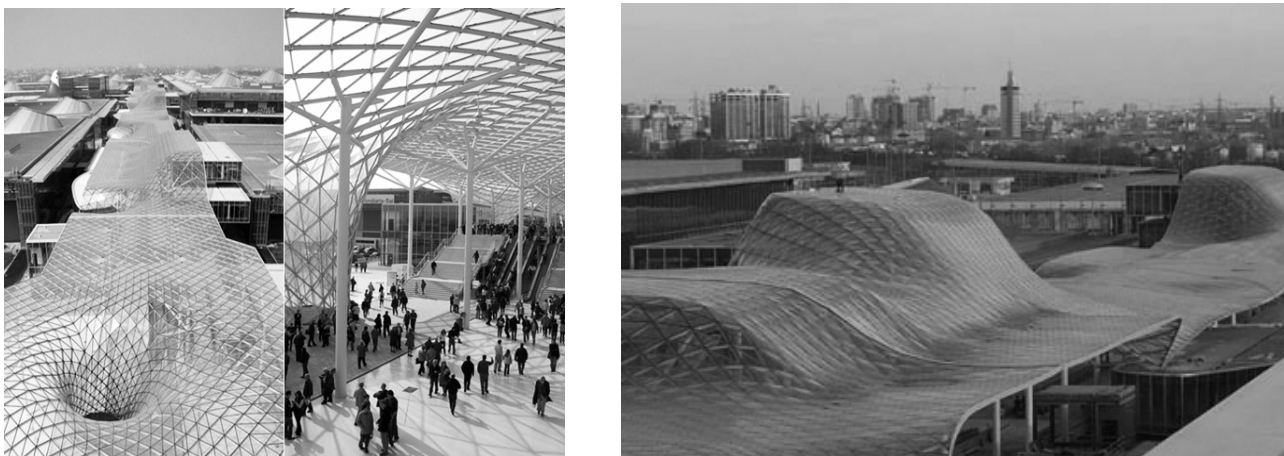


Figure 3. New Trade Fair, Milano, Italy, Massimiliano Fuksas, 2005

9) GLASS WALL (plane, faceted, curved). It passes in front of the structure creating a continuous field on the outside of the façade. This kind of closing allows a continuous glazing, the structure having the role of supporting the transparent façade elements.

Along the history of architecture, certain architectural styles have promoted through their concept, certain opening typologies in the facades that together with the structural system and the building materials used, have determined the specific to the style.

Table 3. Architectural styles and structural systems that have promoted certain opening typologies in the facades.

Window typology	Structural system	Architectural style
Classic window	Brick or stone bearing masonry	Historical styles, Classicism
Standard window	Bearing masonry, reinforced concrete frame structures or metal structures with prefabricated facade panels	Late modernism
Skylight	Metal structures, one-way, grid or space lattice beams systems, folded slabs (prism, pyramid, frame), corrugated membranes and shells	Neo-expressionism, Structuralism
Glasshouse	Structures of one-way, grid or space double layer grid systems, geodesic dome, grid structures, topological structures	Organic, Ecological architecture, Bioclimatic, Fractal architecture
Bow window	Bearing masonry, reinforced concrete frame structures	Historical – Georgian, Postmodernism
Horizontal band	Reinforced concrete frame structures	Modernism, Neo-modernism
Slit	Reinforced concrete structures	Deconstructivism, Minimalism
Panoramic window	Reinforced concrete or metal frame structures	Rationalism, Neo-modernism
Glass wall	Metal or reinforced concrete frame structures	Minimalism , Bioclimatic architecture

### 3. Natural lighting and the destination of buildings

The spacial characteristics of architecture are a decision factor in the natural lighting of space. Two different situations can be distinguished in the architectural floor layout: spacial typologies developed horizontally, that develop their layout with the entire functional scheme on a flat surface and spacial typologies developed vertically, which develop their functional scheme on multiple levels. These two categories contain many more constructional types, from the point of view of the space destination and presume a special relationship of the daylight with the type of space configuration determined by the functional characteristics of its destination (table 4).

Table 4. Typologies of floor layouts in relation to function and natural lighting systems

Space typology/Structural typology	Types of architectural programs	Adequate typologies for natural lighting systems
Horizontal development: Surface Linear Pavilion	1. Sport buildings: stadia, covered swimming pools 2. Buildings for transport: airports, aerostations 3. Cultural buildings: museums, libraries, theatres 4. Commercial buildings: shopping centers, food markets, warehouses	Skylights, lateral glazing panels, structural facets
Vertical development	1. Administrative buildings: offices, courthouses 2. Buildings for tourism: hotels, motels 3. Health buildings: hospitals, clinics, sanatoriums 4. Residential buildings: collective housing	Standard window, bow window, panoramic window, glass wall

There also are buildings with other destinations that don't presume a certain space typology that leads to the lack of discussion about these buildings but these also need an adequate design of the facade openings that bring the daylight inside.

Space typologies with a horizontal development, have a very wide expansion, presume wide interior spaces, with a depth that doesn't allow natural lighting, unless systems with zenith and lateral



lighting and used. The daylight must be captured through natural lighting systems that are correlated with the building's structural system. The structural systems of these types of wide-opening buildings unusually are: post and beam, a frame, portal frame, arches, vaults, domes or systems with three dimensional surfaces, diamatic dome, lamella dome, geodesic dome, cast reinforced concrete shell and monocoque and tensile or pneumatic membrane structures<sup>5</sup>.

“For buildings that have such requirements, designers and engineers have the task of selecting an appropriate structural system capable of resisting the large bending moments and deflections of long spans in as efficient a manner possible without sacrificing safety”<sup>6</sup>.

Depending on the architecture of each building, the windows are in the plane of the closing elements, separate from the structural system elements or their form is determined and directly related with the structural elements that compose the closing of the building (fig. 4).

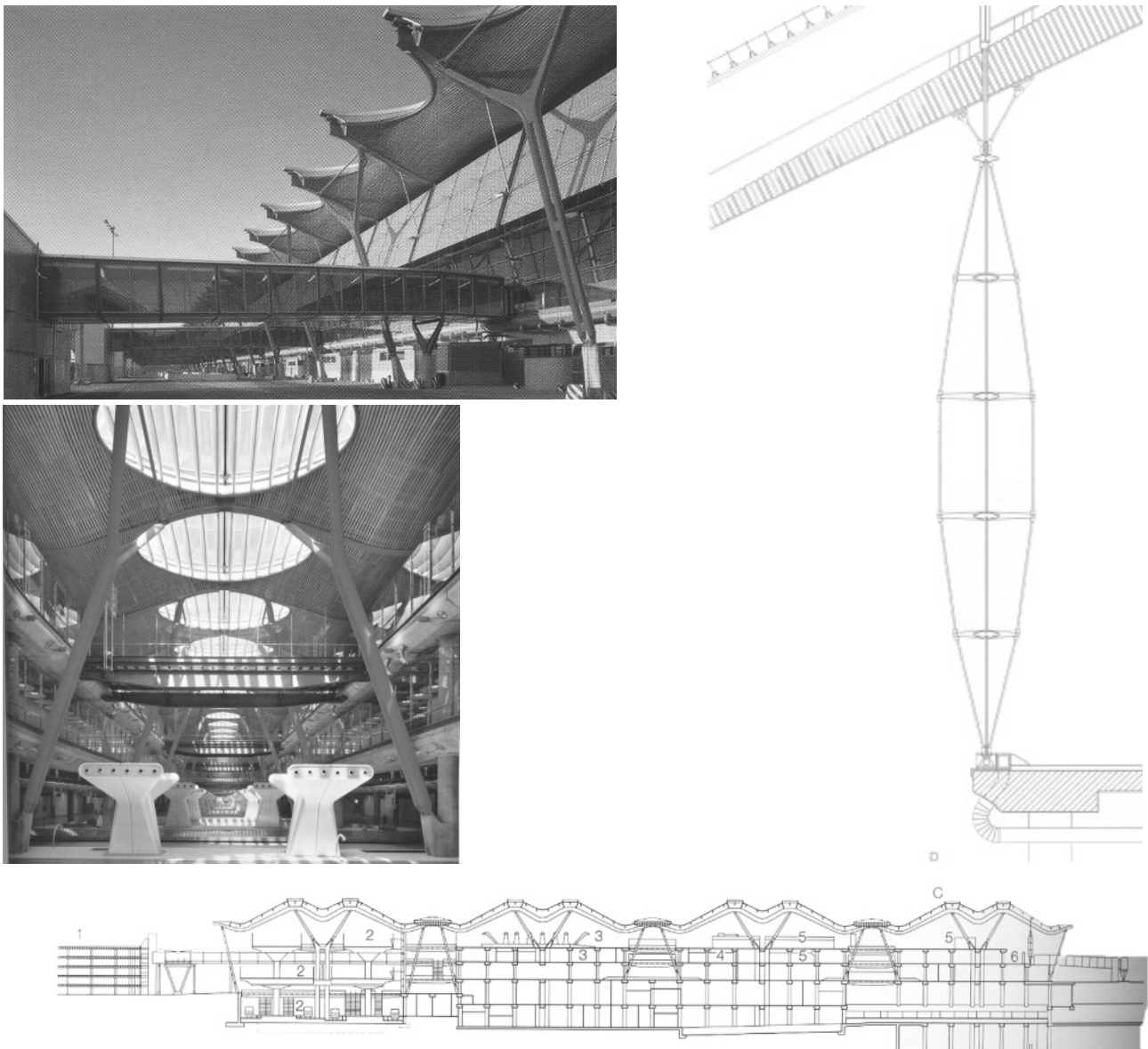


Figure 4. Airport Terminal, Madrid, Spain, Richard Rogers Partnership, 2006

For high-rise buildings, the correlation system of the loads is intimately linked to the configuration and organization of the layout. The load collecting system produces corresponding organization systems of the building layout. A building is considered a high-rise not only because of its height

and its organization on various levels, but also because this kind of a building means an adequate configuration of the structural system, of the layout, a building that means high conditions of design and construction, much more complex than those of the regular type of buildings. “The same basic principles of structural design apply to high rise buildings as for any other type of construction (fig. 5). Individual members and the overall structure must be designed for adequate strength under gravity and lateral loads and there needs to be enough stiffness built into the structure to restrict deflections to acceptable levels”<sup>7</sup>.

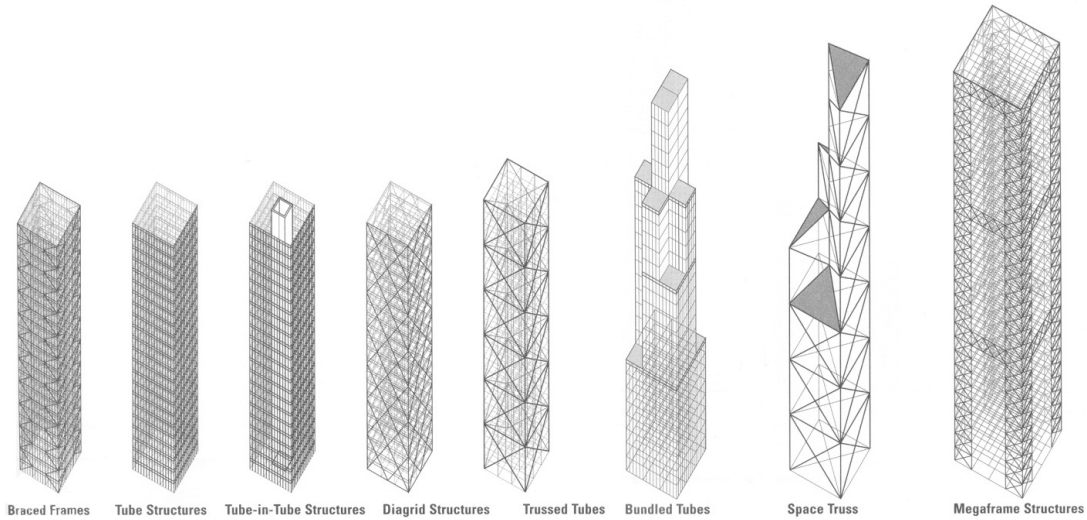


Figure 5. Structural systems for high-rise buildings.

The shape of level layouts of these high-rise buildings has to avoid open, asymmetrical shapes such as L, T, X, C or Z. The layout of these high-rise buildings has to be configured in symmetrical, compact, circular, square or triangular typologies. High-rise structures can be divided in two categories, according to the placement of the structural system: interior structures and exterior structures. “Interior structures are high-rise structures that resist lateral loads primarily through lateral force-resisting elements located within the interior of the structure, such as rigid steel or concrete frame structure or a structure braced by a core consisting of braced frames, moment frames, or shear walls constructed into a closed system that acts as structural tube. Exterior structures are high-rise structures that resist lateral loads primarily through lateral force resisting elements located along the perimeter of the structure”<sup>8</sup>. (fig. 6)

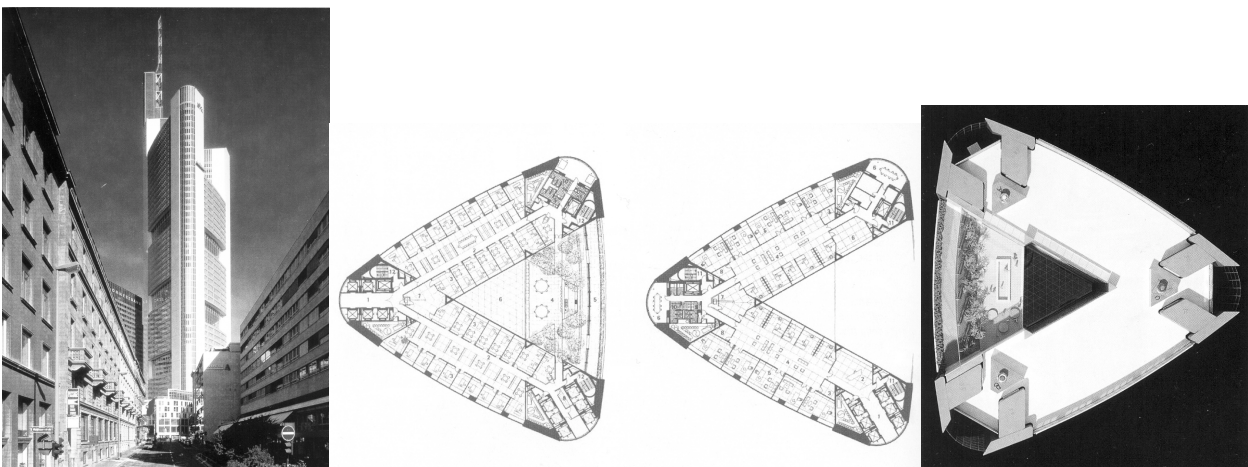


Figure 6. Commerzbank Headquarters, Frankfurt, Germany, Foster & Partners, 1997

#### 4. Daylight and helioplastics

Daylight is used in contemporary architecture just as it was used in the Antiquity and Vernacular architecture, functionally as well as for the aesthetics and ambiance. The creation of special ambient effects in the interior space with the help of lights and shadows is called helioplastics. In contemporary architecture, famous architects such as Tadao Ando, Santiago Calatrava, Zaha Hadid and others, use structural design, shape, texture and the size of openings to capture daylight in an expressive and spectacular way.

By using decorative elements, special colours and embossed textures while guiding daylight towards the interior, different effects in the space perception can be created. Buildings for shows, museums, places of worship, amusement, commercial or administrative buildings have in their functional scheme spaces that can be personalized by creating such helioplastic ambiances. The facades of these buildings, as the surfaces that intermediate the relation between the rooms and daylight, are the ones that can receive special treatments on the level of the closings, on the level of the openings, in the solid-hollow ratio and also in the relation they have with the structural system that supports the façade (fig. 7). So, there are many categories of systems for capturing daylight in a personalized aesthetic special way:

1. Applications on glass, glazing with special treatments: special treatments of the glazing, in the structure of the glass through films, Nano metrics, electro chromatic glass, that modifies its transparency and the translucidity of printed glass or coloured, that through the adding of screen and holographic films offer the possibility to change the ambiance in time, in a managed way.
2. Triforia in the façade plane, parallel to the glass plane of the wall openings: separate fixed elements in front of the openings, which through the geometry of repetitive shapes cast dynamic shadows into the interior space, along the day.
3. Structural members that have the role of fragmenting the lighting surface of the windows: when the façade structure is visually expressed, members such as beams, columns, reticulated systems bring in beams of light and create a spectacular shadow graphic.
4. Independent mechanisms such as sunshade, blinds, shutters, drapery: are attached to the façades with special gradual opening/closing mechanisms that regulate light intensity in heavily lit spaces and also create a pattern of shadows that galvanizes the interior space.

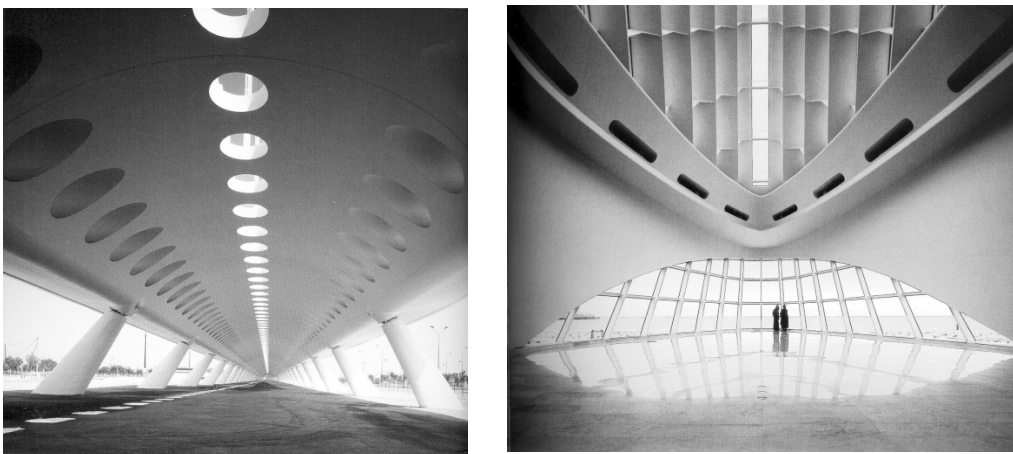


Figure 7. La Cartuja Viaduct and Tenerife Exhibition Centre, Spain, Santiago Calatrava, 1992

## 5. Conclusions

Bringing daylight into interior spaces depends on the structure and geometry of the facades that are the buildings coverings. Facades are directly linked with the structural system, and when choosing it the daylight necessity of the built space must be taken into account.

The shape and size of the openings have an important relevance in the quality of natural lighting from a functional point of view, as well as from an aesthetic point of view.

The destination of the space that defines certain space typologies, determines certain options regarding natural lighting systems on the level of the building covering.

The plastic effects of daylight in the interior space are the result of using certain techniques and advanced technologies from the field of transparent covering materials for openings and of shuttering elements and regulation of the light intensity on the level of the facades.

## 6. Notes:

<sup>1</sup> This type of separation was used by Le Corbusier at the Dominican Friary of La Tourette in 1957

<sup>2</sup> Pracht, Klaus, *Fenster-Planung*, Gestaltung und Konstruktion, Stuttgart, 1982

<sup>3</sup>  $Df = (t \times W \times q \times M) / [A (1 - R_2)]$ , percent equation

T=transmittance of glazing material, W= net area of glazing material, q= vertical angle of sky seen from centre of window, M = maintenance factor, A= total area of interior surfaces, R= area-weighted average reflectance of interior surfaces

<sup>4</sup> Cornelia Barbulescu, *Tehnologia fatadelor, Intefgrarea tehnologica in arhitectura contemporana*, Presa universitara clujeana, 2002

<sup>5</sup> Pete Silver, Will McLean, *Structure and forme: Introduction to Architectural Technology*, Laurence King Publishing

<sup>6</sup> Francis King, Barry Onouye, Douglas Zuberbuhler, *Long Span Structure, Building Structures Illustrated*, John Wiley & Sons, Inc., USA, 2009

<sup>7,8</sup> Francis King, Barry Onouye, Douglas Zuberbuhler, *High-Rise structures - Building Structures Illustrated*, John Wiley & Sons, Inc., USA, 2009

A symmetric configuration of the layout compared to the geometry of the external walls, improves and optimizes the torsion strength of these high-rise volumes.

## 7. References

- [1] Deplazes Andrea, *Constructing Architecture – Materials Processes Structures*, Birkhauser, Second extended edition, 2008
- [2] Francis King, Barry Onouye, Douglas Zuberbuhler, *Building structures illustrated*, John Wiley & Sons, Inc., USA, 2009
- [3] Pete Silver, Will Mclean, *Introduction to Architectural Technology*, Laurence King Publishing, London, 2008
- [4] Tomoko Sakamoto, Albert Ferre, *From control to Design*, Ingoprint SL, 2008
- [5] *Detail - Review of Architecture and Construction Details*, vol. 2/2010, vol. 2/2011, vol. 3/2006
- [6] Thomas Herzog, Roland Krippner, Werner Lang, *Façade Construction Manual*, Birkhauser, 2008
- [7] Philip Joido, *Santiago Caltrava*, Taschen, 2003
- [8] *Tadao Ando Architecture - The colours of light*, Phaidon Press Inc., New York, 2000
- [9] Ariadna Alvarez Garreta, *Skycrapers*, Atrium Group, Spain, 2004.

## Proposal for a network of urban motorways in the Cluj-Napoca urban area

Mihai Grecu<sup>1</sup>

Technical University of Cluj-Napoca, Faculty of Civil Engineering. 15 C Daicoviciu Str., 400020, Cluj-Napoca, Romania

Received 27 June 2011; Accepted 20 September 2011

This article is dedicated to Mr. Ozger Inal of Enka İnşaat ve Sanayi A.Ş., for his outstanding contribution to the construction management of the Transylvania Motorway.

### Abstract

*The existing and currently planned road infrastructure that plays or will play bypass roles for the Cluj-Napoca area is significantly inefficient in serving the interests of both local and transit traffic. In this paper, I propose and discuss a system of urban motorways for the Cluj-Napoca metropolitan area. The system comprises two motorways with a total length of 79.2 km. The first motorway (AUCN 1) is effectively a southern bypass of the city. The second motorway (AUCN 2) serves as a crosstown motorway and then continues south connecting to the Transylvania Motorway. The intraurban sector of AUCN 2 is conceived such as to bring maximum mobility benefits with minimal negative impact, through the usage of existing rights of way. This sector would comprise a submerged section under the Someş river bed and an elevated section following the existing railway line through a mostly industrial area. Complementary measures that should accompany the construction of the urban motorways are proposed, in order to increase the sustainability of Cluj-Napoca and to encourage inhabitants to make carbon-friendly travel choices. A prioritization of the system's eight segments and a set of preconstruction measures are proposed.*

### Rezumat

*Infrastructura rutieră existentă și planificată la ora actuală care oferă sau va oferi posibilitatea ocolirii orașului Cluj-Napoca este ineficientă în a deservi interesele atât ale traficului local cât și ale celui de tranzit. Prezenta lucrare propune și discută un sistem de autostrăzi urbane care să deservească zona metropolitană Cluj-Napoca. Acest sistem cuprinde două autostrăzi cu o lungime totală de 79,2 km. Prima autostradă (AUCN 1) constă într-o centură sudică a orașului. A doua autostradă (AUCN 2) joacă rolul de autostradă transurbană iar apoi continuă înspre sud până la Autostrada Transilvania. Sectorul intraurban este conceput astfel încât să ofere cât mai multe beneficii de mobilitate dar cu un impact negativ minim, prin utilizarea unor coridoare existente. Acest sector ar cuprinde o secțiune subterană construită sub patul râului Someş și o secțiune suspendată de-a lungul căii ferate existente, printr-o zonă majoritar industrială. Sunt propuse de asemenea măsuri complementare ce ar trebui să însoțească construcția sistemului de autostrăzi urbane, pentru a crește sustenabilitatea orașului Cluj-Napoca și pentru a încuraja locuitorii săi să facă alegeri de mobilitate propice pentru mediul înconjurător. Se propune și o prioritizare a celor opt tronsoane ale sistemului precum și un set de măsuri premergătoare construcției.*

**Keywords:** Urban motorways, urban mobility, transport sustainability, underground motorway

---

<sup>1</sup> Corresponding author. E-mail address: grecu20@gmail.com

## 1. Introduction

The provision of an adequate road network that allows for fast and convenient access between the various regions of a metropolitan area is crucial. Of equal importance is that this network provides quick access to the road system intended for long distance trips. When high traffic volumes are involved, controlled-access facilities (expressways and motorways) are usually employed to serve mobility needs.

For the purpose of this discussion, we will arbitrarily classify urban motorways as periurban motorways (they do not cross and are not adjacent to residential areas) and transurban motorways (they have either of these two properties, at least in part<sup>2</sup>).

During the last decades, there has been a general reluctance towards the construction of transurban motorways, ranging from indefinite postponement of such projects to demolishing existing urban motorways (such as in Seoul in 2005). There seems to be a general consensus that the negative impacts of such developments are greater than the positive ones. The point of view that “more roads lead to more congestion” is more popular today than ever.

But maybe it is not the urban motorways *per se* that bring the negative effects, but the way these projects are usually developed. Defining new paradigms in urban motorways development, whereby their construction would be accompanied by the implementation of complimentary measures aimed at improving the usage of other transportation modes (walking, cycling, mass transit, commuter railways) might be a successful solution in solving the mobility problems in today’s cities.

This paper exemplifies such an approach through an urban motorway network proposal for the Transylvanian city Cluj-Napoca.

## 2. Urban motorways and the interests of their local users

In general, the usage of urban motorways is shared between local traffic (this refers to users that perform both local-local trips but also long-distance trips originating from the respective urban area) and transit traffic. Table 1 presents the major interests of the users pertaining to both categories.

Table 1: Interests of various users of urban motorways

Transit users	Local users
<ul style="list-style-type: none"> <li>- Motorway follows the shortest route.</li> <li>- There are few or no speed reductions.</li> <li>- The interchanges are spaced significantly far apart as to not reduce the motorway service level.</li> <li>- Local traffic does not have a significant impact on motorway service level.</li> </ul>	<ul style="list-style-type: none"> <li>- There is convenient access to the motorway.</li> <li>- Motorway provides local-local trip opportunities.</li> <li>- Motorway has limited or no intrusion in the local urban dynamics.</li> <li>- Motorway collects as much of the transit traffic as possible.</li> <li>- Motorway offers future development opportunities for the urban area.</li> </ul>

It can be seen that these interests are often conflicting. Considering urban motorway bypasses, the optimal solution would be to completely separate transit users from local users by building different parallel motorways on completely different alignments, with the transit motorway being as far as convenient from the urban area. A good example in this respect is the city of Milan; motorway A21, routed Brescia (A4) – Piacenza (A1) – Tortona (A7) – Alessandria (A26) – Asti (A33) – Turin

<sup>2</sup> It must be stressed that this classification, as used herein, does not deal with the functionality of the motorways but simply with the absence or presence of residential developments near the motorway corridors.

(A6), provides such a transit bypass that is sufficiently far from the city not only to reduce congestion on the Milan radial motorway, but also on significant lengths of the approach motorway sections towards the city.

A compromise solution is to build a motorway with local-express lanes (or collector-express lanes). This comprises in essence two separated motorways build on the same alignment, with the “inner motorway” serving the transit traffic, and the “outer motorway” serving local traffic. Examples include Highway 401 in Toronto or A14 in Bologna.



Figure 1. Aerial view of A14 north of Bologna, showing “inner” (transit) motorway and “outer” (local) motorway

However, the most commonly used approach is to build a single motorway for both transit and local users. In this case, in order to find a compromise that maximizes the sum of benefits for both types of users, a very good collaboration, starting from the pre-planning stage, should take place between the authority that represents the interests of the transit users (usually the national road administration or similar) and the local authorities. This collaboration should happen regardless of the authority that actually implements the infrastructure project.

### ***2.1 A brief comparison of the local functionality of six motorway bypasses in Romania***

Three major Romanian cities have motorway bypasses in operation. Bypasses of Pitești and Sibiu, part of the future Bucharest – Nădlac A1 motorway, have been opened to traffic in 2007 and 2010, respectively. The motorway bypass of Cluj-Napoca, part of the future Bucharest – Borș A3 motorway, has been opened to traffic in 2009. The Arad – Timișoara motorway is under construction, and by 2012 will provide bypasses for both these cities. Finally, the motorway bypass of Constanța is under construction, also estimated to open in 2012.

Few – if any – comparative analyses of motorway bypasses’ local functionality have been conducted. The purpose of this subsection is to introduce and apply a brief methodology for such a comparison for the Romanian motorway bypasses. In this respect, five criteria have been established and scored for each of the six motorway bypasses.

Criterion *i* deals with motorway accessibility, both for residential, commercial and industrial users, but also for users originating from important local transportation nodes: airport, central railway station and central bus terminal.

Criterion *ii* deals with the various local trip opportunities provided by the motorway. According to their purpose [2], these can be classified as work trips, shopping trips, social or recreation trips,

business trips and school trips.

Criterion *iii* refers to potential negative aspects of the motorway in the urban area, such as: fragmenting existing communities, interruptions or disruptions of established relations and functions, noise effects, impact on areas of value to inhabitants (such as parks and forests) and so on.

Criterion *iv* assesses how much of the transit traffic is actually attracted by the motorway. This is important for the local users, since it reduces congestion on the local roads but also contributes to the reduction of noise and other urban pollution associated with the transit traffic.

Criterion *v* deals with the opening of land adjacent to the urban areas for future developments. This can be important, since otherwise such developments would need their own costly access infrastructure.

Each of these five criteria have been scored with a relative value ranging from 0 (worst situation in the interest of local users) to 5 (best situation in the interest of the local users).

Table 2: Results of the comparison of the six Romanian motorway bypasses regarding the effectiveness in meeting the interests of local users

Interests of the local users	Constanța	Sibiu	Pitești	Arad	Cluj-Napoca	Timișoara	<i>average</i>
<i>i.</i> There is easy and quick access to the motorway	2.5	3	1.5	2.5	0	0.5	1.7
<i>ii.</i> Motorway provides local-local trip opportunities	2	2	1.5	1.5	0	0	1.2
<i>iii.</i> Motorway has limited or no negative effects on the local urban dynamics	5	4.5	5	4.5	5	5	4.8
<i>iv.</i> Motorway collects as much of the transit traffic as possible	5	5	4	4	3	2	3.8
<i>v.</i> Motorway offers future development opportunities for the urban area	4	3	4	3	0	0	2.3
Overall score	3.7	3.5	3.2	3.1	1.6	1.5	2.8

Finally, overall scores have been computed for each city, defined as simply the average of the scores corresponding to the five criteria. A brief discussion of these results follows.

In four cases (Constanța, Sibiu, Pitești and Arad) the motorway bypasses serve the interests of the local users reasonably well. In two other cases (Cluj-Napoca and Timișoara) the motorways bring very few significant benefits to the urban areas, besides collecting some of the transit traffic. This is simply because they are two far from the corresponding urban areas. In both these cases the access to the motorway is (or will be) unreasonably difficult.

The following conclusions, arranged from positive to negative in regards to the utility of the motorway for the local users, correspond to the average results presented in the last column of Table 2.

a). All the bypasses have been planned with careful consideration of avoiding as much as possible any negative effects to the urban areas.

b). In terms of serving as much of the transit traffic as possible, bypasses do an excellent job in the cases of Sibiu and Constanța, a good job in the cases of Pitești and Arad<sup>3</sup>, an average job in

<sup>3</sup> When analyzing the functionality of the motorway, the existing non-motorway bypass sections have been considered too (for Pitești: DN 65B between A1 and DN 65; for Arad: the northern bypass connecting DN 7 westbound, DN 79 northbound and DN 7 eastbound).



the case of Cluj-Napoca and a poor job in the case of Timișoara.

c). Motorways near Constanța, Sibiu, Pitești and Arad offer reasonably good future development opportunities, while motorways near Cluj-Napoca and Timișoara offer virtually no such development opportunities.

d). Overall access to the motorway is reasonable in the cases of Sibiu, Arad and Constanța, rather poor in the case of Pitești and extremely poor in the cases of Cluj-Napoca and Timișoara. Although such projects should be accompanied by new construction or improvements of the access roads to the motorway, there is only one case where this has been done (the extension of the Henri Coandă road in Sibiu to provide a motorway access point for the eastern industrial area).

e). From the point of view of the local users, the worst performance of the bypasses is in terms of providing local trip opportunities: there are limited opportunities in the cases of Constanța and Sibiu, fewer in the cases of Arad and Pitești and none in the cases of Cluj-Napoca and Timișoara.

It can be concluded that the local functionality of these motorways is generally rather reduced, and specifically extremely reduced in the cases of Cluj-Napoca and Timișoara.

Figure 2 clearly shows the opposite approaches that were used when planning the Nădlac – Arad – Timișoara – Lugoj motorway, as it passes Arad (close to the city, multiple access points) as opposed to as it passes Timișoara (far from the city, two access points – one of them on a county road, and the other one is only useful for eastbound traffic – that are very inconvenient to reach from the city).



Figure 2. Different approaches in the routing of the Nădlac – Lugoj motorway near the cities of Arad and Timișoara (ordinary national roads are represented in magenta)

### 3. The existing and currently planned bypass network for Cluj-Napoca

Figure 3 presents those roads that are serving or will serve bypassing roles for Cluj-Napoca.

In addition to the sections opened to traffic or under construction, only other roads that are firmly planned (i.e. the remaining sections of Transylvania Motorway) are included here. There are indeed other ideas for such roads, specifically: the construction of an ordinary road northern bypass, an ordinary road southern bypass between Mănăștur neighborhood and the eastern bypass, and the extension of the eastern bypass from Vâlcele to Ciurila. But these are nothing more than simple ideas.

An analysis of the map presented in Figure 3 brings up serious deficiencies of the plan in serving both the local and the transit users.

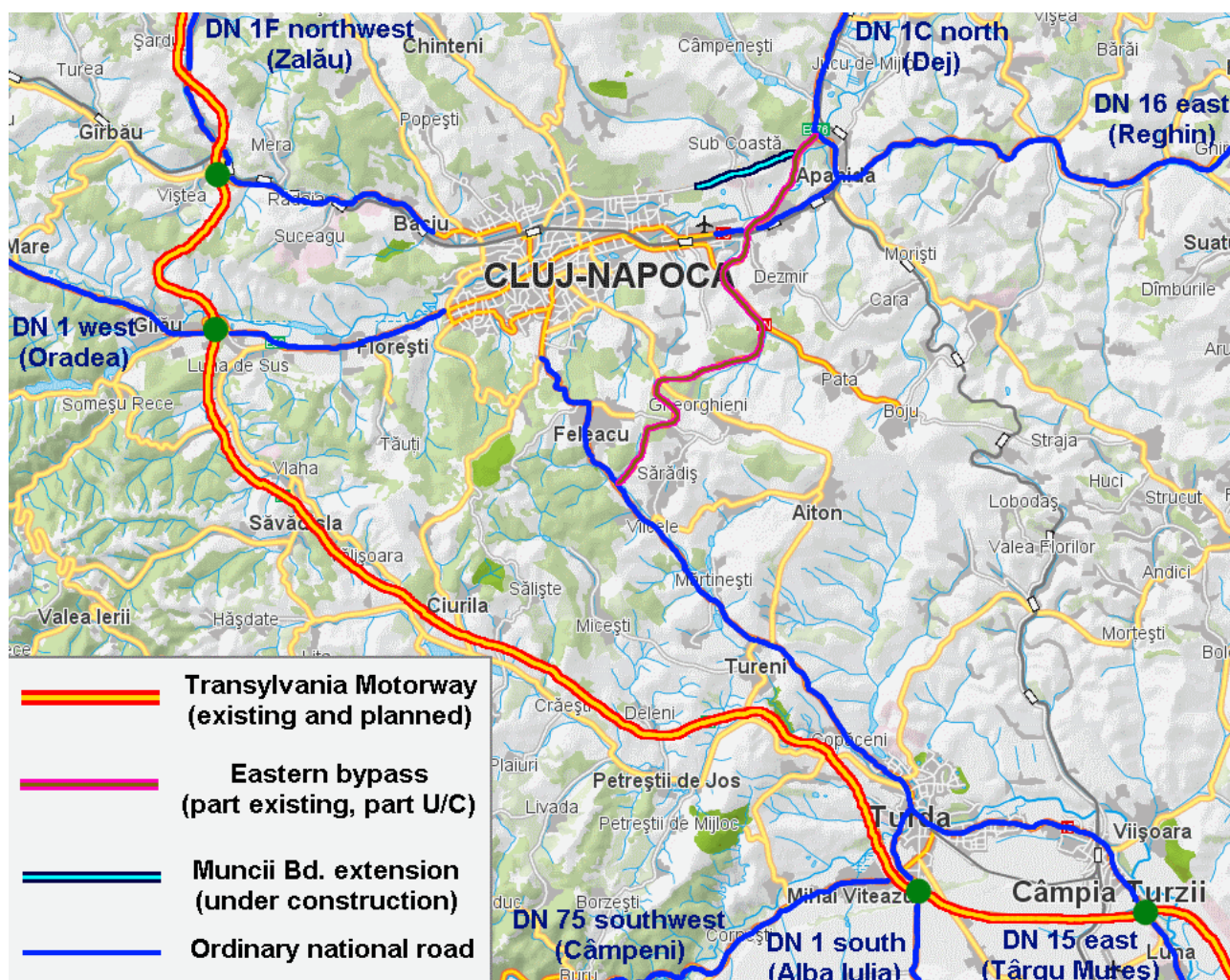


Figure 3. Existing and planned bypass roads for the Cluj-Napoca area

### 3.1 Problems in the functionality for the local users

Access from Cluj-Napoca to the Transylvania Motorway will be possible through three interchanges: interchange Nădășel, positioned on DN 1F; interchange Gilău on DN 1 and interchange Turda on DN 1. Nevertheless, the access from the city to the motorway can be classified as highly inconvenient.

Drivers wanting to use the motorway westbound (towards Zalău, Oradea and Budapest) have two choices: use DN 1F or DN 1 to access interchanges Nădășel and respectively Gilău. The first option, attractive for the inhabitants from the northern part of the city, involves traveling 12 km on an already busy two-lane road, crossing the villages Baciú, Suceagu, Rădaia and Mera. The second option involves traveling 8 km on DN 1 and crossing Florești, a commune that generates a significant amount of commuter traffic, generated by the large number of low- and medium-density residences built in the last years. Users wanting to use the motorway for eastbound and southbound destinations (Târgu Mureș, Brașov, Bucharest) must drive about 20 kilometers on DN 1 south and cross five villages (Feleacu, Vâlcele, Mărtinești, Tureni and Copăceni), and then cross the town of Turda before entering the motorway. In fact, after exiting the city of Cluj-Napoca, drivers have to travel approximately 34 kilometers to reach the motorway access point!

In addition, the currently ongoing and planned new roads will bring only an insignificant improvement to the motorway accessibility. The construction of the Cluj-Napoca south-east bypass will only allow users from the Someșeni neighborhood and from the Cluj-Napoca International Airport to access the motorway (and only eastbound and southbound) somewhat faster.

### 3.2 Problems in the functionality for the transit users

Figure 4 shows the expected relative efficiency of the road transit between any pair of directions among the seven major travel directions that converge in the Cluj-Napoca area.

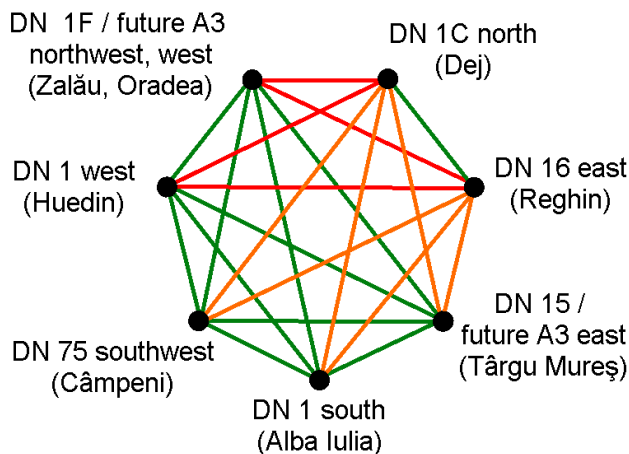


Figure 4. Efficiency of road transit once the projects presented in Figure 3 will be completed (Green = very good; Orange = borderline satisfactory; Red = poor)

One can notice that transit between DN 1C and DN 16 on one hand and all other five directions on the other hand is either borderline satisfactory or very poor. Furthermore, west – east traffic will have to cross the city of Cluj-Napoca. Since DN 1C north continues with DN 17 towards Bistrița and Suceava (a national road which has been recently rehabilitated and constitutes the major access road towards northern Romania), one can estimate that there will be significant transit movements on the west – east axis.

## 4. A proposal for an urban motorways system for the city of Cluj-Napoca

In 2007 – 2008, the Romanian National Company for Motorways and National Roads commissioned a feasibility study<sup>4</sup> for “Autostrada Urbană Cluj-Napoca” (Cluj-Napoca Urban Motorway, herein named „AUCN 1”). Besides improving road transit on the axes characterized by poor transit efficiency in section 3.1, this project would have provided great local functionality: quick access to the Transylvania motorway, the Cluj-Napoca International Airport and the two largest commercial centers of the city. The city’s largest residential areas (Mănăștur, Gheorgheni, Grigorescu, Mărăști) were to be provided with efficient access to this motorway. Figure 5 shows the alignment of the AUCN 1 as it resulted from the feasibility study. However, after 2008, the plans regarding the construction of this motorway have been shelved.

The urban motorway system of Cluj-Napoca envisioned in this article includes, besides AUCN 1, a proposal for another urban motorway (AUCN 2), with a total length of 37.2 km. Figure 6 presents an overall view of the two proposed urban motorways – only the sectors close to Cluj-Napoca city. For a larger-scale view, including the connections with the Transylvania Motorway, please see Figure 13.

<sup>4</sup> At the initiative of the author, who at the said time was the General Director and President of the Board of the Romanian National Company for Motorways and National Roads.



Figure 5. Alignment of the Cluj-Napoca Urban Motorway as it resulted from the feasibility study

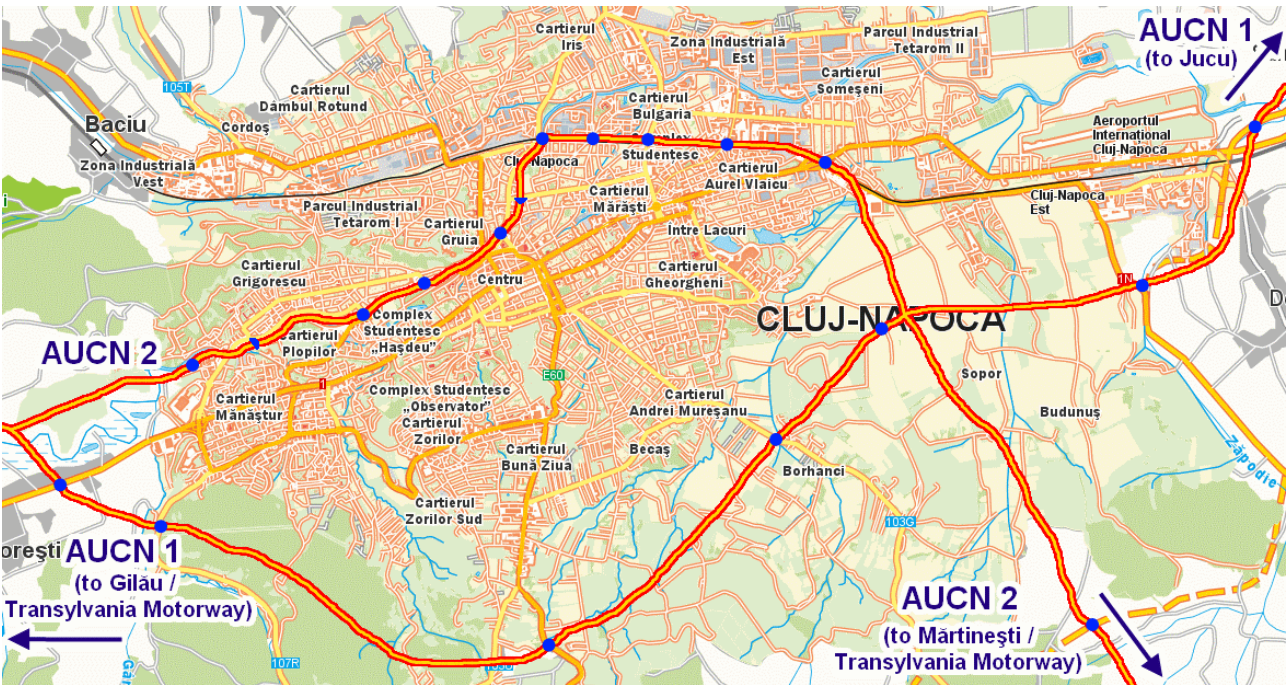


Figure 6. Overview of the proposed urban motorways system (only the sectors close to the city)

#### 4.1 Detailed description of AUCN 2

*Brief overview of the AUCN 2 alignment.* The motorway branches from the AUCN 1 north of Polus Commercial Center, and after allowing for a local interchange with traffic discharging in the 1 Decembrie 1918 bd. / Frasinului st. / Cora roundabout, it submerges under the Someș river bed. The motorway follows this alignment for 5.2 kilometers, until near the railway bridge close to the intersection of the Traian and Decebal streets. At this point, it emerges from below the Someș river and follows the northern side of the railway alignment as an elevated motorway for 4 km until reaching the Selgros area in the Aurel Vlaicu neighborhood. From here it continues as an at-grade

motorway in the south direction, and after an interchange with AUCN 1 it passes east of the Gheorgheni village, west (or east) of Aiton, south of Mărtinești. Then it crosses DN 1 between Mărtinești and Tureni, and ends in the Transylvania Motorway in the km 20-21 region of the latter. The motorway is proposed as a 2x3 (three lanes in each direction) motorway between km 0 and km 6.8 (where the underground section ends), and as a 2x2 motorway for the rest of its alignment. Table 3 presents the proposed location of interchanges along the motorway. Distances have been estimated using the Google Earth application.

Table 3: Interchanges and other critical points on the proposed alignment of AUCN 2.

km	IC #	Description
0.00	IC 0	AUCN 2 starts from its interchange with AUCN 1 (km 0+000 is considered where the directional ramps of opposite directions meet)
1.37	IC 1	Cora interchange
1.64	-	<i>Underground section begins</i>
2.10	IC 2	Acces cart. Grigorescu (partial interchange, ramps only towards/from city center)
3.58	IC 3	Acces Stadion (str. Giuseppe Garibaldi)
4.39	IC 4	Acces Parc (str. Octavian Goga / Splaiul Independenței / P-ța Horea, Cloșca și Crișan
5.49	IC 5	Acces centru (str. Ion Popescu Voitești / Decebal / Traian)
6.01	IC 6	Acces P-ța Abator (str. Daniil Bărceanu) (partial interchange, ramps only towards/from city center)
6.80	-	<i>Underground section ends / Elevated section begins</i>
6.91	IC 7	Acces Gara CFR (str. Traian / Decebal / Oașului)
7.40	IC 8	Acces P-ța 1 Mai (str. Paris / Tăbăcarilor / Porțelanului)
7.99	IC 9	Acces str. Fabricii
9.01	IC 10	Acces str. Fabricii de Zahăr
10.17	IC 11	Acces str. Aurel Vlaicu
10.81	-	<i>Elevated section ends</i>
12.70	IC 12	Interchange with AUCN 1
17.10	IC 13	Centura Cluj-est
33.50	IC 14	DN 1 Mărtinești
37.20	IC 15	Transylvania Motorway junction at km 21 - 22

*Detailed discussion of the AUCN 2 alignment.* AUCN 2 branches from AUCN 1 via an interchange (IC 0) with high-speed directional ramps, that is positioned some 700 m north of the DN 1 interchange near Polus Center. At km 1.37 there is a trumpet interchange (IC 1) with access to the 1 Decembrie 1918 bd. / Frasinului st. / Cora roundabout. At km 1.64 the motorway submerges under the Someș riverbed. Figure 7 shows the proposed alignment of this section<sup>5</sup>.

<sup>5</sup> Readers familiar with the AUCN 1 project will notice that its alignment has been shifted east in Figure 7; according to the feasibility study, the motorway would cross DN 1 west of the Polus commercial center. For reasons discussed in section 5.3 of this article, relocation of AUCN 1 on the alignment proposed in Figure 7 should be investigated.



Figure 7. The western end of AUCN 2

Between kilometers 1.64 and 6.80 of the motorway we find the submerged section that follows the alignment of the Someș river. The author proposes a double-deck structure for this tunnel. In order to reduce the costs of the project, the submerged motorway section is designed only for cars, with an overhead clearance of 2.0 – 2.3 m. The motorway is to have three 3.5 m lanes in each direction, with a fourth lane added where necessary for exit/enter ramps. Construction of this section should be undertaken via cut-and-cover. Without going into great technical detail, a potential constructive method would be to dredge the river bed to create a new cross section (essentially an inverted trapezoid), to prepare the bottom with a suitable rock (or similar) bed and then to realize the tunnel structure, either by laying precast elements or by casting it in situ. This latter approach would need a way to accurately control the volume flow of the Someș river, but this should not be a problem, considering the existing dams upstream of Gilău.

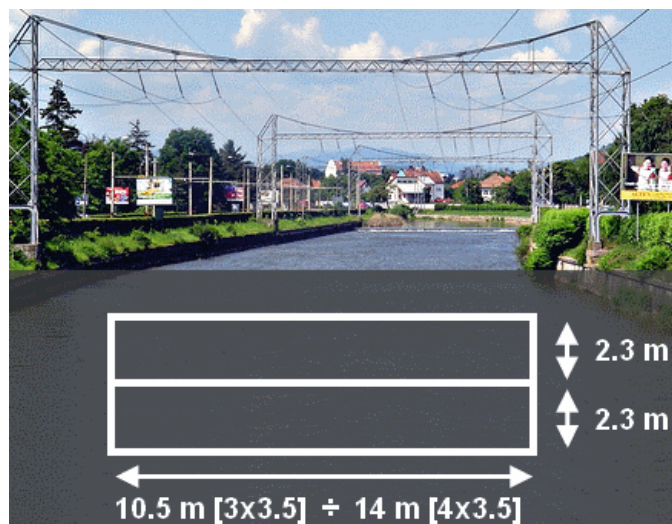


Figure 8. Very basic outline of the proposed cross section for the submerged section of AUCN 2

The proposed cut-and-cover solution is preferred over a TBM solution, since the latter would bring the level of the motorway carriageways much lower, which would imply significantly longer access

ramps to the tunnel, both at the two ends of this section, but also for the five interchanges that would serve the underground section.

A double-deck solution is proposed, since:

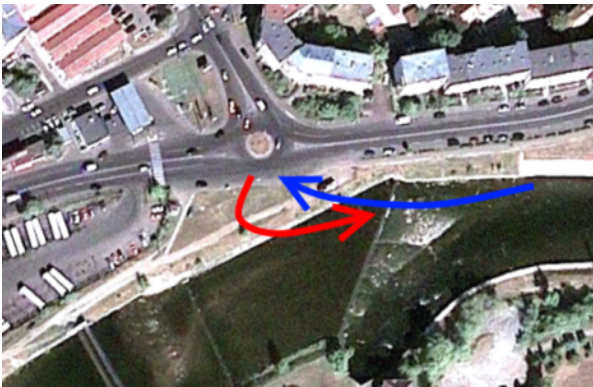
a). It allows for the provision of exits and entrance ramps on either side of the roadway for both motorway directions. This is extremely important, since the existing surface situation where access points are proposed will seriously constrict the position of these access points, as shown in Figure 9.

b). Greater flexibility in designing the tunnel in sections where the riverbed is narrow.

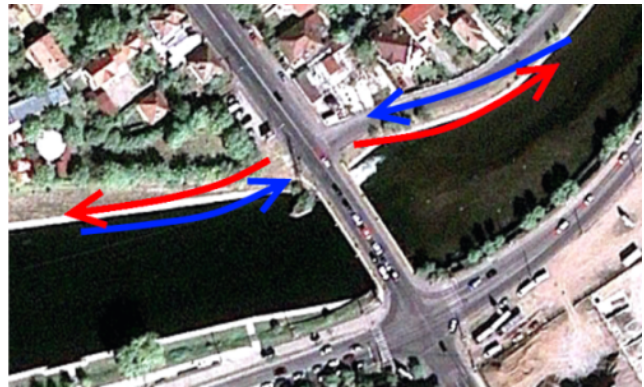
The main disadvantage is that for the

lower carriageway the access ramps will need to be longer, because of the greater height difference (there can be more than 10 meters in vertical difference between surface streets and the pavement level of the lower carriageway).

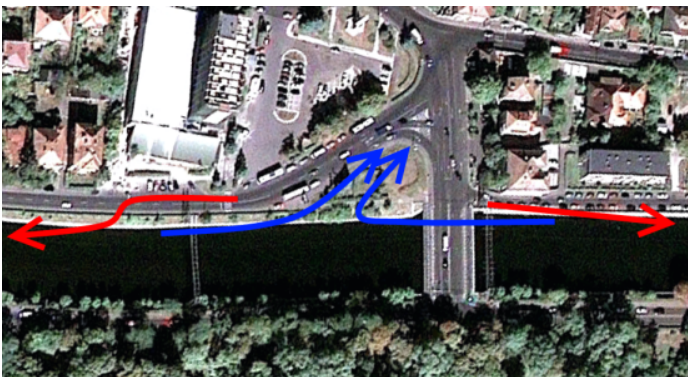
Access points are proposed at five locations (interchanges IC 2 – IC 6) for the underground section. IC 2 (km 2.10) will connect to the roundabout at 1 Decembrie 1918 bd. and Miraslău st. This will serve the Grigorescu neighborhood, and will only have ramps to / from the city center (since westbound access can easily be provided via IC 1). The next three interchanges will be provided around Garibaldi bridge (IC 3 at km 3.58), Napoca bridge (IC 4 at km 4.39) and Ion Popescu Voitești st. bridge (IC 5 at km 5.49). Finally, the last underground interchange, at București st. bridge (IC 6 at km 6.01) will have only westbound ramps, to / from the city center (eastbound access is conveniently provided via IC 8).



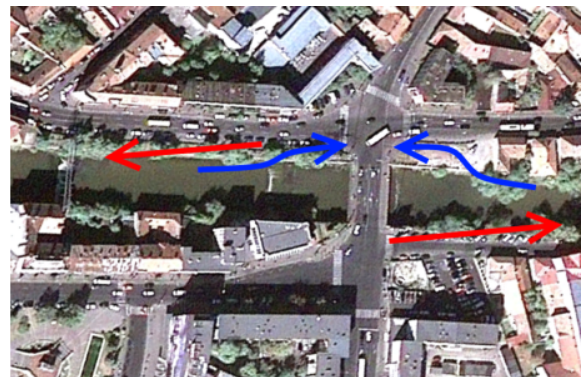
IC 2 (1 Decembrie 1918 / Miraslău)



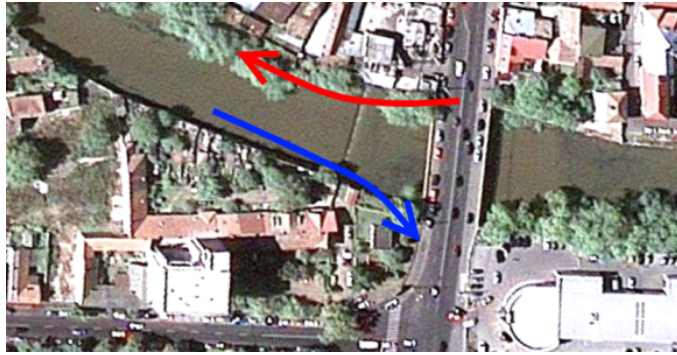
IC 3 (Giuseppe Garibaldi)



IC 4 (Octavian Goga / Splaiul Independenței)



IC 5 (I. Popescu Voitești / Decebal / Traian)



IC 6 (Daniil Bărceanu)

Figure 9. Proposed positioning of access ramps for the five underground interchanges of AUCN 2 (Blue arrows: ramps coming from the tunnel to the surface; Red arrows: ramps going underground)

The selection of these five access points has been made in order to ensure the best functionality of the motorway, but also considering the technical possibilities in providing surface access space for the tunnel ramps. Figure 9 presents proposed locations of the access ramps for the five underground interchanges. It appears as there is little need in expropriating additional surfaces, and no need for demolishing buildings. Nevertheless, some of the bridges will need widening to provide for storage lanes for traffic entering the tunnel. In addition, reconstruction of the foundations and the piers of most bridges will need to be undertaken (constructing inverted V piers to support the bridges and then demolishing the existing piers and foundations is a reasonable solution).

IC 7 is positioned near the intersection of Traian, Decebal and Oaşului streets. This is also the place where the motorway transitions from the underground section to the elevated section.

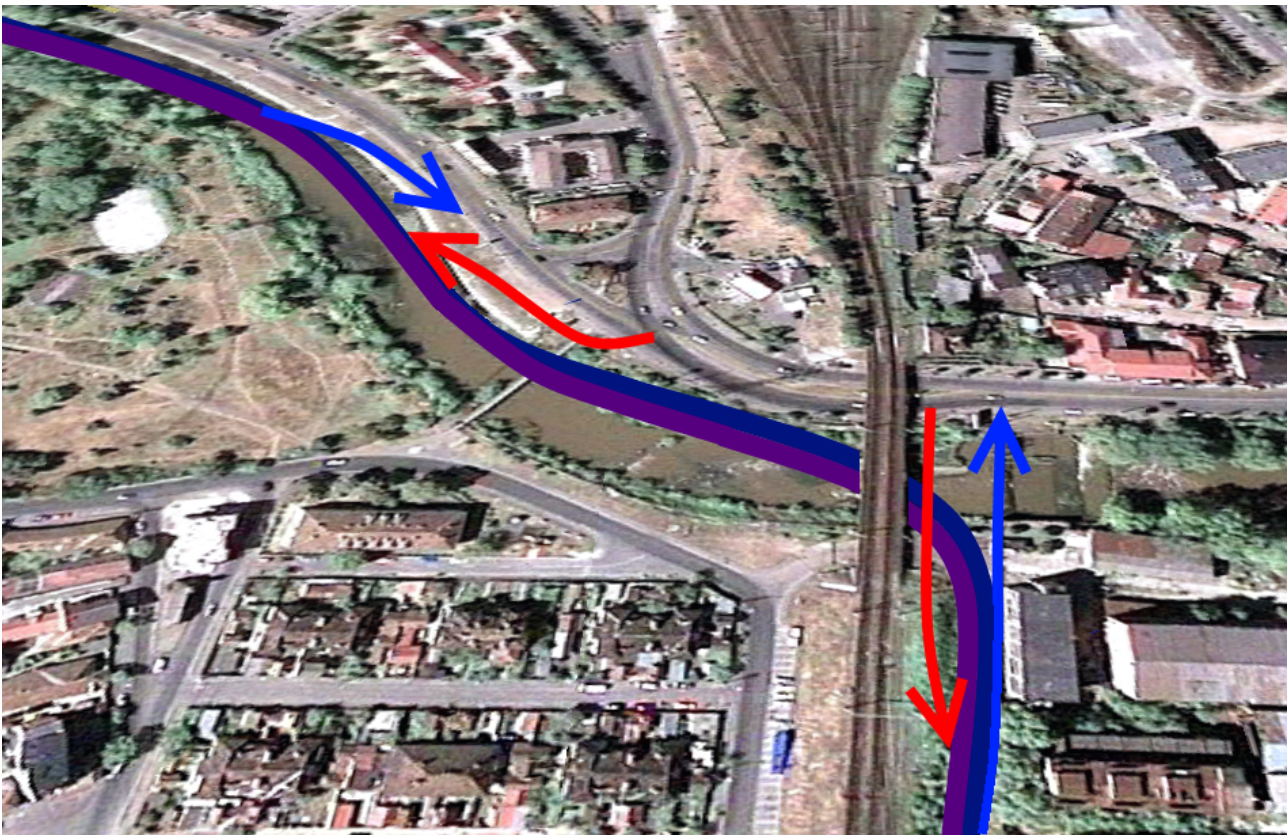


Figure 10. Proposed layout of IC 7 and of the underground – overground transition of AUCN 2



Since the 2.0 – 2.3 m overhead clearance disappears as the motorway becomes elevated, the motorway will be opened east of this point to all motorized traffic. Hence, ramps serving traffic to/from east should connect directly to the surface section of the motorway, to provide truck and bus access towards east starting from this point, as shown in Figure 10.

The corridor north of the railway (currently occupied by a trail as shown in Figure 11) provides sufficient space for the motorway to transition from underground to elevated. In fact, most of the section between IC 7 and IC 8 could be constructed at level, by simply expanding the railway fill to the north.



Figure 11. View of the area where the elevated – underground transition of AUCN 2 should take place. Picture shows the trail between the railway (left part of the trail) and a mostly inactive industrial area (right part of the trail). The arrow in the aerial image on the right shows the point and the direction from where the picture on the left is taken

From here, the motorway follows the north side of the railway corridor. The reason for choosing this side is related to minimizing the disruptions to residential areas. With this solution, only a reduced number of low-density residences found on the Câmpul Pâinii street (the section between Fabricii and Garoafei streets) would be impacted by the motorway, as the rest of the corridor is lined with industrial or commercial developments.

Access points to the motorway are provided at Paris st. / 1 Mai square (IC 8 at km 7.40), Fabricii st. (IC 9 at km 7.99) and Fabricii de Zahăr st. (IC 10 at km 9.01). Basic diamond-type interchanges should be the most appropriate solution for these three cases. However, the motorway red line will need to be shifted north in the interchanges' vicinity, to provide room for the ramps connecting to the eastbound carriageway (these ramps will be located between the railway and the motorway). In addition, some reconstruction of the local streets would be needed, especially in relation to the Câmpul Pâinii / Fabricii st. existing interchange.

The last interchange on the elevated sector is IC 11, near str. Aurel Vlaicu – str. Traian Vuia (DN 1C) railway overpass. At this point the motorway will cross over the existing DN 1C railway overpass, and hence it will reach its highest elevation relative to ground level. It is rather easy to conceive an interchange with no conflicting traffic flows between the two road axes. This takes advantage of the existing (for the southern part) or easily to construct (for the northern part) ramps

connecting DN 1C with the local streets.

Figure 12 presents a proposed layout for this interchange. Besides the fact that turning around is possible for all four directions, only two movements are classified as inconvenient (north to east and south to west), but both are of relatively reduced importance.

After crossing the railway, the motorway exits the urban built area and its elevated section ends at km 10.81. As it heads south, AUCN 2 meets AUCN 1 again at km 12.70. Non-existing space constraints coupled with expected high volumes of exchange traffic between the two urban motorways recommend the construction of a full stack interchange.

The motorway then follows an extraurban area, with interchanges to be provided at km 17.10 (Cluj east bypass) and km 33.50 (DN 1 between Mărtinești and Tureni)<sup>6</sup>. AUCN 2 finally ends at km 37.20, at its junction with Transylvania Motorway, around km 21 – 22 of the latter. A connection to the local road network (to DJ 107L) should also be provided here, to serve the surrounding settlements and the Cheile Turzii area. Hence this last interchange could be configured as a cloverleaf, with collector/distributor lanes installed on the Transylvania Motorway.

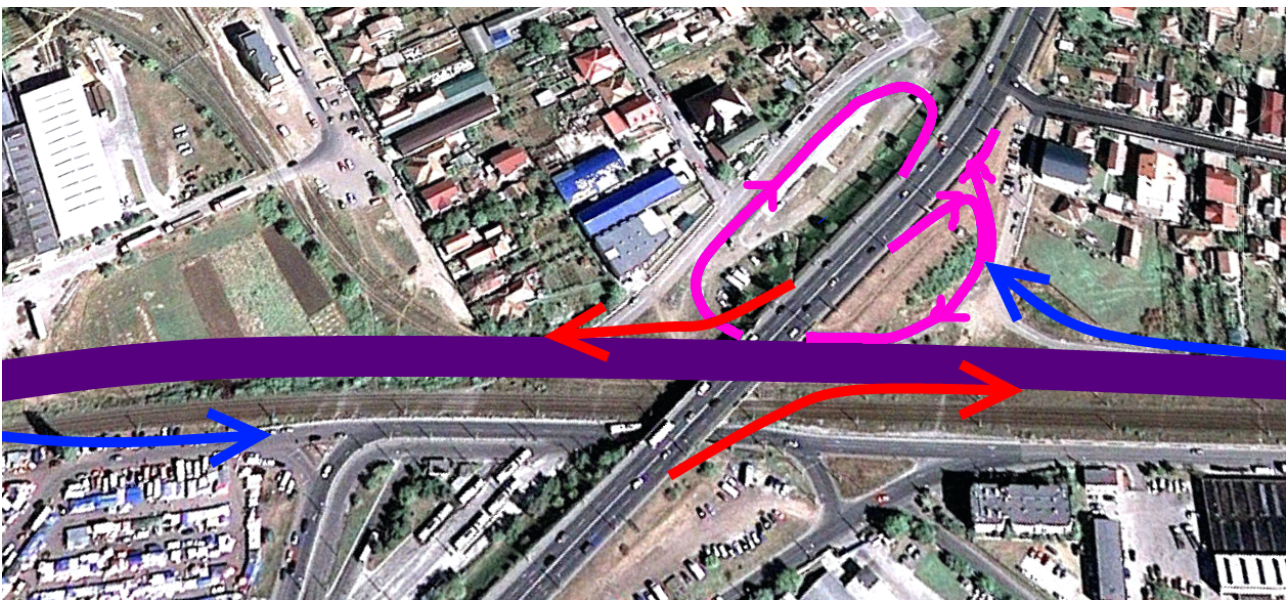


Figure 12. Proposed layout for IC 11. Blue: motorway offramps. Red: motorway onramps. Magenta: additional local ramps to be constructed north of the railway corridor.

## 5. Impact of the motorway system on the sustainability of the Cluj-Napoca metropolitan area

There is a contemporary tendency of looking in a negative way towards the development of urban motorways, especially of the “transurban” (as defined in section 1) sectors. A study on the impact of the M4 motorway in Sydney [3], especially considering the induced traffic growth associated with this development, concludes that the motorway „has not been conducive to improving the sustainability credentials of Sydney” and recommends that mobility-related „policy should be recast to reflect this”. Considering the construction of the A22 transurban motorway in Vienna, Knoflachner [1] draws the following very interesting conclusion: „with the opening of the motorway the speed went up and the kinetic energy in the whole urban structure was enhanced, leading to increased safety hazards and accidents”.

However, maybe it’s not the construction of urban motorways that has generated negative impacts

<sup>6</sup> However, see section 6.3 for potential reasons for additional interchanges.

such as the ones mentioned above, but rather the fact that these projects have not been accompanied by the implementation of complementary measures meant to increase the sustainability of the cities and to encourage inhabitants to make carbon-friendly travel choices.

This section presents such measures that could be taken in conjunction with the development of the proposed urban motorway system in Cluj-Napoca.

### ***5.1. Dedicated public transport lanes***

Even without any action, travel time for public transport in Sibiu has reduced on average with 14% after the opening of the motorway bypass [4]. For public transport routes overlapping with streets that formerly carried transit traffic, the time reduction is on average 22%, with a maximum of 26% for bus route 16.

Cluj-Napoca currently benefits of a 1.69 km dedicated public transport lane on the major west – east axis (eastbound only), between the intersection Str. Moșilor / Str. Petru Maior and the intersection Bd. 21 Decembrie 1989 / Str. Sándor Petőfi. With the construction of the urban motorways, dedicated mass transit lanes could be provided for the major west – east axis (Calea Florești – Calea Mănăștur – Calea Moșilor – Bd. 21 Decembrie 1989 – Str. Aurel Vlaicu) and possibly on other sections throughout the city. This would significantly increase the reliability and speed of the mass transit, and most likely attract more users to this service.

### ***5.2. Provision of bicycle ways***

In surface road corridors adjacent to the new transurban motorway, traffic lanes could be decommissioned and remarked as bicycle-only routes. This could be easily done, for instance, on the entire length of the corridors Bd. 1 Decembrie 1918 – Str. G-ral Dragalina – Str. Horea and Str. Aurel Vlaicu – Bd. 21 Decembrie 1989, as well as on many other connecting routes.

On the other hand, creating a comparable bikeway network in the context of the current surface road system (without constructing the urban motorways) would be much more difficult and possibly even socially unacceptable.

### ***5.3. Provision of Park & Ride facilities***

The urban motorway system should feature Park & Ride facilities that would encourage commuters from the extended urban area to use public transportation. An excellent location for such a facility, serving users from the eastern side of the extended urban area, would be near the Aurel Vlaicu interchange on AUCN 2. This point is connected to the entire city by a large number of bus and trolleybus routes. For the facility serving the western side of the urban area, a very good location would be near the DN 1 interchange on AUCN 1 near the Polus commercial center<sup>7</sup>.

Since the proposed motorway system has exits close to both the central railway station and the airport, similar facilities should be envisioned in these two points.

## **6. Proposed prioritization and action plan**

The two proposed urban motorways form a system that can be arbitrarily divided in eight sections, as shown in Figure 13.

---

<sup>7</sup> A partnership with the owner of this commercial center could be envisioned, especially considering the fact that this facility already has significant parking capacity that sits unused during the weekday working hours.

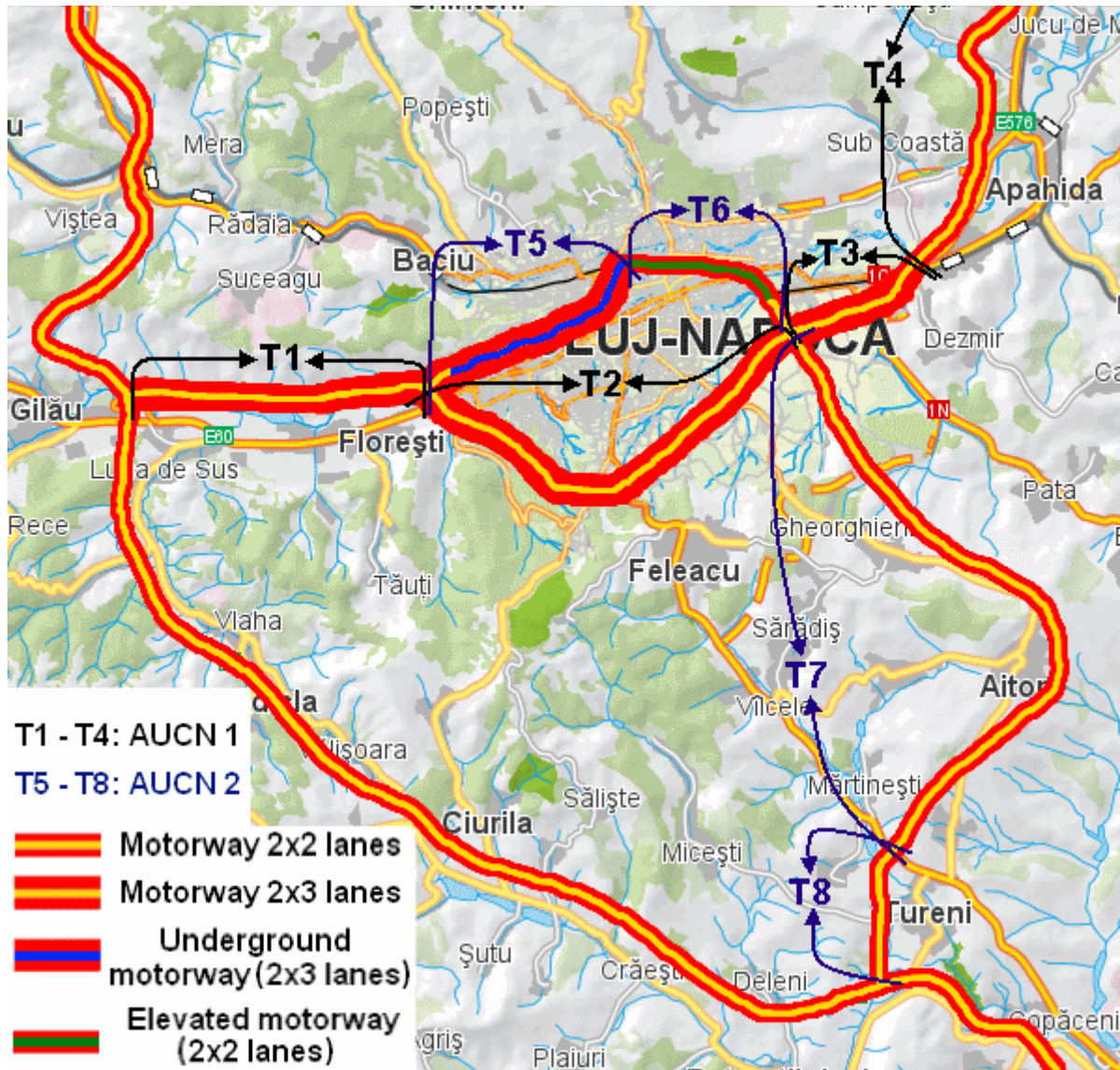


Figure 13. Map of the proposed Cluj-Napoca urban motorways system

### 6.1. Construction prioritization

The table below presents key data about the eight sections (T1 – T8), as well as an arbitrary priority rank (explained in the following paragraphs) and an optimistic construction schedule.

Table 4: Various data pertaining to the sections forming the Cluj-Napoca urban motorway system

Motorway	Section	Length (km)	Lanes	Comments	Priority rank	Proposed construction schedule
AUCN 1 (42 km)	T1	8.15	2x3		2	2012 - 2013
	T2	13.85	2x3		3	2012 - 2014
	T3	5.10	2x3		4	2012 - 2014
	T4	14.90	2x2		8	2014 - 2016
AUCN 2 (37.2 km)	T5	6.80	2x3	<i>underground</i>	5	2013 - 2015
	T6	5.90	2x2	<i>elevated</i>	6	2013 - 2015
	T7	20.80	2x2		7	2014 - 2016
	T8	3.70	2x2		1	2012 - 2013

The rest of this subsection discusses the proposed priority rankings in Table 4.

**a). Construct T8.** This 3.7 km section would bring the important benefit of significantly improving the access to the Transylvania Motorway for eastbound and southbound users, by eliminating the need to cross Turda. Thus, access to the motorway would take place 16 kilometers earlier (which is the distance between the proposed interchange IC 14 on DN 1 between Mărtinești and Tureni on AUCN 2 – see Table 3 – and the existing Transylvania Motorway interchange south of Turda). An estimated time saving of 10 – 15 minutes per vehicle would be obtained by the construction of this segment. In addition, traffic in Turda and Câmpia Turzii would be reduced significantly, as cars traveling on the directions Cluj-Napoca – Alba Iulia and Cluj-Napoca – Târgu Mureș would completely bypass the Turda – Câmpia Turzii area.

**b). Construct T1.** This 8.15 km motorway section would render obsolete the current western access to Cluj-Napoca via DN 1 crossing Florești. Time savings would amount to 5 – 8 minutes for each vehicle. As DN 1 in Florești would be decongested, commuters from Florești would benefit of much easier access to Cluj-Napoca.

**c). Construct T2 and T3.** These sections, totaling 18.95 km, would effectively close the southern bypass of the city between the Polus commercial center and the airport. Time savings of 15 – 25 minutes would be achieved for vehicles crossing the city from the directions Oradea and Zalău to the direction Dej, Bistrița, Suceava and Reghin. Also, Cluj-Napoca west – east crosstown traffic would drop significantly.

**d). Construct T5 and then T6.** These 12.7 km of AUCN 2 (of which 6.8 km underground and 5.9 elevated) will greatly reduce congestion on a significant number of arterials throughout Cluj-Napoca. After their construction, there will be serious changes in the urban traffic patterns in this city.

**e). Construct T7.** This 20.8 km section will furthermore improve access to the Transylvania Motorway for eastbound and southbound users, by eliminating the need to use the existing winding national road that crosses Feleacu, Vâlcele and Mărtinești.

**f). Construct T4.** The eastern section of AUCN 1 is the least urgent, since the existing Apahida bypass provides a reasonable access towards DN 1 towards Gherla and Dej. However, traffic on this two-lane road section is constantly increasing.

## **6.2. Measures to be taken for the construction of the urban motorway system**

a). Immediately analyze the land availability for constructing AUCN 1. When the feasibility study and preliminary design were conducted in 2007 – 2008, no major problems were identified regarding the availability of the corridor needed for the construction. An analysis should be conducted to see if this is still the case, and adjust the alignment or the proposed design where this is needed.

b). Block any new developments in the AUCN 1 corridor by means of local and country councils decisions.

c). Conduct preliminary design for all sections of AUCN 2, and then block developments in the needed corridor.

d). Start, as soon as possible, critical pre-construction activities (archeological clearance, utility relocation design, land acquisition<sup>8</sup>).

e). Devise a preliminary strategy for the project structuring and financing. The total costs of the construction of the entire urban motorway system (with a total length of 79.2 km) could be anywhere between 1.8 billion EUR (considering an average cost of 23 million EUR per km) and 3 billion EUR (considering an average cost of 35 million EUR per km).

<sup>8</sup> As a general statement, central and local governments should use periods of economic downturn (such as the current one) to do as much land acquisition for motorway and other infrastructure development as possible, given the low market prices of land.

### 6.3. A proposal for financing the construction of the system

While financing the motorway construction from public sources might be an option, due to their reduced availability, alternatives should be sought to involve private capital. Such an alternative could rely on the capitalization of the existing public land available along the motorway corridors. The alignments of at least T7 and T1 are adjacent to large tracts of public land. If a private consortium would be established with the purpose of building the motorway system, these tracts of land could be donated by the public authorities to this consortium, and the latter could develop them into residential, commercial, industrial or logistic areas – with motorway access. Since this land would significantly appreciate with the construction of the motorway, this appreciation could cover a significant cost of the motorway construction.

## 7. Conclusions

Since the existing and most of the currently planned road infrastructure around the Cluj-Napoca urban area fails to adequately serve the interests of both the local and transit road users, new road infrastructure developments are needed as a remedy to this situation.

This paper proposes the construction of an urban motorways system for the city of Cluj-Napoca, with an estimated total length of 79.2 km. This includes a crosstown motorway that would bring significant mobility benefits to the city, and that can be constructed using existing rights of way (under the Someș river and near the existing railway line crossing a mainly industrial area) and thus bring very limited negative impacts.

The construction of these urban motorways should be accompanied by complementary measures designed to stimulate the usage of alternative transport modes and to improve the quality of life in the city. With very good planning and implementation of the construction, the entire system could be built between 2012 and 2016.



Figure 14. A proposal for a motorway network serving Cluj county

Looking outside the Cluj-Napoca metropolitan area, it is only natural that AUCN 1 would be extended further north / east towards Gherla, Dej and then Bistrița on one hand and west up to Huedin on the other hand. Considering also the proposed expressway or motorway from Turda to Sebeș, one reaches what the author likes to call a “reasonably good” motorway network for Cluj county, as presented in Figure 14.

### **Acknowledgements**

This paper was supported by the project "Improvement of the doctoral studies quality in engineering science for development of the knowledge based society-QDOC" contract no. POSDRU/107/1.5/S/78534, project co-funded by the European Social Fund through the Sectorial Operational Program Human Resources 2007-2013.

### **8. References**

- [1] Knoflach H. Success and failures in urban transport planning in Europe - understanding the transport system. *Sadhana - Academy Proceedings in Engineering Sciences*, Vol. 32, Part 4, pp. 293–307, August 2007.
- [2] Meyer MD, Miller EJ. *Urban Transportation Planning*. 2nd edition. New York: Mc Graw Hill; pp. 149-150, 2001.
- [3] Zeibots ME. Before and after Sydney’s M4 Motorway: did it make the city more sustainable? *State of Australian Cities National Conference*. Sydney, December 2003.
- [4] Maier S. Fără trafic greu prin oraș. Tursib – cu 14% mai rapid și cu 8 % mai eficient. *Tribuna*, 10/02/2011, (<http://www.tribuna.ro/stiri/eveniment/tursib-cu-14-procente-mai-rapid-si-cu-8-procente-mai-eficient-61673.html>).

## **Thermal shrinkage bending test in characterizing reinforcement advantages over bituminous mixtures**

Mihai L. Dragomir<sup>\*1,2</sup>, Christophe Petit<sup>2</sup>

<sup>1</sup> *Technical University of Cluj-Napoca, Faculty of Civil Engineering, 15 C. Daicoviciu Str., 400020, Cluj-Napoca, Romania*

<sup>2</sup> *Limoges University, GEMH-Civil engineering and Durability Laboratory, Bd. J.Derche, 19300 Egletons, France*

*Received 27 June 2011; Accepted 20 September 2011*

### **Abstract**

*Cracking in pavements is a permanent preoccupation for a lot of researchers in roads domain, because this is the most frequent phenomenon that happens on site, making a lot of problems. In the same time the road entertaining in our country, like all over the world, is a permanent preoccupation for all road builders but also for the beneficiaries, who wishes to realise durable works respecting some costs limits.*

*This paper wish's to present a French laboratory test equipment, named Thermal Shrinkage-Bending Test, for crack propagation in different types of bituminous materials in controlled conditions of time and temperature.*

*The tested materials are issues from an international experimental-program TG4 (Task-Group4), RILEM, group that is in a constant research in the field of cracking in pavements.*

*For this purpose we have realised a number of thermal shrinkage bending tests, over two types of double layer systems, each one of it with a different type of interface.*

### **Rezumat**

*Aparitia fisurilor in imbracamintile rutiere este o permaneneta preocupare a multor cercetatori din domeniul, datorita aspectului general pe care acest tip de degradare il are in situ. In acelasi timp, intretinerea drumurilor in tara noastra, ca de altfel peste tot in lume, este o preocupare permanenta pentru toti constructorii si beneficiarii de drumuri, care-si doresc realizarea unor lucrari durabile in anumite limite de cost.*

*Lucrarea doreste sa prezinte o metoda franceza, denumita tractiune-incovoiere, asupra propagarii unei fisuri prin diferite tipuri de complexe bituminoase in conditii de temperatura si timp controlate.*

*Materialele testate provin din cadrul unui grup international de cercetare in domeniul soselelor: RILEM, prin cel de al patrulea proiect experimental, TG4(TasckGroup4) ce studiaza fenomenul de fisurare. In cadrul campaniei de incercari am realizat un numar de teste de laborator cu acest dispozitiv de tractiune incovoiere, pe doua tipuri de complexe bistrat primite, fiecare dintre acestea avand un alt tip de interfata uzura-legatura.*

**Keywords:** Laboratory testing, Thermal Shrinkage-Bending Test, Cracking, Durable, RILEM-TG4;

---

\* Corresponding author: Tel. / Fax.:

E-mail address: [mihai.dragomir@etu.unilim.fr](mailto:mihai.dragomir@etu.unilim.fr) / [mihai\\_construct@yahoo.com](mailto:mihai_construct@yahoo.com)



## 1. Introduction

Cracking in pavements is a constant preoccupation for all researchers in the roads domain, because this phenomenon is the base of all damages that cause finally, the lost of the entire system.

Nowadays, the problem posed by all organisms is to obtain durable works respecting the environmental conditions. The raw materials for infrastructures are not regenerative sources, and from this point of view our task is to find all types of solutions, to respond affirmative to this task: Respect the environment and assure durable infrastructure works.

Today, the project engineers have the tendency to create roads systems with a reduced thickness. This economy in mixture associated with the traffic that nowadays is more and more aggressive and with the thermal variations, leads to cracking. After the crack arrives at the surface is very difficult to stop its plane propagation (its ramification).

Our task is, to block the crack most time possible or to stop it's propagation at the source. The crack velocity depends by various factors that we will discuss in this article, after a laboratory test campaign named thermal shrinkage – bending test.

This article wishes to met in evidence, by the thermal shrinkage – bending test, the cracking performances of two different mixture complexes. The tested materials are issued from an experimental site, realized at Ancones Italy in TG4 RILEM project. Task Group4 is the name of this international project, started by RILEM (International Union of Laboratories and Experts in Construction Materials). Every four years, by 1989, an international congress is dedicated to this topic: cracking in pavements.

## 2. Cracking in pavements: causes and solutions

The cracking phenomenon has like reasons [1], [2]:

- the traffic, that nowadays is more and more aggressive;
- the thermal variations, a problem that cannot be solved;
- the mixture fatigue: caused by the increased traffic levels, frost-defrost cycles and very long periods without maintenance;
- the contraction, at the level of hydraulic stabilized layers;
- support ground movements or with a low carrying capacity;
- construction errors: working in cold season or when it's raining, dirty surfaces;
- aging effect, because bitumen is an organic material, that changes his characteristics in time;

The crack will be formed by a couple, [3], not by every single factor mentioned above. This couple it's called fatigue. A phenomenon that is responsible for all damages, because is the sum of two factors that is difficult to be kept under control. The temperature from this couple is responsible for 50% of the cracks length [4]. Temperature is also responsible for its initiation that after a developing period is peaked by the traffic for the rest of 50%. The temperature effect is mentioned also by [5] like having an 80% effect and traffic the rest of 20%. We have to mention, that first affirmation [4] is made over a semi-rigid structure, and the second [5] over a supple structure, more vulnerable at cracking. It's important to remark that the influence of the temperature is decisive. In Fig. 1 the couple is separated, for a better look over it.

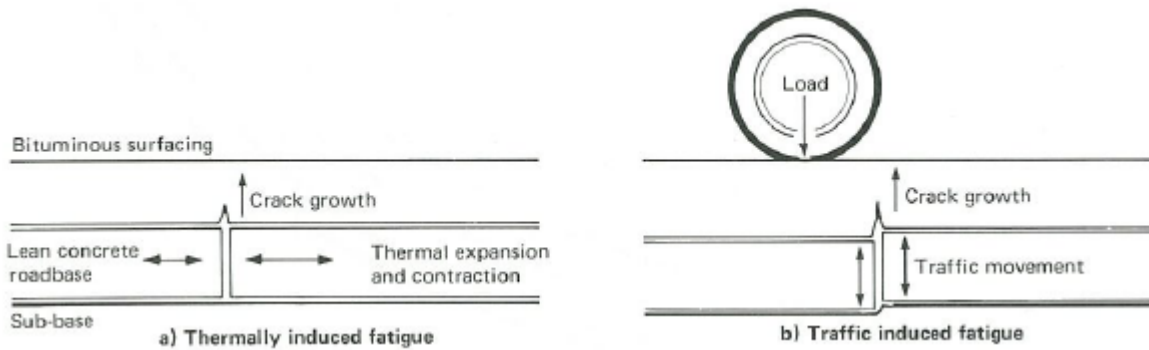


Figure1. Crack developing schema, by [6]

To reach a durable structure is important to have a perfect bonding between bituminous layers interfaces [3], [7]. If the bituminous layers are not very well bonded, the road life time will be reduce with 90 % [8].

Fig. 2 gives a simple explication, showing the two principal manners in crack propagation. A first one, crack propagation without debonding at interface level: under traffic and thermal contraction in very well bonded interfaces. A second one, the crack propagates horizontally from debonded interface zones, followed by the vertical propagation just at the road surface.

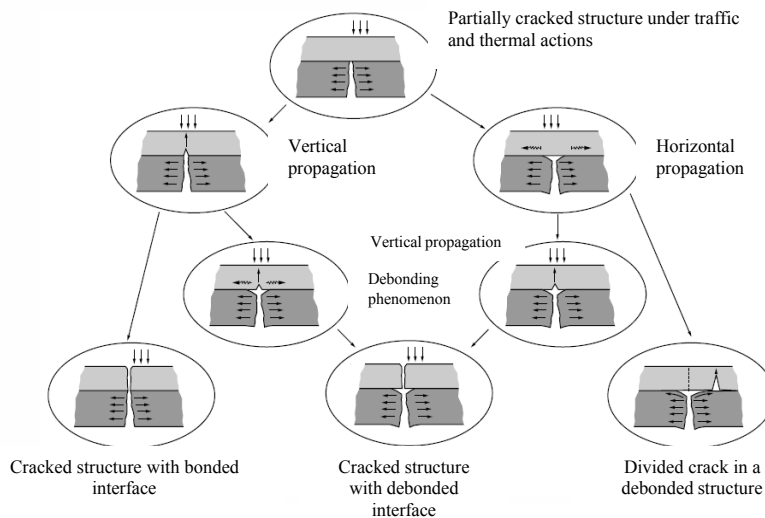


Figure2. Crack propagation in different interface conditions, after [9]

Solutions to assure durability:

- insertion of an interface system that will be able to delay or stop the crack transmission;
- assuring a good bonding between the superiors mixture layers;
- realize good quality works, respecting the prescription and standards;
- do not reduce excessively the height of mixture layers;
- use good quality bitumen and modified emulsions, were the grids are not used ;

If the system will be correctly bonded results [10], [11]

- good distribution of efforts ;
- durability of all structure, because the system will work entirely ;
- the crack will be delayed or stopped by the reinforcement element from the interface ;

### 3. Tested materials

Like we already said, the tested materials are issued from an experimental site, realized at Ancones Italy in TG4-Rilem international research activity. This experimental site is made by a double layer AC11 mixture (Asphalt Concrete 11mm) each layer having 50mm thickness. It's realized in three sections, every one of it, with a different type of interface between the two AC11 mixture layers. One section is the UN (Unreinforced), the second is FP (Fiber Glass Polymer) and the third CF (Carbon Fiber).

In this article we show the results after thermal shrinkage bending laboratory test campaign over UN and FP samples. UN having at the interface a tack-coat with an emulsion described above, in a dosage of: 210 g/m<sup>2</sup>. The particularity of FP is that the grid has a big rigidity being impregnated and protected by a special green polymer.

In bellow tables are showed the geometrical and mechanical characteristics of tested materials.

<b>FP</b>	Grid netting [mm*mm]	Bar section [mm <sup>2</sup> ]	Tensile strength [kN/m]	Elongation strength [%]	Elastic modulus [N/mm <sup>2</sup> ]
	33*33	10	105	3	23000

Table1. FP- Glass grid characteristics

Tested samples	Length [mm]	Width [mm]	Thickness [mm]
	560	110	95

Table2. Samples geometry

<b>UN</b>	H <sub>2</sub> O content [%]	Breaking speed	pH	Pseudo - viscosity Engler [°E]	Polymerized bitumen SBS [%]
	29-31	80-120	2-4	16-25	69

Table3. UN- Cationic modified emulsion-characteristics

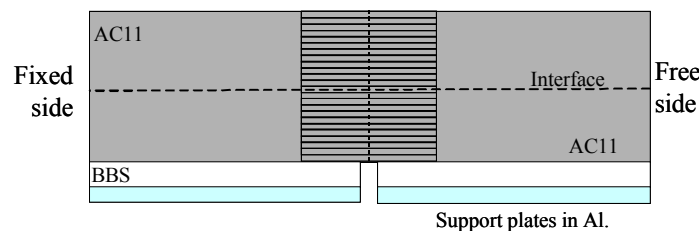


Figure3. Cracking gage implantation (see also Fig. 4)

### 4. Test principle and instrumentation

Thermal shrinkage bending test, a laboratory French testing equipment is represented in Fig. 4. It consists of a testing machine where the samples are tested under two different types of solicitations at 5°C (temperature from the testing chamber):

- a traction, that is the equivalent of thermal shrinkage with a speed of 0.01mm/min ;
- a flexion, that simulates the traffic action with a frequency of 1Hz and 0.2mm flesh;

The particularity of this equipment is that, quite big samples (560mm length) are tested under two

actions, which are the two most important actions that exist on site in reality.

In the literature this equipment has been used by the research team from Autun Laboratory Departement [12] and also by Ph.D. students [13].

Tested samples are realized in three steps:

- 1<sup>st</sup> is cutting the received double layer that has 100mm thickness, at 80mm thickness respecting the placement of the interface at the middle of the sample;
- 2<sup>nd</sup> over the binder layer, we have realized a special bituminous layer called BBS of 15mm height- Béton Bitumineux Soufré, (Asphalt Concrete with soufre- a yellow special filler that in contact with high temperature becomes liquid);
- 3<sup>rd</sup> this BBS layer will be cut at the ½ of samples length, having like this a pre-cracked layer under the new anti-cracking complex ; The realized crack has 4mm width and 15mm depth.

Under the double solicitations: traffic (simulated by the 1Hz frequency and 0.2mm fleshe) and thermal shrinkage (simulated by the constant traction of 0.01mm/min), the crack can develop in two manners [12]:

- directly at the surface, maintaining bonded the interface;
- just at interface level;

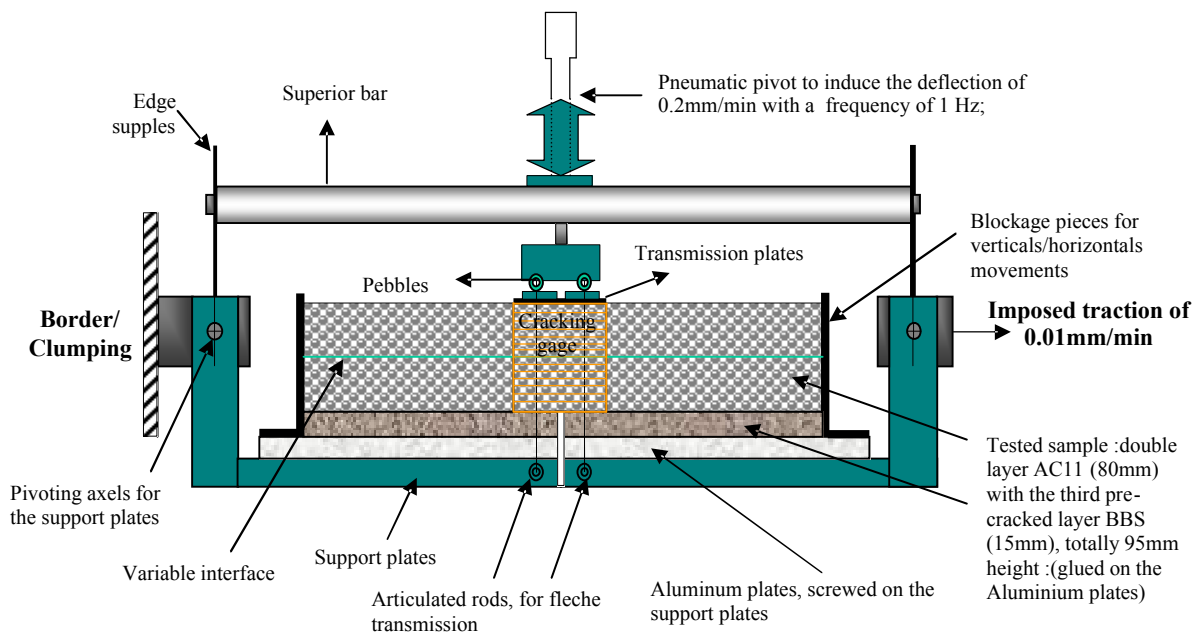


Figure4. Thermal shrinkage bending test principle schema

In Fig. 4 (frontal view of the machine) is represented the principle schema of thermal shrinkage bending test equipment, remade after a primary principle schema of [14]. The frontal side of the sample is implanted with a cracking gage. This cracking gage has 24 copper filaments that function by a very simple principle. If the support surface is intact, all the 24 filaments will function. After the test begins, and the crack starts to propagate in the material, every filament will deliver at the acquisition centre the moment when the crack arrives at their level, by breaking. We can follow in this manner the crack propagation in time under the double solicitation. We have used also in our instrumentation strain gages, for the back side part of the sample, but their exploitation will be done in a future paper.

## 5. Results

The results presented in this paper give a better look over the differences between two types of different interface anti-cracking systems.

We have notice that, over the test duration there are three zones of interest, in both cases:

The first zone is the starting or the boot zone. The material is for the first time in interaction with the double solicitation. It's clear that this first zone, boot zone, is quite particular because the (simulated) thermal shrinkage starts to grow. The flexion like we already said is constant for all test duration 0.2mm flesh at 1Hz frequency. The traction has instead a constant width developing from 0 mm to maximum 7.2 mm. This width developing is associated with the 0.01mm/minute or 0.6mm/hour for maximum test duration of 12 hours.

A second zone, named by us reflective cracking zone, that characterize the biggest part of the test, represents the destruction of tested material. This is the down-top cracking, that happens on side because of an old crack recovered by a new layer of bituminous mixture. This will characterize the bituminous material performances and also the interface response.

A third one, that is proper to the top-down cracking phenomenon that has been remarked by us after this first campaign of exploitations. This region has been observed also by [15], after another experimental campaign named DST, due at construction errors and bad tack-coat interface conditions.

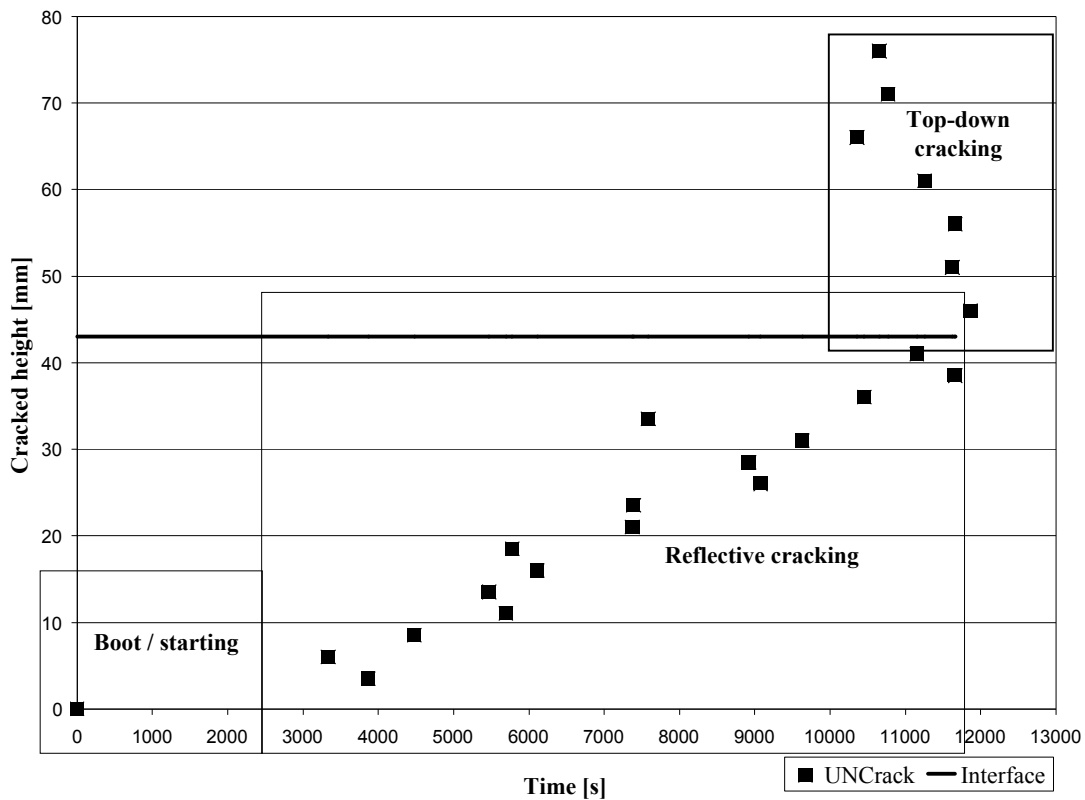


Figure5. UN cracking

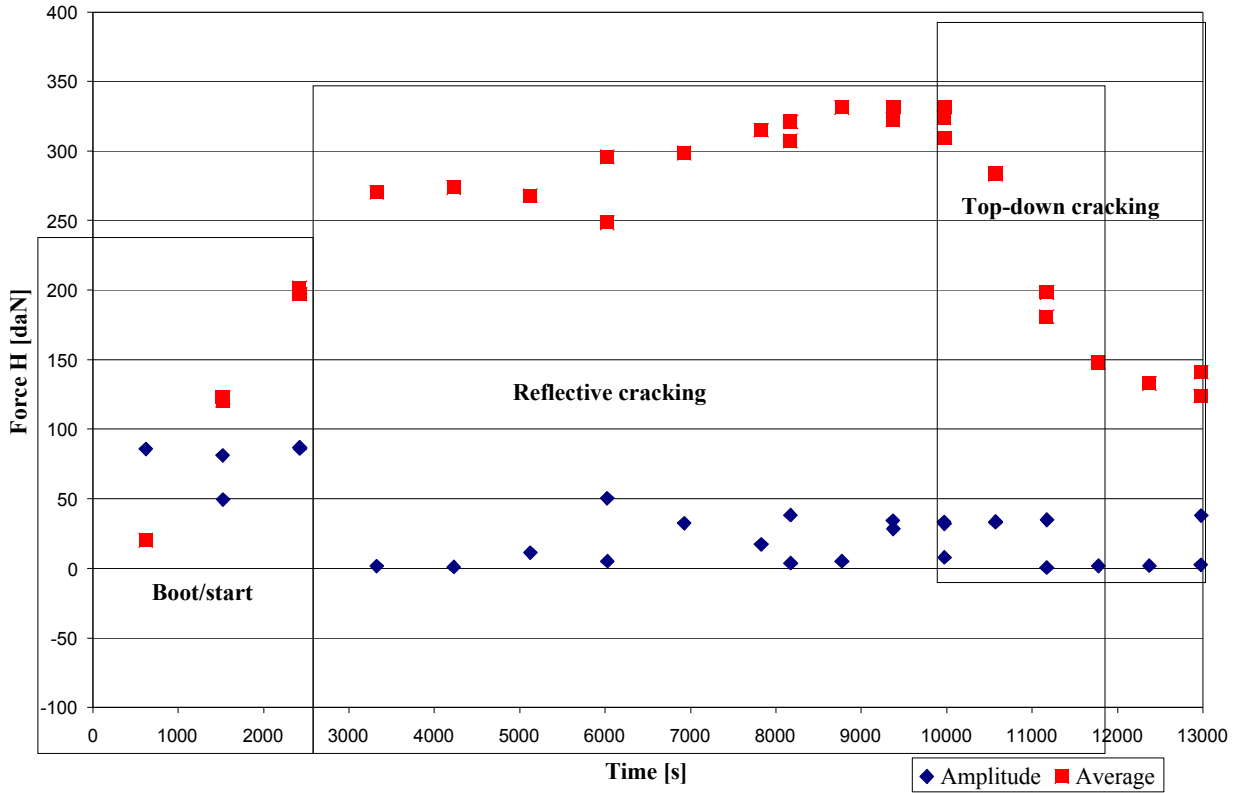


Figure6. Force average and amplitude, for UN

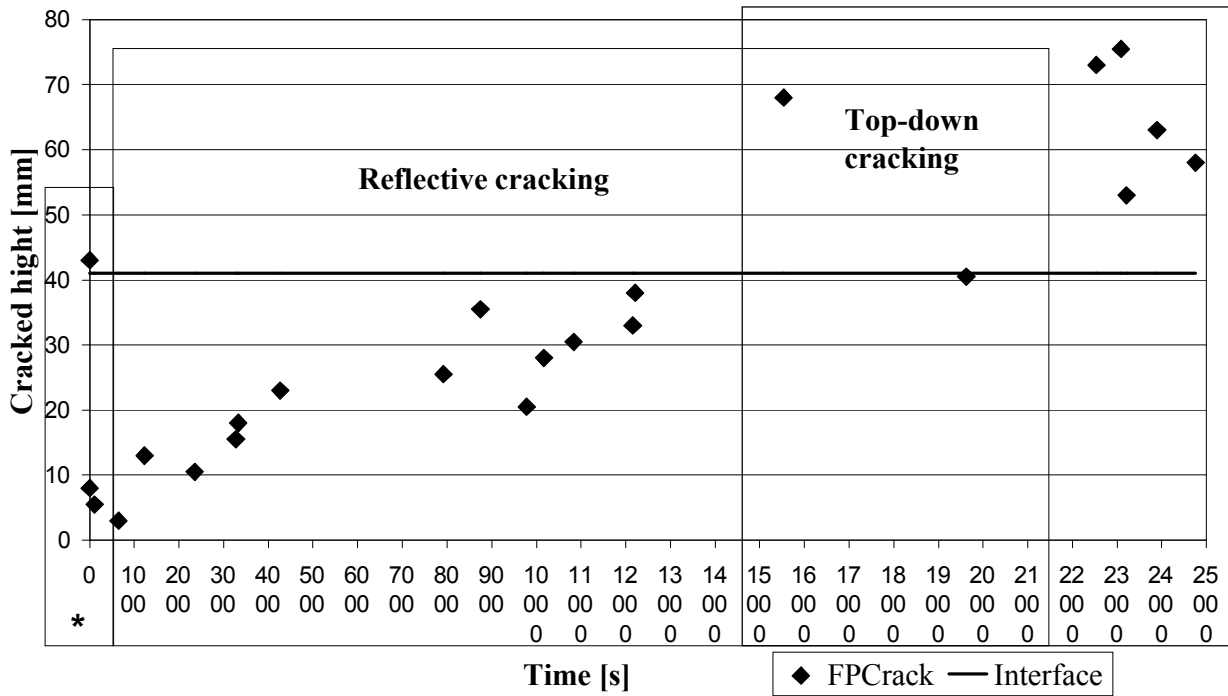


Figure7. Crack developing for FP sample (\*Boot period)

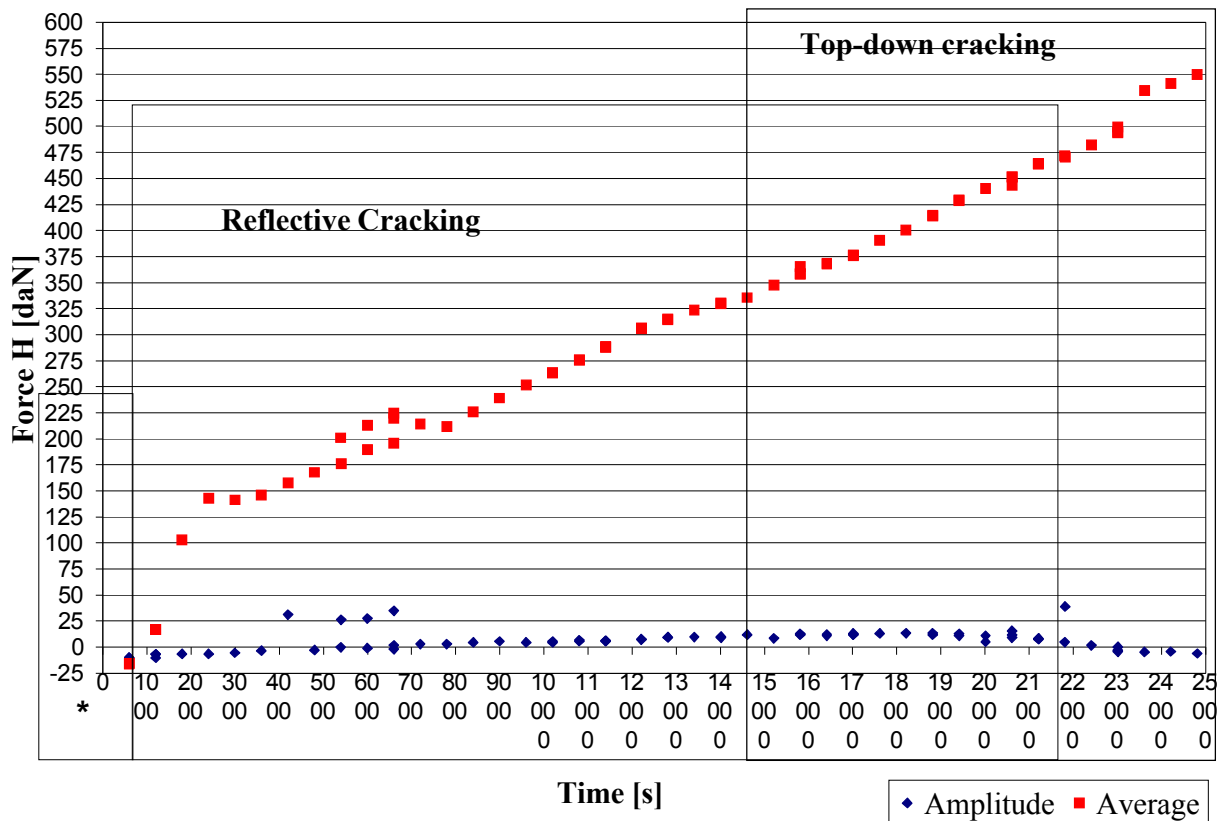


Figure8. Force average and amplitude, for FP (\*Boot period)

## 6. Conclusions

From this first results exploitation we can conclude that:

- The witness sample UN reported at FP reinforced sample, has an extra boot zone, that is represented by the 2500 seconds instead of 500 seconds for the FP reinforced sample;
- This period will be kept in all figures because the time scale is the same for the cracking figure like for the force;
- This difference of boot-starting zone is caused by the difference of rigidity, between the two materials;
- Like we already said, the glass grid has a big rigidity and also by regarding at Tab. 1, geometrical characteristics give reason at this explanation;
- The reflective cracking zone, where the crack arrives at the interface, is very different. The UN crack arrives at the interface in approximately 12000 [s] and the FP in 21000 [s];
- This crack propagation and also its blockage is due to interface conditions;
- We remark that for FP sample the crack growth is very different than UN crack. The crack linearity is not respected in FP case;
- Regarding force growing, it's very clearly from the Fig.6 and Fig.8, that the maximum force will ever be reached by the UN;
- Due to this great difference of rigidity it is clear that between a unreinforced and a glass grid reinforced material is a great difference;

- The influence of bonding conditions is very important also. There are better bonding conditions in UN case that in FP case, due at tack coat layer, that is absent from FP case;
- This is the explication because the UN sample acts like this, and has this crack linearity between the reflective and top-down cracking zones, the meeting will be quite normal;
- The top down cracking happens because at a certain moment, the constant flexion fatigue and damage the upper layer. We can make the connection between our results and the literature review.

After this primary exploitation campaign, of thermal shrinkage bending test results, we can say that the presence at the interface of a reinforcement system will reduce the crack developing and also its velocity. The different force values, between our samples, show this good effect of the reinforcement presence at the interface and also confirm the literature results. Is important to mention that the effect of thermal shrinkage is most significant that the traffic one. Top down cracking is due at traffic frequency that fatigues the upper mixture and conducts it at the reflective one.

## 7. References

- [1] Vanelstraete A., Franken L., RILEM Report 18, *Prevention of reflective cracking in pavements*, State of art report of Rilem committee 157 PRC, Belgian Road Research Center, Bruxelles, Belgium, E&F Spon, 1997.
- [2] Colombier G., *Fissuration des chaussées nature et origine des fissures moyennes pour maitriser leur remontee*, Reflective Cracking in Pavements, Assessment and Control 8-10 mars 1989, Liège, Belgium, pp.3-22.
- [3] De Bond A., *Effect of reinforcement properties*, Reflective Cracking in Pavements Research in Practice, Proceedings of the 4th International RILEM Conference, Ottawa, Ontario, Canada, 26-30 March, 2000, pp.13-22.
- [4] Laveissiere D., *Modélisation de la remonte de fissure en fatigue dans les structures routières par endommagement et macro-fissuration- de l'expérimentation à l'outil de dimensionnement pour l'estimation de la durée de vie*, Ph.D. thesis, Limoges University, 2002.
- [5] Nunn M.E., *An investigation of reflection cracking in composite pavements in the United Kingdom*, RILEM 1<sup>st</sup> Congress Liege 1989, pp.146-153.
- [6] Foulkes M.D., *Assessment of asphalt materials to relieve reflection cracking of highway surfacing*, Ph.D. thesis at Plymouth Polytechnic, 1988.
- [7] Tran Q.T., Toumia A., Turatsinze A., *Modelling of debonding between old concrete and overlay: fatigue loading and delayed effects*, Materials and Structures 40(2007), pp. 1045-1059.
- [8] Fock G., *The use of paving felts to influence the life expenctancy and permanent adhesion of asphalt road surfaces*, Proceedings of 1<sup>st</sup> RILEM International congress, Liège, 1989, pp.95-102.
- [9] Goacolou H., Marchaud J.P., *Fissuration des couches de roulement*, 5<sup>eme</sup> Conférence internationale sur les chaussées bitumineuses, 1982.
- [10] Vanelstraete A., Francken L., *On site behaviour of interface systems*, Reflective Cracking in Pavements Research in Practice, Proceedings of the 4<sup>th</sup> International RILEM Conference, Ottawa, Ontario, Canada, 26-30 March, 2000, pp.517-526.
- [11] Zielinski P., *Fatigue investigation of asphalt concrete beams reinforced with geosynthetics interlayer*, Pavement Cracking 6<sup>th</sup> RILEM Conference, Chicago, SUA, 2008, pp.751-759.



- [12] Vecoven J., *Méthode d'étude de systèmes limitant la remontée de fissure dans les chaussées*, 1<sup>st</sup> RILEM Congress, Liège 1989, pp.57-62.
- [13] Florence C., *Etude expérimental de la fissuration réfléctive et modélisation de la résistance de structures cellulaires*, ENPC Ph.D. thesis , 2005.
- [14] Dumas Ph., Vecoven J., *Processes reducing reflective cracking, synthesis of laboratory test*, Reflective Cracking in Pavements State of Art and Design Recommendations- Proceedings of the 2<sup>nd</sup> International RILEM Conference, Liege, Belgium, March 10-12, 1993, pag.246-253.
- [15] Diakhaté M., Millien A., Petit C., Phelipot-Mardelé A., Pouteau B., *Experimental investigations of tack-coat fatigue performance : towards an improved life time assessment of pavement structure interfaces*, Construction and Building Materials 25(2010), pp.1123-1133, ISSN 0950-0618.